Delivery, Design, and Mechanism of Antimicrobial Peptides

by
Tanguy Chau
B.S., Chemical Engineering
University of California, Berkeley, 2004

Submitted to the Department of Chemical Engineering
in Partial Fulfillment of the Requirements for the Degree of
Doctor of Philosophy in Chemical Engineering Practice
at the
Massachusetts Institute of Technology

May 26, 2010
[September 2010]

Signature of the author .....

Tanguy M. Chau
Department of Chemical Engineering
May 26, 2010

Certified by .....

Gregory N. Stephanopoulos
Bayer Professor of Chemical Engineering
Thesis Supervisor

Accepted by .....

William M. Deen
Professor of Chemical Engineering
Chairman, Committee for Graduate Students

Abstract

Each year, 2 million people contract hospital-acquired bacterial infections, which causes the death of 100,000 patients and costs the US healthcare system over $21 billion. These infections have become dangerously resistant to our existing line of antibiotics and are rapidly spreading outside of hospitals and into communities. As molecular targets to develop new antibiotics are becoming exhausted, clinicians and scientist are concerned that antibiotic resistant infections will wipe out most of the major health benefits acquired over the last century. The work described in this thesis develops new antimicrobials strategies against bacterial infections, focusing on antimicrobial peptides (AmPs).

We first delivered genes inducing the toxic expression of AmPs and other lytic agents directly into bacteria using reengineered bacteriophages. Expression of these lytic agents in lysogenic bacteriophages resulted in bactericidal activity, and demonstrated, for the first time, a long-term cidal effect for over 20 hours. We then enhanced the efficacy of our approach by expressing the same agents in lytic bacteriophage, which resulted in complete suppression of the bacterial culture and prevented bacterial regrowth and resistance to bacteriophages.

Since a large fraction of medical infections originates at the surface of implantable devices, we developed film coatings that release active AmPs to cover these surfaces and prevent bacterial colonization. We incorporated AmPs in layer-by-layer films and demonstrated that the kinetics of AmP release can be adjusted. These released AmPs still actively prevented bacterial growth and remained non-toxic towards mammalian cells.

While natural AmPs have broad activity against pathogens, they are not optimized for a specific antimicrobial function or bacterial target. Thus, researchers have tried for decades to design highly active and specific *de novo* AmPs. One approach is to design new peptides using conserved motifs identified from the amino acid sequence of natural AmPs. We improved this

approach by measuring the antimicrobial activity of a large database of natural AmPs and incorporating this activity information in the design algorithm. This strategy improved the success rate of designing *de novo* peptides from 45% to 73% and increased the antimicrobial strength of the designed peptides.

Finally, we developed new potentiating strategies by studying the mode-of-action of the family of ponericin AmPs. First, we measured their cidal behavior and differentiated bactericidal ponericins from bacteriostatic ones. Using a modified AFM and a microfluidic device, we observed that the action of AmPs led to cellular death through the corrugation of bacterial, while sub-population of cells resisted the action of the AmPs longer than others. Focusing on the ponericin G1 AmP, we correlated these visual observations with various membrane stress sensing mechanisms. We concluded that bacteria's ability to develop resistance to ponericin G1 requires the sensing and repair of misfolded membrane proteins via the CpxAR system, as well as DNA repair via induction of the SOS response by RecA. Using microarrarys, we showed that ponericin G1 targets tRNA synthetases in the ribosome. Finally, we demonstrated 99.999% killing of antibiotic resistant bacteria by potentiating ponericin G1 with the ribosomal antibiotic kanamycin, whereas no killing is observed when these two agents are applied independently. untreta

The PhDCEP capstone requirement finalizes the work of this thesis by analyzing market entry and expansion strategies for an antimicrobial company commercializing genetically engineered bacteriophages. In conclusion, this thesis establishes new advances in the delivery, the design and the potentiation of AmPs in order to eradicate resilient bacterial infections.

à Maman,

Sache qu'ici reste de toi
comme une empreinte
indélébile

Acknowledgments

Family:

- **Papa**, **Chloé**, et ma famille: pour votre amour, et soutien constant.

Best buddies:

- **Doktor Michael Koeris**: Ohne dich mein Bruder, ich würde nirgends.
- Aspiring Doctor **Christopher Jongsoo Yoon**: 당신의 헌신과 열정에 감사드립니다.
- Professor **Timothy Lu**: 謝謝你鼓勵 我對科學的熱愛, and turning on the headlights when I was lost.
- **Christopher Loose**, and **Joel Moxley**: for teaching me to play football with the Irish.

Collaborators:

- **Bernice Huang**: for making late night gel electrophoresis such fun.
- **Rana Ghosh**: for introducing me to the phage world.
- **Orhan Karsligil:** for bringing rational to AmP designs.
- **Helen Chuang**, and **Anita Shukla**: for stuffing AmPs into coatings.
- **Robbie Barbero** and **Georg Fantner**: for sharing my passion to kill bacteria.

Mentors:

- My advisors, **Robert Langer** and **Gregory Stephanopoulos**, for inspiring me to be my best.
- My committee members **Christopher Love** and **Dr. Robert Rubin** for their guidance.
- **Jim Collins** for your contagious enthusiasm and support of my work.
- **Steve Lerman** for making my experience at MIT an enjoyable, diverse and rewarding one.

Friends:

- **My friends** for allowing me to vent my frustration in front of a good beer.
- Ma cousine **Corinne Tram** pour faire ma lessive pendant quatre ans.
- To **Robert Wang** and the **Graduate Student Council** for giving me a purpose and helping me create a dental plan for MIT graduate students.

Table of contents

– Blank Page –

List of figures

List of tables

Chapter 1. Critical need for new antibiotics

1.1. The rise of antibiotic resistant infections

Antibiotic-resistant microbes infect more than 2 million Americans and kill over 100,000 each year (*1*). They are one of the biggest and fastest growing clinical problems today (*2*) and constitute a global threat that has the potential to wipe out many of the major health benefits that have occurred over the last century (*3*).

These infections pose a risk to everyone from infants, to college athletes, to elderly in nursing homes and hospitals. For example, the 2009 MRSA outbreak at Beth Israel Hospital maternity ward infecting over 30 mothers and infants. In 2008, New England Patriot's quarterback Tom Brady contracted an MRSA during a knee surgery and required several IV antibiotics treatment to eradicate the infection, which ended his football career for the year. Antibiotic resistant infections have spread beyond the hospital settings and now threaten communities. Nationwide outbreaks have already occurred shutting down in schools, and athletic events while claiming many lives. MRSA alone kills more Americans than AIDS, Parkinson's disease or homicide. (*4*)

The populations with the highest risk of mortality following infection are infants and young children, elderly and immuno-suppressed patients (*5*). These groups are at increased risk as a result of a suppressed immune system, increased exposure to numerous pathogens, or because of restriction on the antibiotics they can be administered. Thus, infections are the fourth most common cause of death for children in their first year (*6*), are the most common cause of hospitalization for older adults, and are responsible for 30 percent of the deaths in senior citizens (*7*). Patients with particular medical conditions such as cancer, diabetes, HIV/AIDS, transplants, etc. are also extremely vulnerable to infections. Even the

healthiest individual becomes exposed to antibiotic-resistant pathogens every time they enter hospitals, even for the most benign interventions (*8*).

Infections are not only a health problem but also an economical one. Resistance to antibiotics significantly extent the length of hospital stay typically by 6 additional days and increases the total cost of treatment by $24,000 per patient (*9*). John Paul, retired CFO of the University of Pittsburgh Medical Center explains that the ability to control hospital-based infections would add tens of millions of dollars straight to a medical center's bottom line (*10*).

Consequently, there is an unmet need to develop new antimicrobial solutions that decrease morbidity and mortality in patients, to reduce hospital costs or to prevent and control nationwide outbreaks.

1.2. A multifaceted problem

The problem of antibiotic resistance in bacterial infections is multifaceted and the reasons for their recent rise are multiple. Firstly, the sheer number of infections has increased rapidly by 200% in the last 5 years, with over 2 million cases and 99,000 deaths per year in 2007 (*11*).

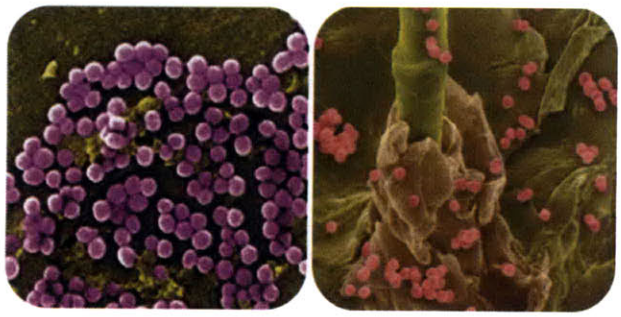

Figure 1-1: Methicillin-resistant S. aureus and vancomycin-resistant Enterococcus are two resistant pathogens spreading rapidly. Figure adapted from (12).

Secondly, these infections are becoming increasingly difficult to treat. Figure 1-2 shows the rapid spread of resistant strains. Methicillin resistance in staphyloccal infections (MRSA), one of the most

common hospital pathogen, rose from just 3% in the 1980s to over 60% by 2007 (*12*). Over 30% of hospital infections today are due to infections resistant to all but one antibiotic, vancomycin which is considered to be the last resort antibiotic (*13*). Already, cases of high-level resistance to vancomycin are being reported worldwide. Many physicians worry that if these strains were to spread like MRSA has, death rates would likely increase to pre-antibiotic era at greater than 50% (*14*).

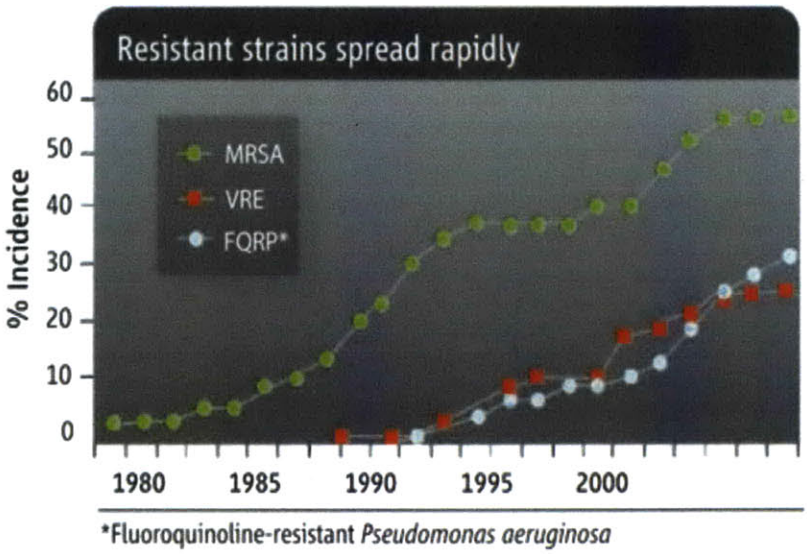

Figure 1-2: Rise in resistance strains. The green curve shows the increase in methicillin resistance nosocomial Staph. infections. Less than 3% of those infections were resistant to methicillin by 1980, whereas today over 60% are resistant to methicillin and other commonly used antibiotics. The red and silver curve shows the rise in vancomycin-resistance enterococcus infections and fluoroquinoline-resistant Pseudomonas aeruginosa. Figure adapted from (12).

Antibiotic resistance in bacterial infections result in increased morbidity and mortality in patients (*15*). A study by the Duke University medical center shows that patients infected by methicillin resistant *S. aureus* were seven times more likely to die and 35 times more likely to be readmitted within 90 days than those infected by *S. aureus* sensitive to methicillin (*9*). Figure 1-3 shows the increase in number of death either directly caused or correlated with the methicillin resistant infections in England and Wales.

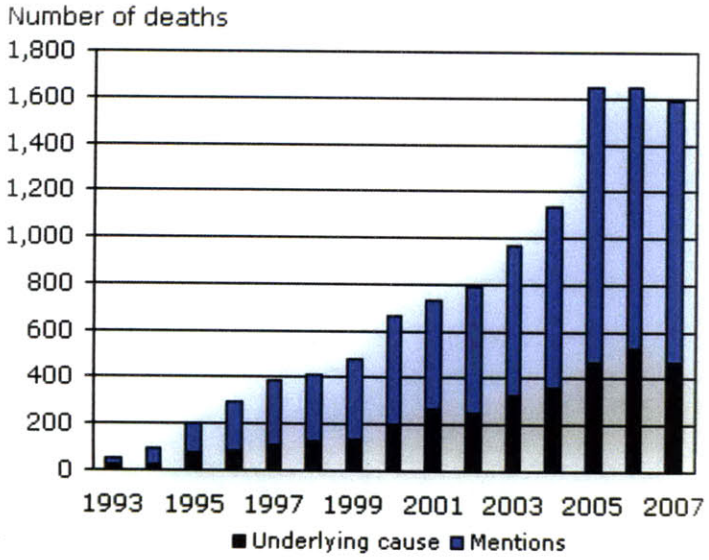

Figure 1-3: Rise in mortality. Number of death certificates mentioning Staphylococcus aureus by methicillin resistance in England and Wales. The number of death certificates mentioning Methicillin-resistant Staphylococcus aureus (MRSA) decreased to 1,593 in 2007 and then decreased further to 1,230 in 2008, a fall of 23 per cent. The number of death certificates in England and Wales mentioning Staphylococcus auras (including those not specified as resistant) was 1,500 in 2008, a decrease of 27 per cent compared to 2007.

Finally, the threat of antibiotic resistant bacteria is further accentuated by a decline in the development of new antibiotics. Although the $25B global market for antibiotics is attractive, drugs for chronic diseases offer much greater return on investments says Steve Projan, vice president of biological technologies at Wyeth. Pharmaceutical companies developing new antibiotics are also faced with a Catch-22; the better their antibiotic, the less health experts want to see it used to avoid the development of resistance. This led to an exodus of pharmaceutical companies from antibiotic development starting in the 1980s. Of the 15 major pharmaceutical companies that once had flourishing antibiotic discovery programs, only five – GlaxoSmithKline, Novartis, AstraZeneca, Merck, and Pfizer – still have antibiotic discovery efforts. As a result there has been a decrease in the number of new antibiotics available to clinical doctors to treat infections and many researchers also suggest that the intracellular metabolic

targets for antibiotic discovery are being depleted (*16*). Figure 1-4 shows the decrease in the number of antibiotic products approved by the FDA over time (*12*). These antibiotics actually only constitute two new classes of antimicrobials discovered since the 1980s – oxazolidinones (linezolid) and cyclic lipopeptides (daptomycin). All of these new classes of antibiotics target only Gram positive bacteria and no new Gram-negative antibiotics have been developed since quinolone in the 1960s (*17*). Gram-negative bacteria tend to be harder to kill because of their cell membrane which the antibiotics needs to penetrate and additional defense mechanisms such as shutting down protein channels through which the antibiotic penetrates or activating efflux pump to excrete the antibiotics.

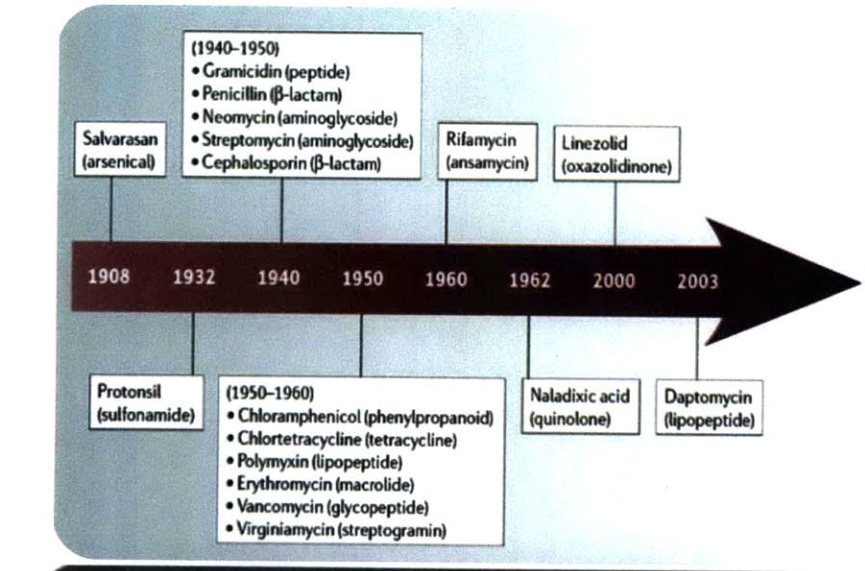

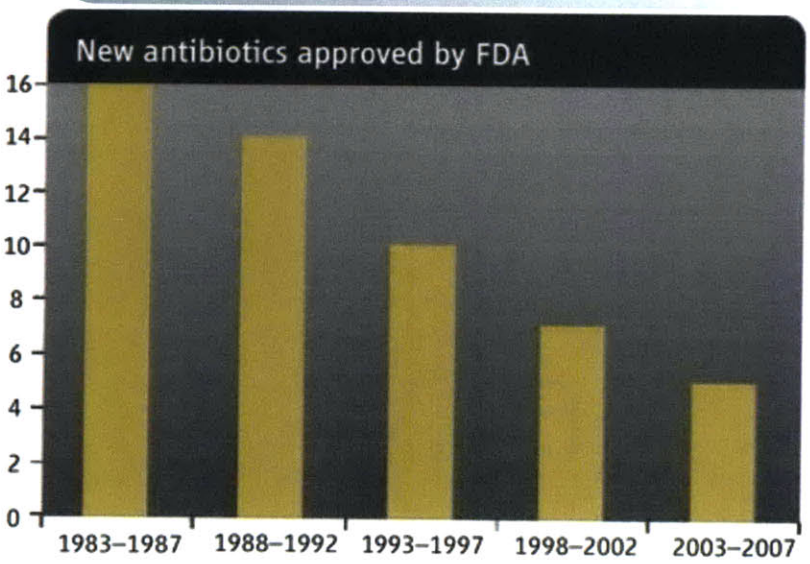

Figure 1-4: Timeline of antibiotic drug discovery and new antibiotics approved by FDA. Only two new classes of antibiotics have been discovered in the past 50 years and the number of new antibiotics approved by the FDA has been decreasing continually since the 1980s. Figure adapted from (12).

1.3. Thesis objective and organization

This thesis aims at providing an advance in the development of new antimicrobial therapies. The work explores the use and the design of novel antimicrobial peptides and engineered bacteriophages to treat bacterial infections. The thesis is organized into the following six chapters:

- *Chapter 2. Antimicrobial peptide overview* – provides background and review on antimicrobial peptides, the central element of this thesis and introduce them as new human antimicrobial therapeutics.
- *Chapter 3. Engineered bacteriophages expressing AmPs* – offers an approach to deliver genes expressing antimicrobial peptides and other lytic antimicrobial agents using bacteriophages.
- *Chapter 4. Controlled delivery of AmPs from LBL surfaces* – describes an approach for the controlled release of antimicrobial peptides using layer-by-layer biodegradable polymer films coated on the surfaces of implantable devices.
- *Chapter 5. Motif-based rational design of AmPs* – discusses advances made in the design of novel peptides using conserved sequences founds in natural AmPs.
- *Chapter 6. Mechanism and potentiation of AmPs* – gives insight on the mechanism of antimicrobial peptides, their intra- and extra-cellular targets, and outlines an approach to potentiate AmP-based therapeutics.
- *Chapter 7. Therapeutic opportunities for engineered bacteriophages (PhDCEP Capstone)* – describes a market entry and expansion strategy for an antimicrobial start-up company commercializing genetically engineered bacteriophages.

1.4. References

1. B. Spellberg, *Rising Plague: The Global Threat from Deadly Bacteria and Our Dwindling Arsenal to Fight Them*. (2009).
2. J. Katz, *Oral communication*, (2009).
3. M. P. M. Shnayerson. The Killers Within: The Deadly Rise of Drug-Resistant Bacteria (2002).
4. R. M. Klevens *et al.*, in *Public Health Rep.* (2007), vol. 122, pp. 160-6.
5. K. F. Shea, M., Barlam, J., *Environmental Defense*, 1 (Mar 12, 2002).
6. Gotoff, *Infections of the Neonatal Infant*. R. M. K. Behrman, and H.B. Jenson, Ed., Nelson Textbook of Pediatrics (2000).
7. M. S. a. D. Kaye, *Infectious Disease Clinics of North America*, 357 (2000).
8. R. P. W. a. M. B. Edmond, *New England Journal of Medicine* **343**, 1961 (2000).
9. D. J. Anderson *et al.*, *PLoS ONE* **4**, e8305 (2009).
10. D. L. C. Loose, J. Moxley, *Stericoat Business Plan*.
11. K. Krul, *Kalorama Information*, (2009).
12. G. Taubes, *Science* **321**, 356 (July 18, 2008, 2008).
13. C. Loose, MIT (2007).
14. *Staph Bacteria*. Science Blog (Rockefeller University, 1997), vol. June 11.
15. http://www.statistics.gov.uk/cci/nugget.asp?id=1067. (Office for National Statistics).
16. G. D. Wright, *Nature Reviews Microbiology* **5**, 175 (2007).
17. M. S. Daniel Becker, Claudia Rollenhagen, Matthias Ballmaier, Thomas F. Meyer, Matthias Mann and Dirk Bumann, *Nature*, 303 (2006).

Chapter 2. Overview of antimicrobial peptides

2.1. Executive summary

Antimicrobial peptides are part of the innate immune systems of many living organisms and serves as a first line of protection against invading bacterial, viral or fungal infections. They represent an exciting potential new class of antibacterial therapies as their novel mode of action prevents bacteria from easily evolving resistance to AmPs. AmPs are small cationic amphipatic peptides between 15 and 30 amino acids that typically form alpha helices ad intercalates within the bacterial cell membrane to form pores; eventually leading to cell lysis. In order for bacteria to evade the action of AmPs, they are required to significantly alter their cell membrane composition, which drastically decreases their viability. For these reason, resistance to AmPs is uncommon which constitutes one of their greatest advantage of the tradition small-molecule antibiotics used in hospitals today.

2.2. Antimicrobial peptides as antibiotics

Antimicrobial peptides (AmPs) are an exciting potential new class of antibiotic because their unique mode of action is unlikely to introduce drug resistance. AmPs are typically short peptides composed of 15 to 30 amino acids that have strong antimicrobial properties. AmPs are an important component of the innate defense mechanism of many living organisms where they constitute a first non-specific line of defense against invading pathogens (*18*). For example, many AmPs are been isolate from skin secretions of, such as dermaseptin from the South American frogs, where they protect against pathogens in the natural living environment. AmPs, such as histatins from human saliva or magainin from the Xenopus laevis frog, play a role in protection from ingested pathogens. Cathelicidins, another family of AmPs, have

been isolated from many mammalian species, such as mice, rabbits, sheep, horses, and humans. Defensins from human neutrophils are found inside the host body indicating varied biological roles in host defense.

To date, more than 800 AmPs have been reported. Their range of antimicrobial activity is unusually broad as their primary role is non-specific. AmPs have been found to be active against Gram-positive (e.g. *S. aureus*) and Gram-negative (e.g. *E. coli*) bacteria, viruses (e.g. HIV, Herpes virus), protozoa (e.g. *T. brucei*) and fungi (e.g. *C. albicans*). More recently, they have been shown to bind selectively and prevent the growth of cancer tumors (*19*) and also to play an important role in recruiting the innate immune systems (*20, 21*).

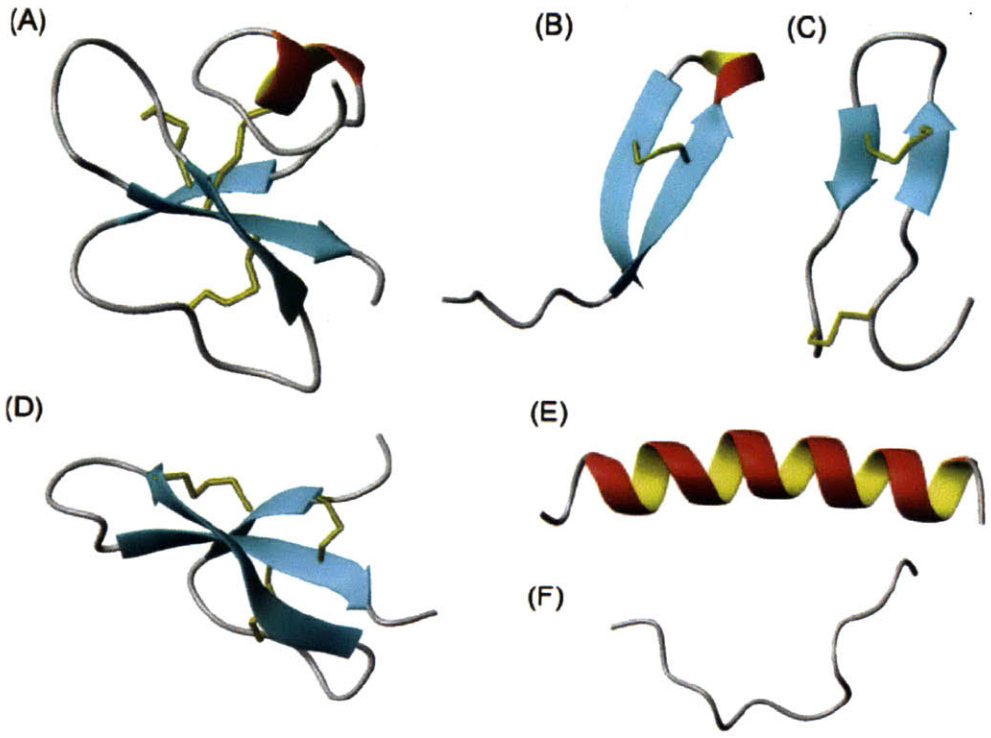

Figure 2-1: Structural classes of AmPs. (A) Mixed structure of human β-defensin-2; (B) looped thanatin (C) β-sheeted polyphemusin; (D) rabbit kidney defensin-1; (E) α-helical magainin-2; (F) extended indolicidin. The disulfide bonds are indicated in yellow, and the illustrations have been prepared with use of the graphic program MolMol 2K.1. Figure adapted from Jenssen 2006.

In contrast with their enormous diversity in activity, AmPs share several common characteristics and are generally categorized into four structural classes: α-helix, β-sheet, loop or extended structure (Figure 2-1). These short peptides are predominately positively charged. AmPs typically assume an amphipatic three-dimensional structure where, for α-helix peptides, the hydrophilic positively charged residues are localized on one side of the helix and the hydrophobic residues are on the other side. This amphipatic structure and the net positive charge give AmPs an affinity for bacterial membranes over eukaryotic membranes. AmPs selectively coalesce and bind to bacterial membrane leading to membrane permeation and the death of the bacteria through cell lysis. While the exact mechanism of action by which killing occurs is not clearly understood, several models have been proposed (*22*) and are explained below.

2.3. Mode of action of AmPs

One model describing the killing mechanism of AmPs is the barrel-stave model shown in Figure 2-2A. The AmPs aggregate and insert perpendicularly into the membrane bilayer so that the hydrophobic peptide regions align with the lipid core region and the hydrophilic peptide regions form the interior region of the pore. In a second model, the toroidal model shown Figure 2-2B, the AmPs aggregate and induce the lipid monolayers to bend continuously through the pore so that the aqueous core is lined by both the inserted peptides and the lipid head groups. In this model, the peptides are always associated with the lipid head group even when they are perpendicularly inserted in the bilayer, which is not the case in the barrel-stave model. Finally, in the carpet model in Figure 2-2C, the peptides disrupt the membrane by orienting parallel to the surface of the lipid bilayer and forming an extensive layer or carpet. Some AmPs do not induce cell lysis but instead they permeate through the membrane and kill the bacteria by acting on intracellular targets (*23*). Such AmPs have been shown to inhibit DNA, RNA and protein synthesis. Inhibition of enzymatic activities and of the formation of structural components, such as the peptidoglycan or cell walls, are other known intracellular targets for AmPs.

Because the uptake of AmPs is self-promoted -- based on peptide charge-- and non-specific, bacteria are less likely to develop resistance to AmPs since it would require the bacteria to completely change the properties and structure of their membranes (*20*). As a result, AmPs have been killing bacteria for millions of years, yet bacteria have developed very little resistance and the few resistant strains have significantly reduced viability because of the numerous changes introduced to their membranes (*24*).

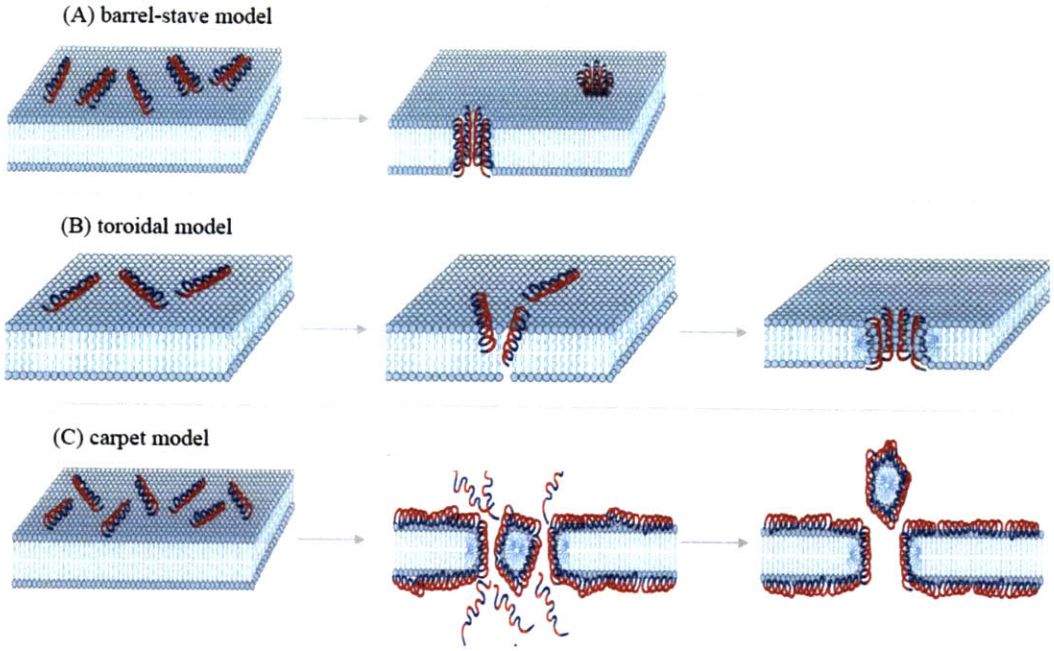

Figure 2-2: Proposed models of AmPs induced killing. (A) In the barrel-stave model, the AmPs insert perpendicularly into the membrane bilayer. (B) In the toroidal model, the AmPs induce the lipid monolayers to bend continuously through the pore. (C) In the carpet model, the peptides align parallel to the surface and disrupt the membrane. Hydrophilic regions of the peptide are shown colored red, hydrophobic regions of the peptide are shown colored blue. Figure adapted from Brogden 2005 (22).

2.4. AmPs compared to traditionnal antibiotics

Several characteristics make AmPs particularly attractive compounds to develop as novel antibiotics (*20*). Firstly, because AmPs are non–specific and act on multiple targets, bacteria are less

likely to develop resistance to them. On the other hand, traditional antibiotics typically act on single metabolic or intracellular targets, which the bacteria can modify to evolve antibiotic resistance. Gram negative bacteria also posses additional defense mechanism such as the ability to modulate their protein channel to reduce the uptake of antibiotic or to activity efflux pump to secrete and reduce intracellular antibiotic concentration. Secondly, AmPs exhibit a broad spectrum of activities including against Gram-negative, Gram-positive, multi-drug resistant bacteria and non-bacterial target such as viruses, fungi, or cancerous cells. Traditional antibiotics are only efficacious on bacteria and are sometimes specific to sub-classes of bacteria. For example, vancomycin is active only against gram-positive bacteria as it inhibits the biosynthesis of cell wall, which gram-negative bacteria do not posses. Thirdly, AmPs kill bacteria in a rapid and bactericidal manner through cell lysis where as some antibiotics are bacteriostatic and only prevent the growth of bacteria with out actually killing them. Finally, AmPs have the additional effect of boosting and recruiting the overall innate immune system of the host (*25*). These properties give AmPs great advantages over traditional antibiotics.

The main obstacles for the clinical development of AmPs are their high manufacturing cost, their short in-vivo lifetime due to protease degradation, and a general lack of understanding of their systemic toxicity. However, recent scientific and technological improvements have addressed some of these issues. Improvement in solid phase chemical synthesis of custom peptides has driven down the manufacturing cost of a typical 20-mer peptide from $500 to $30 per peptide (*26*). Other synthesis methods such as recombinant production have been developed for larger size manufacturing and are continuously improved upon. Researchers were also able to improve the stability of AmPs to protease degradation by introducing unusual or D- (rather than L-) amino acids, the use of non-peptidic backbones, and special formulation such as in liposomes (*25*). Finally, the concern about systemic toxicity can be addressed by developing topical applications for AmPs or through local drug delivery methods such the immobilization or release of AmPs from the surface of implantable devices.

Table 2-1: Selected characteristics of AmPs vs. traditional antibiotics

	Antimicrobial peptides (AmPs)	Traditional antibiotics
Advantages of AmPs		
1. Bacterial resistance	Less Likely Non-specific, act on multiple target	Resistance common through reduced uptake, increased efflux, altered target
2. Activity spectrum	Broad spectrum: Gram +/- bacteria, viruses, fungi	Bacteria only and can be specific to sub-classes
3. Bactericidal/static activity	Bactericidal activity through cell lysis	Some antibiotics are bacteriostatic and only prevent cell growth
4. Additional effect	Recruit and supports the host innate immune system	
Obstacles with AmPs and recent improvements		
1. Manufacturing cost	Expensive (~$100/gram) • Shorter peptides manufactured by chemical synthesis, decreasing costs	Cheap (<$1/gram)
2. In-vivo stability & Pharmacokinetics	Short systemic half-life due to protease degradation • Use unnatural or D-amino acids; non-peptidic backbones, liposome formulation	Stable and long half-life up to 1 week
3. Toxicity	Systemic toxicity not well studied • Localized delivery	Well studied and relatively safer

2.5. References

1. M. Zaiou, in *J Mol Med.* (2007), vol. 85, pp. 317-329.
2. Lehmann *et al.*, in *European Urology.* (2006), vol. 50, pp. 141-147.
3. A. Marr, W. Gooderham, R. Hancock, in *Current opinion in pharmacology.* (2006).
4. N. Mookherjee, R. Hancock, in *Cell. Mol. Life Sci.* (2007).
5. K. Brogden, in *Nat Rev Micro.* (2005).
6. H. Jenssen, P. Hamill, R. E. W. Hancock, in *Clinical Microbiology Reviews.* (2006), vol. 19, pp. 491-511.
7. H. G. Boman, in *Jounral of Internal Medicine.* (2003), pp. 197-215.
8. R. E. W. Hancock, H.-G. Sahl, in *Nat Biotechnol.* (2006), vol. 24, pp. 1551-1557.
9. C. Loose, in *MIT PhD Archive.* (2007).

Chapter 3. Engineered bacteriophages express antimicrobial peptides

3.1. Executive summary

The rise of antibiotic resistant infections has led to a renewed interest in alternative treatments such as bacteriophage therapy. However, the therapeutic use of bacteriophage has been contested, as bacteria are able to rapidly evolve resistance to bacteriophages. In this work, we engineered bacteriophages to overexpress antimicrobial peptides and lytic enzymes to enhance their cidal activity. We demonstrate that M13 lysogenic bacteriophages expressing the lytic CHAP+ enzyme result in a 10,000-fold decrease in viable cell counts relative to the unmodified phage and the effect is maintained for over 20 hours. Engineered T7 lytic bacteriophages expressing CHAP+ lead to long term suppression of bacteria culture and prevent the evolution to bacterial resistance to bacteriophages. This work establishes an engineering approach to confer new functionalities to bacteriophages and enable them to eradicate difficult-to-treat bacterial infections.

3.2. Introduction

3.2.1. Bacteriophages and their therapeutic potential

A naturally occurring countermeasures to bacteria are bacteriophages, viruses that infect and multiply in bacteria. Phages specifically recognize and attach to bacterial membranes, inject their genomes and utilize the host replication system to multiply. This process subsequently leads to new phage progeny that are released either through extrusion in the case of lysogenic phages or by inducing cell lysis in the case of lytic phages. The therapeutic potential of lytic bacteriophages was recognized early (*27, 28*) when they were successfully used in the 1920s to treat and control the spread of cholera and to disinfect water sources. The discovery of cheap, broad-spectrum antibiotics in the 1950s halted

the development of bacteriophages in the West though some efforts have continued up to this day in the former Soviet Republic (*29, 30*). The spread of antibiotic resistance has led to a recent regained interest in bacteriophage therapy (*31*) with several clinical trials carried out worldwide (*32-36*). However, criticism for phage therapy still remains. Two primary concerns are their high specificity and the rapid evolution of bacterial resistance (*37*). Modern molecular biology has now made it feasible to re-engineer bacteriophages and express foreign proteins to address these concerns and confer new functionality.

We have previously shown that expression of a biofilm-degrading enzyme (DspB) from a T7 bacteriophage infecting *E. coli* increases the disruption of bacterial biofilms (*38*). In another model, we showed that expression of a repressor protein of the SOS response (LexA3) from an M13 bacteriophage administered as an antibiotic adjuvant suppressed the evolution of bacterial resistance to antibiotics and increased bacterial susceptibility (*39*). Both models demonstrated the feasibility of engineering bacteriophages without compromising their natural infectivity, replication, packaging and lytic activity.

3.2.2. Engineered phages expressing AmPs and lytic enzymes

In this work, we address the concern of bacterial resistance to phages by overexpressing antimicrobial peptides and lytic enzymes during infection and increase bacterial killing. Antimicrobial peptides were introduced in the Chapter 2. Lytic enzymes (lysins) are another new class of prospective antimicrobials. These biologics range in size from 50 to several hundreds of amino acids, and are typically used by bacteriophages to lyse bacterial membranes and escape from their hosts (*40, 41*). Lysins act in concordance with holins, which permeabilize cell membranes (*42*) while lysins degrade peptidoglycan cell walls (*43*). When applied exogenously, phage lysins exhibit immediate and strong bacteriolytic activity (*44*). One well-studied phage lysin is the CHAP+ protein, an optimized derivative of the LysK staphylococcal phage K endolysin truncated to the first 165 amino acids of its active domain (*45*).

While promising, peptide and enzyme-based therapeutics suffer several practical challenges for systemic application. They are subject to protease degradation when administered *in-vivo*. Their distribution and pharmacokinetics and pharmacodynamics are also not well characterized. As a result,

their toxicity levels and potential immune reactions at required active physiological concentrations are undetermined (*46-48*). More practically, their cost of production and purification is still prohibitively high compared to that of small molecule antibiotics.

We first determined the minimum inhibitory concentrations (*49*) and the bactericidal activities of a panel of five AmPs. We selected the two most active AmPs candidates, Ponericin W3 and Ponericin W5, along with the CHAP+ lytic enzyme for expression in our bacteriophage system. To confer cidality to lysogenic bacteriophages, we expressed these lytic proteins fused to an ompA secretion signaling peptide in an M13 phage infecting *E. coli* EMG2 K12. To further increase bacterial killing, we then combined the activity of these proteins with the innate lytic activity of a T7 bacteriophage (Figure 3-1). Through this work, we demonstrate that overexpression of broad-spectrum lytic agents increases the efficacy of bacterial killing, prevents bacterial resistance to bacteriophages and enables the long-term suppression of bacterial cultures for at least 40 hours.

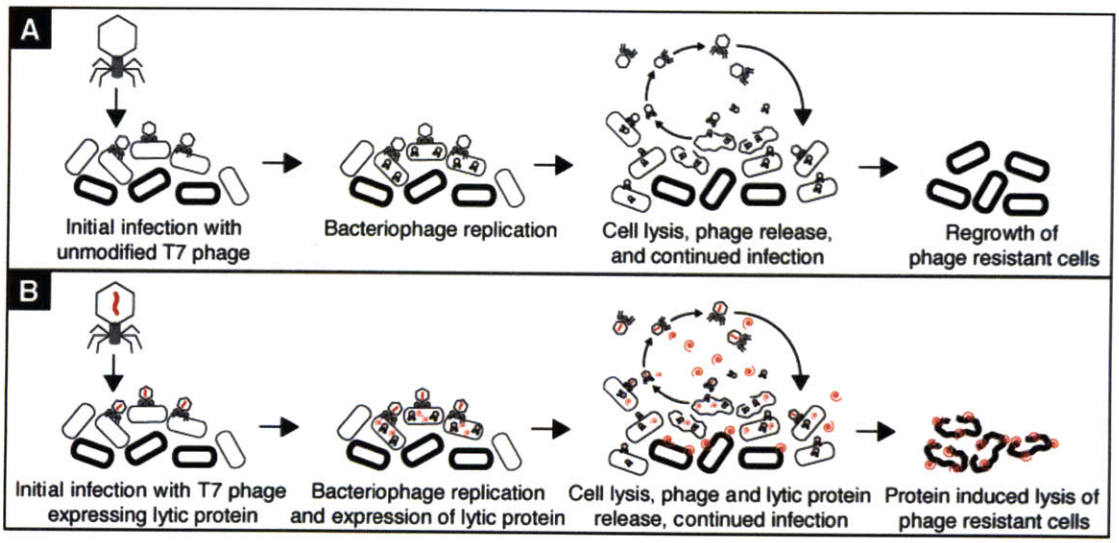

Figure 3-1: Engineered bacteriophages expressing lytic proteins. Upon initial infection, bacteriophages multiply and express lytic agents in the bacterial host. New phages progeny and lytic agents are released upon cell lysis. The phage system then enters a continued infection cycle leading to the complete eradication of the bacterial culture where phage resistant bacteria are suppressed by lytic agents.

3.3. Materials and Methods

3.3.1. Synthesis of Cationic Antimicrobial Peptides

All antimicrobial peptides were synthesized by Fmoc (fluorenylmethoxycarbonyl) chemistry on an Intavis Multipep Synthesizer (Intavis LLC, San Marcos, CA) at the Massachusetts Institute of Technology's Biopolymers Lab core facility. Mass spectrometry was routinely used to confirm the accuracy of the synthesis and typical purities obtained with the synthesizer were >85%.

3.3.2. Bacteriostatic of Antimicrobial Peptides

The Minimum Inhibitory Concentration (MIC) was measured using a standard assay based on the NCCLS M26A and the Hancock assay for cationic peptides (*50*). Serial two-fold dilutions of peptides were performed, starting with a base concentration ten times higher than the highest assay concentration, i.e. at 2560μg/ml in 0.2% Bovine Serum Albumin and 0.01% Acetic acid. *E. coli* and *S. aureus* were grown in Mueller Hinton Broth (Becton-Dickinson, Franklin Lakes, NJ) to an OD_{600} = 0.1 – 0.3 and diluted down to ~5 x10^5 CFU/ml in fresh MHB. Ten μL of the peptide dilutions were incubated with 90 μL of the target in a 96-well plate (Corning Life Sciences, Lowell, MA) for 16-20 hrs. The MIC was defined as the minimum concentration that prevented growth based on OD_{600}.

3.3.3. Bacteriocidality of antimicrobial peptides

E. coli and *S. aureus* were inoculated from a -80ºC culture the day before the assay, into 3ml LB plus any appropriate antibiotic, in a 14ml Falcon snap-cap tube (BD Biosciences), incubated overnight, shaking at 300rpm and 37ºC. On the day of the assay the overnight stationary phase culture is diluted 1:5000 into 50ml LB + any appropriate antibiotic in a 250ml Erlenmeyer flask, shaking at 300rpm at 37ºC. The culture is monitored by taking samples and measuring the absorption of the culture at 600nm to determine the optical density (OD_{600}). The culture is grown until it reaches an OD_{600}=0.2—0.4, but preferably 0.3. A 96-well plate (Corning) is loaded with 180μL of the bacterial culture and 20μL of AmP

stock solution to yield a final concentration of 192μg/ml or 640μg/ml. The plate is sampled every 5 minutes using an automated 96-well optical assay plate reader (Bio-Tek, Winooski, VT) capable of reaching and maintaining a temperature of 37ºC and orbital shaking between reads.

3.3.4. Construction of Recombinant M13 Expressing Antimicrobial Peptides and Polypeptides

To construct recombinant M13 expression AmPs, we used M13mp18 as a backbone (Novagen / EMD Biosciences, Gibbstown, NJ) as a starting point. Ponericin W5 was built by combining two long DNA oligomers and amplifying them via PCR to form the initial template for cloning 5'-AGTAAACATATGTTTTGGGGCGCGCTGATTAAAG-3'and 5'-ATCGAGGATCCTTACTGTTTTTTTTTTTTAAACAGGCCCACCACG-3'. The resulting fragment is cloned between the *Kpn I* and *Hind III* cut sites of M13mp18, yielding phage M13mp18.PonW5. In order to facilitate export into the extracellular space, an ompA-signal peptide sequence was attached via PCR-elongation of the initial amplicon of PonW3 using primers 5'-GGTACCATGTTTTGGGGCGC-3' and 5'-AAGCTTTTACTGTTTTTTTTTAAACAGGCCCACCACGCTC-3'. Again the construct is ligated into M13mp18 between the *Kpn I* and *Hind III* cut sites, yielding phage M13mp18.ompA.PonW5. Similarly, the CHAP+ fragment was initially amplified from phage K gDNA using 5'-CATATGATGAAAAAGACAGCTATCGCGATTGCAGTGGCACTGGCTGGTTTCGCTACCGTAGCGCAGGCC-3' and 5'-ATCGACCTAGG-3'. An ompA–signal peptide was added using primers 5'-GCAGCTTTCGAACTATGCTTTTACAGGTATTTCAATGA-3' and 5'-GCAGCTGGTACCATGGCTAAGACTCAAGCAGAAATA-3' and the resulting amplicon inserted into M13mp18 between *Kpn I* and *Hind III* for phage M13mp18.ompA.CHAP+. The two phages containing the signal peptide were transformed into *E. coli* XL-10.

3.3.5. Construction of Recombinant T7 Expressing Antimicrobial Peptides and Polypeptides

Engineered T7 bacteriophages were created starting from the T7SELECT415-1 phage display system (Novagen / EMD Biosciences, Gibbstown, NJ) and using standard molecular biology techniques (*51*). We designed the T7SELECT phage to express the inserted antimicrobial products intracellular, instead of on the surface as is intended through the SELECT system. The AmP ponericin W5 (PonW5) was built by combining two DNA oligomers and amplifying them via PCR to form the initial template for inserting into the T7-shuttle vector pET9a; 5'-AGTAAACATATGGGCATTTGGGGCACCCTGGCGAAA-3'and 5'-ATCGAGGATCCTTACTGTTTTTTTTTTTTCAGCATGCTAATCACG-3'. The amplicon is inserted into pET9a via Nde I and Bam HI cut sites, forming pET9a-PonW5. To amplify CHAP+ from phage K gDNA and insert it into pET9a, the following primers were used 5'-AGTAAACATATGGCTAAGACTCAAGCAGAAATA-3' and 5'-TAGCTGGATCCCTATGCTTTTACAGGTATTTCAATGA-3', yielding pET9a-CHAP+. The shuttle vectors are then amplified with two primers to yield compatible insertion ends for ligation into the T7 arms; 5'-TACTCGAATTCTTAAGTAACTAACGAAATTAATACGACTC-3' and 5'-AAATATAAGCTTCGGGCTTTGTTAGCAGCC-3'. The constructs are ligated to the T7 arms using *Eco RI* and *Hind III* restriction cut sites, yielding T7.PonW5 and T7.CHAP+, respectively.

All amplicons CDS were therefore placed under the control of the strong T7 φ10 promoter downstream of the T7select415-1b 10B capsid gene and stop codons in all reading frames to create T7.PonW5 and T7.CHAP+ precursors. Packaging of the recombinant genome was achieved with the T7SELECT packaging extracts using the manufacturers recommended protocol, with the modification of only using 0.5μL of the packaging extract. The control phage, T7control-precursor, was generated previously (*38*). All bacteriophage constructs in their packaging were allowed to infect a mid-log culture of BL21 for amplification.

3.3.6. Preparation of Infective Bacteriophage Solution

Bacteriophages were amplified in a re-diluted overnight culture of *E. coli* XL-10 in the case of M13mp18-based phages or BL21 in the case of T7415-1b-based phages. The culture was grown until it reached mid-log phage at approximately an OD_{600}=0.3, at which point 10^4 – 10^6 PFU/ml of the respective phage was added. Following clearing or lysis of the culture, the culture was centrifuged for 5 min at 16,100g. The supernatant was collected and filtered through a 0.2μm filter for sterilization. The infective phage solutions were tittered through the standard plaque assay described earlier. All phage solutions were normalized to a concentration of 10^9PFU/ml via dilution into LB media. Before treatment, the T7 bacteriophages were amplified on E. coli BL21 and purified.

3.3.7. Bacteriophage Plaque Assay

The appropriate host strain is inoculated in LB medium and incubates shaking at 37°C and 300rpm until an OD600 = 1.0 is reached. A sufficient volume of top agarose (0.5%) to provide 5 ml for each dilution being plated is melted in a heat block or microwave. The molten agarose is transferred to a 45–50°C water bath and allowed to adjust temperature. A dilution series is conducted using an initial 1:100 dilution of 10μL of sample to 990μL of medium. Serial dilutions were performed by adding 20μL first to 1:100 dilution to 180μL medium. For plating 100μL of the respective dilutions of the phage are combined with 300 μL of overnight *E. coli* BL21 culture and 4–5 ml of 50°C LB top agar [0.7% (wt/vol) agar]. This solution was mixed thoroughly, poured onto LB agar plates, inverted after hardening, and incubated for 4–6 h at 37°C until plaques were clearly visible. In the case of M13mp18, modifications to the protocol were made. in order to facilitate blue/white screening based on lacy activation/inactivation, XL-10 cells were mixed in with 3 ml top agar, 1mM IPTG, and 40μL of 20 mg/ml X-Gal, and poured onto LB agar containing chloramphenicol (30μg/ml). After overnight incubation at 37 °C, plaques were counted.

3.3.8. Bacteriophage Lytic Assay

The host strain to be assayed is inoculated from a -80ºC culture the day before the assay, into 3ml LB plus any appropriate antibiotic, in a 14ml Falcon snap-cap tube (BD Biosciences), incubated over night shaking at 300rpm and 37ºC. On the day of the assay the overnight stationary phase culture is diluted 1:5000 into 50ml LB + any appropriate antibiotic in a 250ml Erlenmeyer flask, shaking at 300rpm at 37ºC. The culture is monitored by the measuring the absorption of the culture at 600nm to determine the optical density (OD_{600}). The culture is grown until it reaches an OD_{600}=0.2—0.4, but preferably 0.3. A 96-well plate (Corning) is loaded with 180µL of the bacterial culture and the appropriate amount of bactericidal agents. The plate is sampled every 5 minutes using an automated 96-well optical assay plate reader (Bio-Tek, Winooski, VT) capable of reaching and maintaining a temperature of 37ºC and orbital shaking between reads.

3.4. In vitro bactericidal activity of lytic proteins

To determine optimal lytic protein candidates to express from bacteriophage, we measured the minimal inhibitory concentrations (MICs) of natural AmPs against 10^5 CFU/ml of *Escherichia coli* (ATCC 25922) and/or *Staphylococcus aureus* (ATCC 25923) in accordance to standard MIC determination protocols (*49*). A panel of five AmPs with strong MICs was assembled and tested for hemolytic activity against human red blood cells as a measure of toxicity (Table 3-1). Since MICs do not necessarily correlate with lytic activity, we determined the bactericidal activity of these AmPs against log-phase bacterial cultures with optical-density-based killing assays over time (Figure 3-2). We found that there was little correlation between MICs and killing behavior (Figure 3-2). For example, Dhvar5 delayed growth but did not demonstrate significant bactericidal or bacteriostatic activity against *E. coli* or *S. aureus*. Though Hyphancin IIIE has a very low MIC against *E. coli*, it only exhibited significant bactericidal activity at very high concentrations. Moronecidin showed bacteriostatic activity against both *E. coli* and *S. aureus* at low and high concentrations. Finally, both Ponericin W3 and Ponericin W5 (Figure 3-2E and

F) showed strong bactericidal behavior for *E. coli* and *S. aureus*. We observed a rapid drop in OD upon treatment with high concentrations of Ponericin W3 and Ponericin W5, which was indicative of cell lysis and also observed no cell regrowth up to at least 10 hours after treatment.

Table 3-1: Minimum Inhibitory Concentration (MIC) of selected panel of AmPs measured against E. coli and S. aureus. HC_{50} denotes the 50% hemolytic concentration indicative of the peptide's toxicity.

AmP Name	Amino Acid Sequence	MIC (μg/ml)		HC_{50}
		E. coli	*S. aureus*	(μg/ml)
Dhvar5	LLLFLLKKRKKRKY	32	16	512
Hyphancin IIIE	RWKFFKKIERVGQNVRDGLIKAGPAIQVLGAAKAL	2	256	256
Moronecidin	FFHHIFRGIVHVGKTIHKLVTG	32	64	256
Ponericin W3	GIWGTLAKIGIKAVPRVISMLKKKKQ	16	8	64
Ponericin W5	FWGALIKGAAKLIPSVVGLFKKKQ	64	4	32

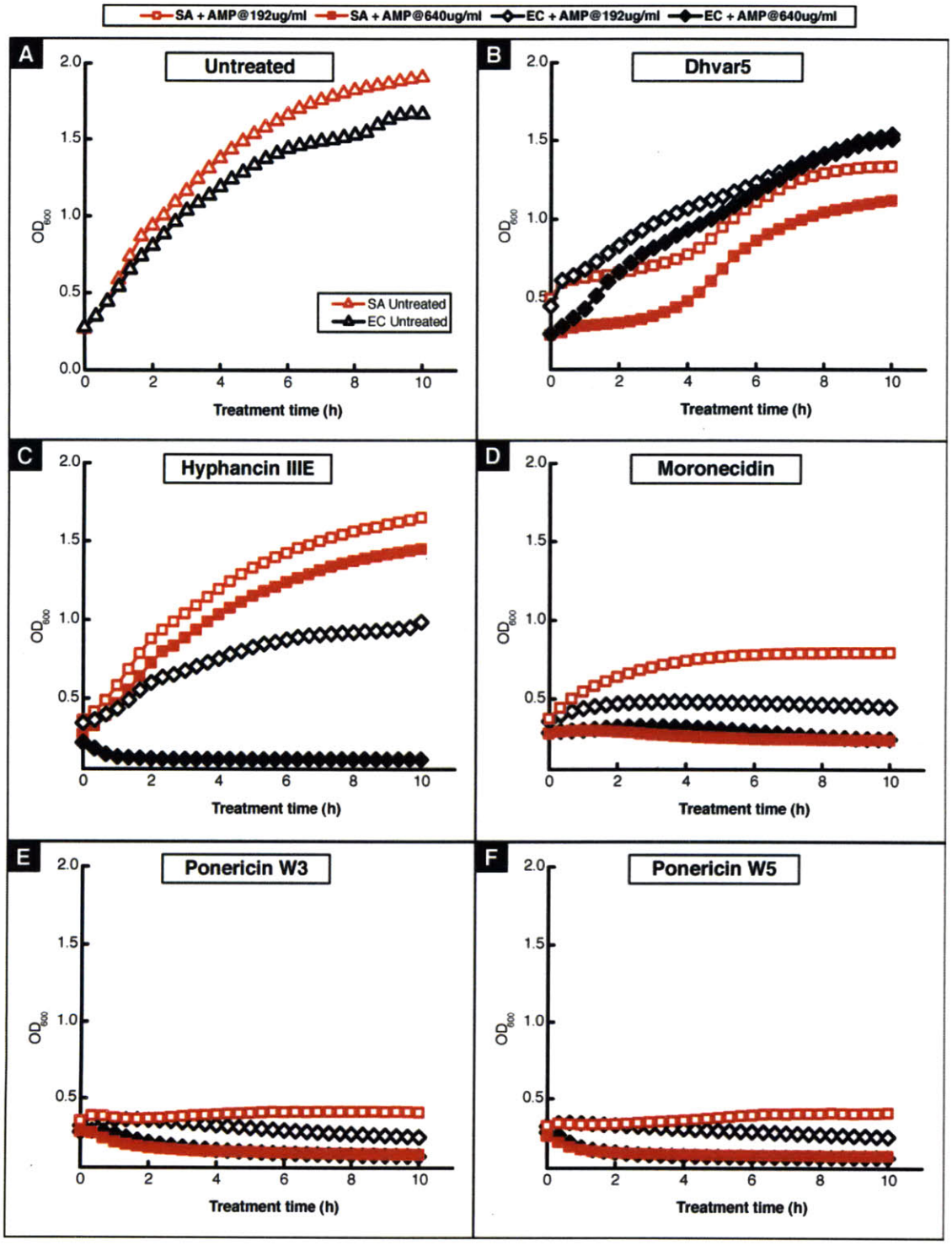

Figure 3-2: In vitro bactericidal activity of selected AmPs was measured against E. coli (EC) and S. aureus (SA) at an intermediate concentration of 192μg/ml and a high concentration 640ug/ml and compared to (A) the growth profile for the untreated culture. All experiments were carried out in

duplicates and the averaged OD, which was within standard error, is reported. (B) Dhvar5 is inefficient at killing the cultures and only slightly delays the growth of E. coli and S. aureus. (C) Hyphancin IIIE induces strong killing of E. coli at high concentration but shows no effect on S. aureus. (D) Moronecidin has bacteriostatic activity against both E. coli and S. aureus and the magnitude of the effect is concentration dependent. (E-F) Ponericin W3 and Ponericin W5 induce growth arrest for both E. coli and S. aureus at the intermediate concentration with slight decrease of OD towards the end of the 10-hour treatment period. At high concentrations, the peptides induce strong killing and no re-growth.

3.5. Engineered lysogenic bacteriophage expressing antimicrobial agents

Since Ponericin W3 and Ponericin W5 had strong bactericidal efficacies, low MICs, and minimal bacterial regrowth, we selected them as candidates for expression in our engineered bacteriophage platform. In addition, we chose to express CHAP+, a lytic protein derived from the first 165 amino acids of the LysK lysin of *Staphylococcus* phage K.

We engineered lysogenic M13mp18 phages to overexpress Ponericin W3, Ponericin W5, and CHAP+. Because M13 phages are non-lytic, we fused an OmpA-derived signal peptide (*52-54*) to the amino end of the antimicrobial agents to target the translated precursor for secretion. Upon secretion of the precursor, the OmpA signal sequence is cleaved, leaving the attached protein in its natural unmodified state in the bacterial periplasm (*55*). The gene coding for the expression of these antimicrobial agents was placed under the regulation of the synthetic $P_L$tetO promoter (*56*) followed by a synthetic ribosome-biding-sequence. The $P_L$tetO promoter is inducible in the presence of the TetR repressor, and is, thus, constitutively expressed in EMG2 cells that lack TetR.

To test the antimicrobial activity of our phages, we performed killing assays with engineered phage against *E. coli* wild-type EMG2 cells (Figure 3-3:). We calculated viable cell counts by counting colony-forming units (CFU) during treatment with no phage or with 10^8 plaque-forming-units/ml

(PFU/ml) of phage. Figure 3-3: demonstrates that cells infected with engineered phage expressing Ponericin W3 (M13.ompA.PonW3) eventually regrew by 6 hours after infection to levels similar to that of cells infected with control phage (M13.Unmodified). In contrast, cells that were infected with engineered phage expressing CHAP+ (M13.ompA.CHAP+) demonstrated a strong and long-term bactericidal effect starting at 2 hours. M13.ompA.CHAP+ exhibited a 10,000-fold increase in bacterial killing compared to control phage (M13.Unmodified) with no bacterial regrowth up to 20 hours.

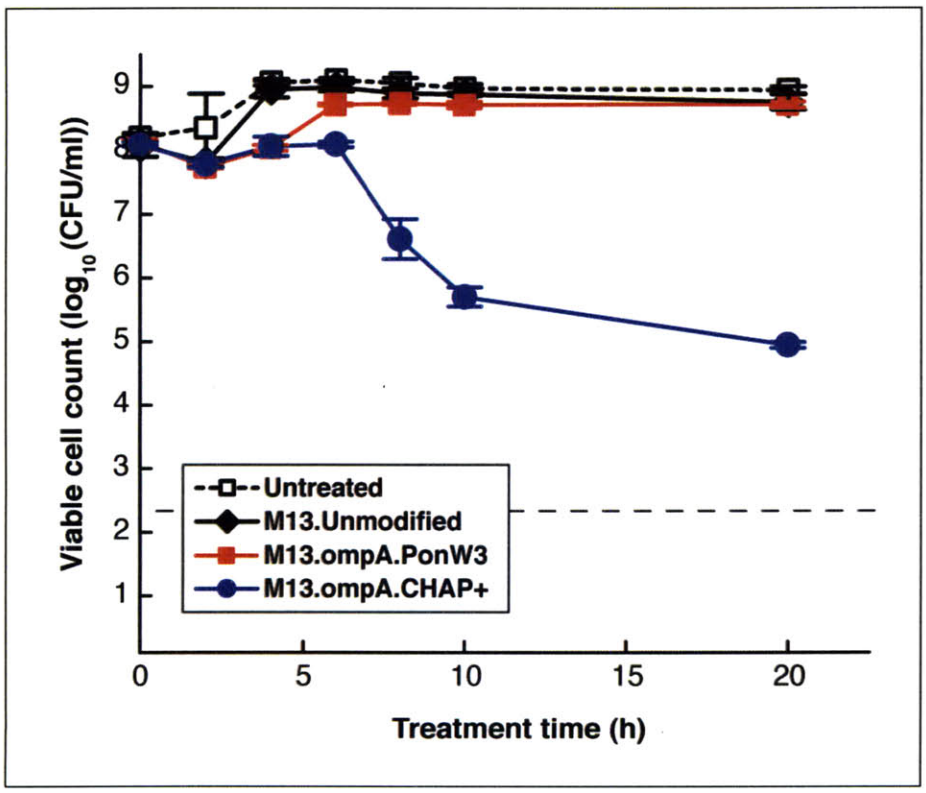

Figure 3-3: Viability and time course treatment of E. coli EMG2 cultures with 10^8 PFU/ml of unmodified M13 phage or engineered phage expressing Ponericin W3 or CHAP+. Treatment with phage expressing CHAP+ resulted in a long-term decrease in viable cell counts by 10,000-fold compared to treatment with the unmodified M13 phage. All experiments were carried in triplicates with the standard error shown. The horizontal dotted line denotes the detection limit of our viable cell count assay.

3.6. Engineered lytic bacteriophage expressing antimicrobial agents

Although we demonstrated that lysogenic bacteriophage that express antimicrobial agents can indeed increase bactericidal activity and suppress cultures, we sought to combine the bactericidal activity of lytic phage with antimicrobial agents to obtain even better bacterial killing. To do so, we cloned antimicrobial peptides under the control of the strong T7 promoter into T7 bacteriophage. Since lytic phage break open their host cells using their own native lysozymes, we chose to omit the ompA signal sequence from the expression cassettes inserted into our engineered lytic bacteriophage (*57, 58*).

Initial optical-density-based killing studies showed that at least 10^4 PFU/ml of engineered phage expressing CHAP+ (T7.CHAP+) suppressed bacterial regrowth for at least 14 hours. Thus, we tested control phage (T7.Unmodified), engineered phage expressing Ponericin W5 (T7.PonW5), and engineered phage expressing CHAP+ (T7.CHAP+) at varying phage concentrations from 10^4 PFU/ml to 10^8 PFU/ml against *E. coli* BL21 cells up to 40 hours. We found that the control phage was able to rapidly kill *E. coli* populations but allowed bacterial regrowth to occur starting at about 10 hours, indicating the presence of phage-resistant populations. In contrast, we determined that T7.PonW5 at 10^8 PFU/ml was sufficient to suppress bacterial cultures up to 40 hours while it was unable to prevent regrowth at 10^6 PFU/ml or 10^4 PFU/ml. This threshold effect suggests that there are important dynamics involving AmP production, phage replication, bacterial growth, and evolution of phage resistance that determine whether a substantial phage-resistant population can develop. In comparison, T7.CHAP+ showed significant long-term bactericidal efficacy against *E. coli* at concentrations ranging from 10^4 PFU/ml to 10^8 PFU/ml up to 40 hours.

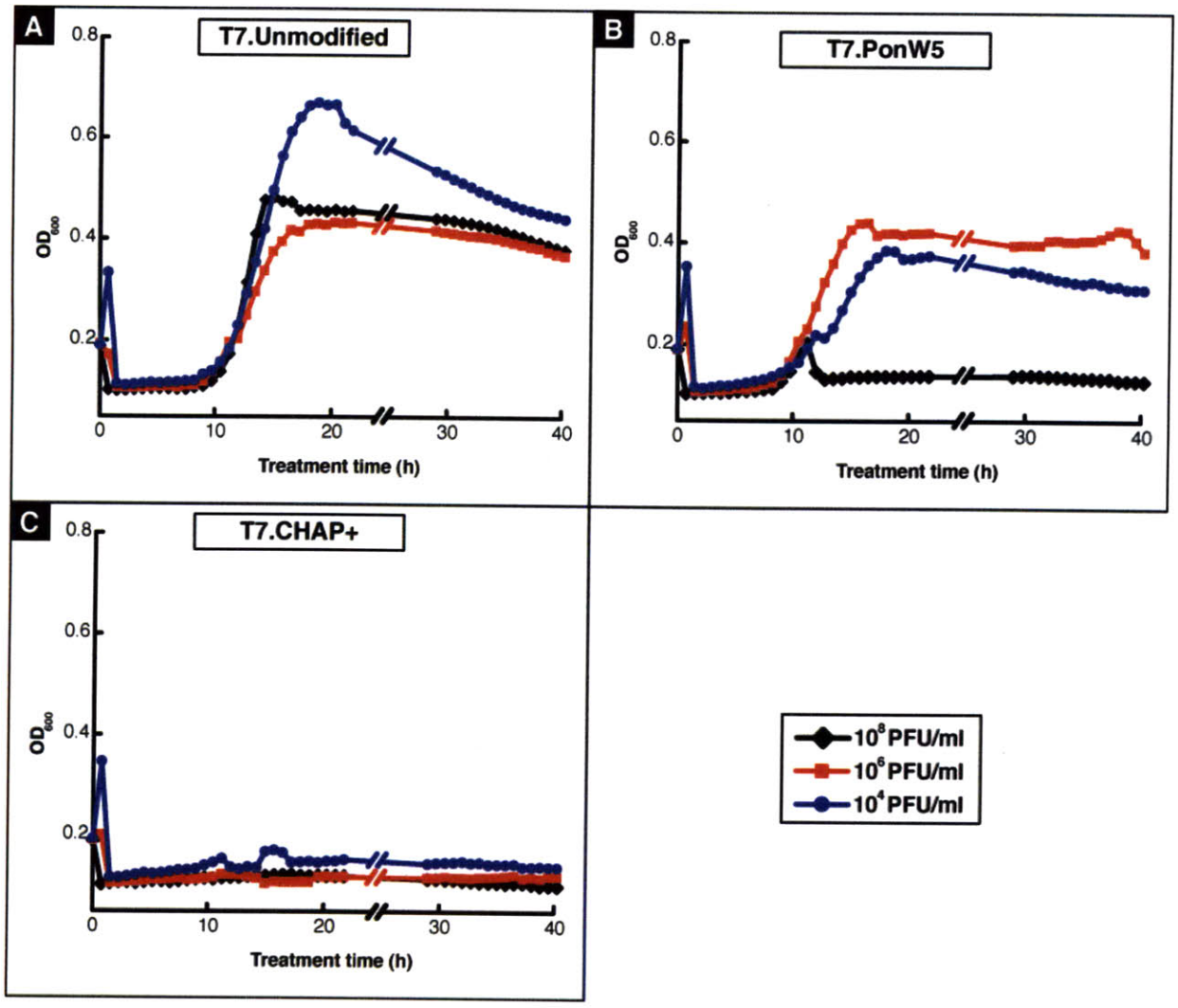

Figure 3-4: Optical density and time course treatment of an E. coli BL21 culture with unmodified T7 phage and engineered T7 phage expressing Ponericin W5 and CHAP+ with an initial phage count of 10^8, 10^6, and 10^4 PFU/ml. (A) Treatment with unmodified T7 phage results in a rapid drop in optical density resulting from the natural lytic action of the bacteriophage. However, after 10 hours of treatment the culture is able to regrow due to bacterial resistance to T7 regardless of the initial phage concentration. (B) Treatment with T7 phage expressing Ponericin W5 is able to overcome the cell regrowth for initial phage counts at 10^8 PFU/ml or above. (C) Treatment with T7 phage expressing CHAP+ completely suppresses regrowth of resistant cells starting at phage counts of 10^4 PFU/ml or above thereby resulting in long-term suppression of the bacterial culture.

To confirm the accuracy of the optical-density-based killing assays, we obtained viable cell counts of treated cultures (Figure 3-5:). In Figure 3-5:, 10^4 PFU/ml of phage was applied to bacterial cultures that were sampled every 12 hours. T7.Unmodified and T7.PonW5 showed a decrease in viable cell counts between 12 and 24 hours that were not statistically significant from each other. These results are consistent with the optical-density-based assay which showed bacterial regrowth occurred at about 10 hours for both T7.Unmodified and T7.PonW5 when 10^4 PFU/ml phage were applied. In contrast, we found that T7.CHAP+ reduced viable cell counts to our detection limit without any significant regrowth up to 36 hours. We also diluted T7.CHAP+ treated cultures into fresh media at a ratio of 1:1000 at each time point and determined that none of the sub-dilutions showed re-growth, a result that is consistent with sterilization or near-sterilization of the treated cultures.

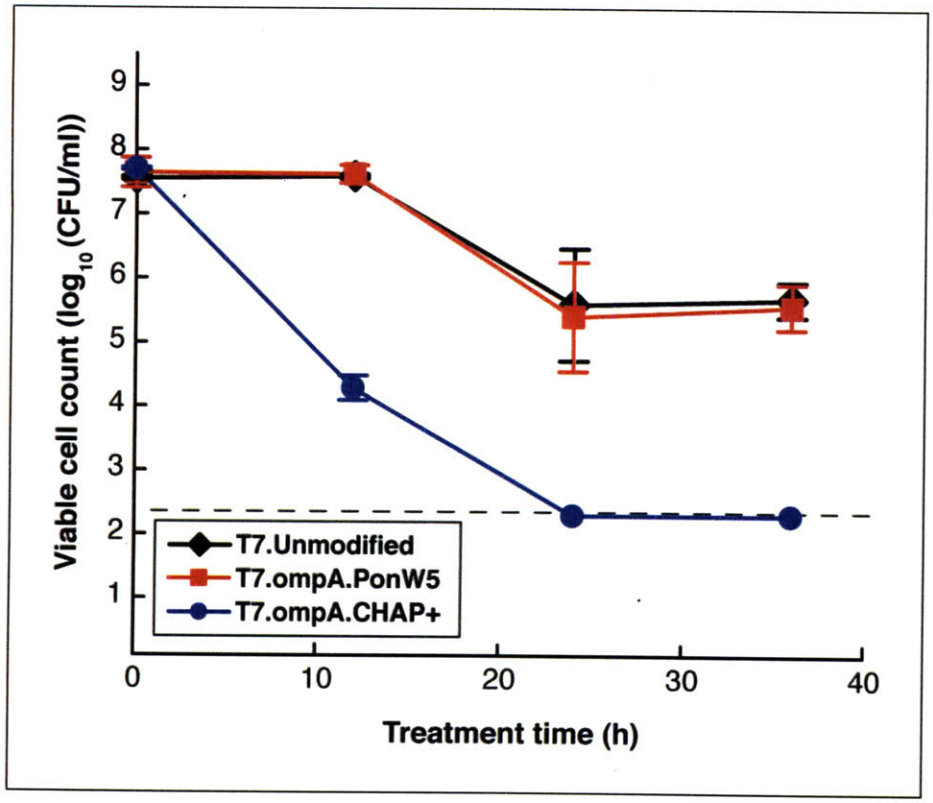

Figure 3-5: Viability and time course treatment of E. coli BL21 cultures with 10^4 PFU/ml of unmodified T7 phage or phage expressing Ponericin W5 or CHAP+. Treatment with phage expressing CHAP+ resulted in a long-term decrease in viable cell counts by 10,000-fold compared to treatment with the unmodified T7 phage, resulting in a viable cell count below our assay detection limit of 200 CFU/ml. All experiments were carried out in triplicates with the standard error shown. The horizontal dotted line denotes the detection limit of our viable cell count assay.

3.7. Expression of other lethal proteins from bacteriophages

In this work, we demonstrated that the expression of lytic proteins confers long-term cidality to lysogenic bacteriophages and suppresses bacterial culture and regrowth caused by phage resistance in the case of lytic bacteriophages. We demonstrated our approach with two classes of lytic proteins, phage-based lysins and antimicrobial peptides. We selected the optimized antimicrobial enzyme CHAP+ derived

from the phage K lysin and the antimicrobial peptides, Ponericin W3 and Ponericin W5, based on their low *in vitro* MIC values and bactericidal activities.

For expression in the M13 lysogenic phage model, an *ompA* signaling sequence was fused to the antimicrobial agents. This sequence allows for extracellular export and release of expressed protein, which was necessary since M13 does not induce cell lysis. We found that while Ponericin W3 has a low MIC value and strong cidal properties, its expression from the M13 phage vector only resulted in a moderate lytic effect upon infection. Though we observed a decrease in viability at 4 hours post treatment, the culture eventually regrew to untreated levels at 6 hours. These results are similar to those reported by previous authors who have delivered lethal genes in lysogenic bacteriophages. Hagens (*59*) observed regrowth starting at 3 hours for recombinant M13 phage expressing holins and for phages encoding restriction enzymes. Westwater (*60*) observed increased viable cell counts beginning at 4 hours for M13 phagemids expressing toxins. Both authors infected *E. coli* ER2738, a strain engineered to maintain the F-plasmid that is required for M13 infection. Loss of the F-plasmid is one of the primary modes of resistance to M13 bacteriophages (*61*). We, on the other hand, used a more challenging bacterial target and benchmarked our activity measurements against a wild-type strain of *E. coli* EMG2 K12, which has the ability to lose the F-plasmid. Expression of CHAP+ from M13 bacteriophages led to the long-term suppression of cellular viability, by 6,000-fold over 20 hours compared to treatment with unmodified M13 phage. The strong cidal activity and lack of bacterial regrowth in our engineered phage are key improvements over previously published M13 phages expressing lethal agents. While the M13 phage expressing CHAP+ did not completely sterilize the culture, the significant decrease in bacterial cell counts could be sufficient to allow the immune system to counteract the infection if applied in a therapeutic setting (*42*).

Expression of lytic agents in T7 did not require the *ompA* signaling sequence for release since T7 naturally lyses its host as part of its normal lifecycle. We demonstrated that expression of the CHAP+ lytic

protein increased the bacterial killing efficacy of T7 bacteriophages by 10,000-fold and completely suppresses bacterial resistance to phages.

3.8. Possible expansion to target other pathogens

While our proof-of-concept bacteriophages target *E. coli*, we believe our approach could be extended to different lytic agents expressed from the multitude of phages already isolated to target other relevant bacterial pathogens (*62, 63*). For example, 60% of MRSA infections today are resistant to all but one antibiotic, vancomycin (*64*). Already, cases of high-level resistance to vancomycin are being reported worldwide (*65*) raising concerns that if these were to spread as MRSA did, death rates would increase to those in the pre-antibiotic era and wipe out many of the health benefits of the last century (*14, 66*). Human clinical trials using bacteriophages are currently ongoing in Belgium to address multi-drug-resistant *S. aureus* as well as *P. aeruginosa* infections (*36*). The difficulty in treating *P. aeruginosa* results from it high-level resistance to antibiotics and its ability to form protective biofilms. *Legionella pneumophila* also shares these characteristics, making them difficult to eradicate. As a result these two pathogens are common causes of infections but are also present in industrial settings such as HVAC systems in hospitals (*67, 68*). Current methods of treating industrial HVAC systems and hospital surfaces have been less than successful (*69-72*). However, the increasing interest in alternative antimicrobial strategies led to the first report of bacteriophages infecting *Legionella* (*73*), while *Pseudomonas* phages are now becoming utilized for these purposes (*74*). Thus, our ability to increase the bacterial killing efficacy of engineered phage extends far beyond medical settings into the decontamination of industrial, agricultural and food processing settings as well (*75-84*).

3.9. Addressing the concerns of both bacteriophage and AmP-based therapy

The approach presented here is novel in that it combines and addresses concerns associated with both phage therapy, namely the evolution of resistance to phage, as well as protein-based antimicrobial therapy, namely delivery issues to the site of infection. Phage resistance can occur in many ways as

bacteria have developed different mechanisms to counteract each step of the phage lifecycle. These mechanisms involve blocking phage adsorption and injection, preventing early and late replication including suppression of the host transcriptional machinery, and inhibiting packaging and escape from the bacterial host that can occur via lysis or continuous extrusion (*85*). Our approach prevents bacteria from evolving phage resistance not by combating individual phage resistance mechanism but by optimizing the lethality of bacteriophages through the expression of extracellular lytic factors. The antimicrobial agents expressed and released during infection target adjacent bacteria that may have otherwise escaped the initial phage infections and evolved resistance.

Traditional AmP- or protein-based antimicrobial therapies also suffer difficulties of their own. For example, these proteins are subject to protease degradation *in vivo*, they may elicit immune reactions and their systemic toxicities at the active concentrations are not well understood. As a result, the *in vivo* delivery of synthesized AmPs and proteins can be challenging. However, our approach to deliver genes encoding and exporting these proteins circumvents many of these problems. We achieve the effects of combination treatments without the need to produce, purify and deliver antimicrobials and the bacteriophages separately. The actual antimicrobial agents are produced and released directly at the sites of infection by virtue of the targeting and multiplication of bacteriophages without requiring high systemic concentrations.

3.10. Limitations of the approach

3.10.1. Production of antimicrobials vs. phage-induced cell lysis

However, the approach presented in this work has some limitations. We rely on the cell's ability to produce antimicrobial agents before the cell is killed. There is thus a competition between the production of antimicrobials from the cell and its killing, especially in the case of lytic phages. It would thus be of interest to model and compare the kinetics of cell growth, antimicrobial production and phage replication and lysis. One approach to optimize the efficacy of our engineered phage would be to alter the

kinetics of the phage lifecycle such as by increasing the phage replication time or delaying lysis. Slower lytic kinetics can be achieved through mutations in the phage holing (*86, 87*) or deletion of the lysin gene and mutations in the transglycosylase domain of the entry protein (*57, 88*). This optimized system would produce more antimicrobial agents prior to cell lysis and may be able to treat heterogonous cultures where the antimicrobials agents suppress the growth of a strain of bacteria that is not affected by the phage. Other future improvements could include any number of combinations of antimicrobial agents, factors targeting intracellular processes (*39*), agents secreted extracellularly such as biofilm degrading enzymes (*38*) or cell wall degrading enzymes (*89-91*).

3.10.2. Specificity of bacteriophages

The high specificity of bacteriophages also limits the spectrum of the technology. Rather than looking to supplant antibiotics, phage therapy should be used to enhance the effect of broad-spectrum antibiotics. Our ability to suppress the regrowth of a bacteria culture for over 40 hours suggests the potential that combining these phages with broad-spectrum antibiotics could have significant benefit for treating clinical infections. The antibiotic would target the potentially broad heterogeneous bacterial population while our engineered phage would effectively eradicate the resistant population. Despite their potential benefits, phage have yet to be accepted into clinical practice because of a number of other issues, such as phage immunogenicity, efficacy, target bacteria identification and phage selection, host specificity, and toxin release (*59, 92, 93*). To reduce the risk of leaving lysogenic particles in patients after treatment, our adjuvant phage could be modified to be non-replicative (*93*). We do also recognize that real-world usage may necessitate the use of phage cocktails to ensure efficacy. The prospect for such combination treatment appear positive as the FDA is currently establishing new and faster development pathways specifically for drug cocktails (*94*).

There also exists other ways to address the concern of phage specificity that do not rely on combination treatments. Phage specificity results from the interaction between their tail fibers and their recognized receptor domains on the surface of bacterial cells (*95, 96*). While phages are able to infect

closely related sub-species of bacteria, they are rarely able to infect bacteria from different strains (*97*). Recent work has, however, shown that this specificity is an artifact of historical isolation procedures, which selects for the greatest burst size and infectivity within one bacteria species (*98*). It is feasible to alter the isolation protocols to select for broad-host-range bacteriophages capable of infecting multiple bacterial host species (*99*). The isolation of broad-spectrum bacteriophages with only minor alterations in isolation protocols makes the use of single bacteriophages in anti-infective settings more feasible.

3.11. Chapter conclusion

In conclusion, the rise of antibiotic resistance has led to a regained interest in phage therapy. However, the ability of bacteria to develop resistance to bacteriophages has been a major concern and hurdle to the adoption of phage therapy. By overexpressing lytic antimicrobial proteins, we suppressed bacterial resistance to phages and significantly increased the cidal activity of lytic and lysogenic phages. In addition to prior designs (*38, 59, 60, 100*), this work demonstrates the potential for engineering platforms that confer new functionalities to phages that enable them to eradicate difficult-to-treat bacterial infections in clinical, environmental and industrial settings.

3.12. References

1. Klevens, R.M., et al., Estimating health care-associated infections and deaths in U.S. hospitals, 2002, in Public Health Rep. 2007. p. 160-6.

2. Anderson, R.N., Deaths: Leading Causes for 2000, in National Vital Statistics Reports. 2002. p. 1-8.

3. Wenzel, R.P. and M.B. Edmond, The Impact of Hospital-Acquired Bloodstream Infections, in Emerging Infectious Diseases. 2001. p. 174-177.

4. Taubes, G., *The Bacteria Fight Back*, in *Science*. 2008. p. 356-361.

5. Schmid, M.B., Do targets limit antibiotic discovery?, in Nat Biotechnol. 2006. p. 419-20.

6. Zasloff, M., Antimicrobial peptides of multicellular organisms, in Nature. 2002. p. 389-95.

7. Giangaspero, A., L. Sandri, and A. Tossi, *Amphipathic alpha helical antimicrobial peptides*, in *Eur J Biochem*. 2001. p. 5589-600.

8. Boman, H.G., Antibacterial peptides basic facts and emerging concepts, in Jounral of Internal Medicine. 2003. p. 197-215.

9. Cegelski, L., et al., *The biology and future prospects of antivirulence therapies.* Nat Rev Microbiol, 2008. **6**(1): p. 17-27.

10. Keller, L. and M.G. Surette, *Communication in bacteria: an ecological and evolutionary perspective.* Nat Rev Microbiol, 2006. **4**(4): p. 249-58.

11. Veiga-Crespo, P., et al., Enzybiotics: a look to the future, recalling the past, in J Pharm Sci. 2007. p. 1917-24.

12. Young, R. and U. Bläsi, Holins: form and function in bacteriophage lysis, in FEMS Microbiol Rev. 1995. p. 191-205.

13. Matsuzaki, S., et al., Bacteriophage therapy: a revitalized therapy against bacterial infectious diseases, in J Infect Chemother. 2005. p. 211-219.

14. Horgan, M., et al., Phage Lysin LysK Can Be Truncated to Its CHAP Domain and Retain Lytic Activity against Live Antibiotic-Resistant Staphylococci, in Applied and Environmental Microbiology. 2009. p. 872-874.

15. Fischetti, V.A., Bacteriophage lytic enzymes: novel anti-infectives, in Trends Microbiol. 2005. p. 491-6.

16. Nilsson, J.B., et al., The effect of streptokinase neutralizing antibodies on fibrinolytic activity and reperfusion following streptokinase treatment in acute myocardial infarction, in J Intern Med. 2002. p. 405-11.

17. Squire, I.B., et al., Humoral and cellular immune responses up to 7.5 years after administration of streptokinase for acute myocardial infarction, in Eur Heart J. 1999. p. 1245-52.

18. Twort, F.W., An investigation on the nature of ultra-microscopic viruses. Lancet, 1915(2): p. 1241-3.

19. d'Herelle, F., *An invisible antagonist microbe of dysentery bacillus.* Comptes Rendus Hebdomadaires des Seances de L'academie des Sciences, 1917. (165): p. 373-5.

20. Deresinski, S., Bacteriophage Therapy: Exploiting Smaller Fleas. CLIN INFECT DIS, 2009.

21. Stone, R., *Bacteriophage therapy. Stalin's forgotten cure.* Science, 2002. **298**(5594): p. 728-31.

22. Merril, C.R., D. Scholl, and S.L. Adhya, *The prospect for bacteriophage therapy in Western medicine.* Nature reviews Drug discovery, 2003. **2**(6): p. 489-97.

23. Bruttin, A. and H. Brüssow, Human volunteers receiving Escherichia coli phage T4 orally: a safety test of phage therapy, in Antimicrob Agents Chemother. 2005. p. 2874-8.

24. Rhoads, D., et al., Bacteriophage therapy of venous leg ulcers in humans: results of a phase I safety trial., in J Wound Care JO -. 2009. p. 237-233 DO -.

25. Sulakvelidze, A., Z. Alavidze, and J.G. Morris, *Bacteriophage therapy*, in *Antimicrob Agents Chemother.* 2001. p. 649-59.

26. Sulakvelidze, A., Phage therapy: an attractive option for dealing with antibiotic-resistant bacterial infections., in Drug Discov Today JO -. 2005. p. 807-809 DO -.

27. Merabishvili, M., et al., Quality-controlled small-scale production of a well-defined bacteriophage cocktail for use in human clinical trials, in PLoS ONE. 2009. p. e4944.

28. Skurnik, M. and E. Strauch, *Phage therapy: facts and fiction.* Int J Med Microbiol, 2006. **296**(1): p. 5-14.

29. Lu and J.J. Collins, Dispersing biofilms with engineered enzymatic bacteriophage. Proc Natl Acad Sci USA, 2007.

30. Lu, T. and J. Collins, Engineered bacteriophage targeting gene networks as adjuvants for antibiotic therapy. Proc Natl Acad Sci USA, 2009.

31. Barry, A., et al., Methods of Determining Bactericidal Activity of Antimicrobial Agents; Approved Guideline, in Clinical and Laboratory Standards Institute. 1999. p. M26-A.

32. Lilly, A.A., J.M. Crane, and L.L. Randall, Export chaperone SecB uses one surface of interaction for diverse unfolded polypeptide ligands, in Protein Science. 2009. p. 1860-1868.

33. Xian, M., et al., Sorting signal of Escherichia coli OmpA is modified by oligo-(R)-3-hydroxybutyrate, in Biochim Biophys Acta. 2007. p. 2660-6.

34. Freudl, R., M. Klose, and U. Henning, Export and sorting of the Escherichia coli outer membrane protein OmpA., in J Bioenerg Biomembr. 1990. p. 441-9.

35. Takahara, M., et al., The ompA signal peptide directed secretion of Staphylococcal nuclease A by Escherichia coli, in J Biol Chem. 1985. p. 2670-4.

36. Lutz, R. and H. Bujard, Independent and tight regulation of transcriptional units in Escherichia coli via the LacR/O, the TetR/O and AraC/I 1-I 2 regulatory elements, in Nucleic acids research. 1997. p. 1203-1210.

37. Heineman, R.H., I.J. Molineux, and J.J. Bull, Evolutionary robustness of an optimal phenotype: re-evolution of lysis in a bacteriophage deleted for its lysin gene, in J Mol Evol. 2005. p. 181-91.

38. Inouye, M., N. Arnheim, and R. Sternglanz, Bacteriophage T7 lysozyme is an N-acetylmuramyl-L-alanine amidase, in J Biol Chem. 1973. p. 7247-52.

39. Hagens, S. and U. Bläsi, Genetically modified filamentous phage as bactericidal agents: a pilot study, in Lett Appl Microbiol. 2003. p. 318-23.

40. Westwater, C., et al., Use of genetically engineered phage to deliver antimicrobial agents to bacteria: an alternative therapy for treatment of bacterial infections, in Antimicrob Agents Chemother. 2003. p. 1301-7.

41. Burke, J.M., C.P. Novotny, and P. Fives-Taylor, Defective F pili and other characteristics of Flac and Hfr Escherichia coli mutants resistant to bacteriophage R17, in J Bacteriol. 1979. p. 525-31.

42. Mann, N.H., *The third age of phage.* Plos Biol, 2005. **3**(5): p. e182.

43. Breitbart, M., et al., *Genomic analysis of uncultured marine viral communities.* Proc Natl Acad Sci USA, 2002. **99**(22): p. 14250-5.

44. Lowy, F.D., Antimicrobial resistance: the example of Staphylococcus aureus, in Journal of Clinical Investigation. 2003. p. 1265-1273.

45. Hiramatsu, K., et al., Methicillin-resistant Staphylococcus aureus clinical strain with reduced vancomycin susceptibility, in J Antimicrob Chemother. 1997. p. 135-6.

46. *Staph Bacteria*. Science Blog. Vol. June 11. 1997: Rockefeller University.

47. Shnayerson, M. and M.J. Plotkin, The Killers Within: The Deadly Rise of Drug Resistant Bacteria. 2002.

48. Vinodkumar, C.S., S. Kalsurmath, and Y.F. Neelagund, Utility of lytic bacteriophage in the treatment of multidrug-resistant Pseudomonas aeruginosa septicemia in mice. Indian J Pathol Microbiol, 2008. **51**(3): p. 360-6.

49. Vinodkumar, C.S., Y.F. Neelagund, and S. Kalsurmath, Bacteriophage in the treatment of experimental septicemic mice from a clinical isolate of multidrug resistant Klebsiella pneumoniae. The Journal of communicable diseases, 2005. **37**(1): p. 18-29.

50. Makin, T., Legionella bacteria and water systems in health care premises. Nurs Times, 2005. **101**(39): p. 48-9.

51. Roig, J., M. Sabria, and M.L. Pedro-Botet, *Legionella spp.: community acquired and nosocomial infections.* Curr Opin Infect Dis, 2003. **16**(2): p. 145-51.

52. Atlas, R.M., Legionella: from environmental habitats to disease pathology, detection and control. Environ Microbiol, 1999. **1**(4): p. 283-93.

53. Lin, Y.S., et al., *Disinfection of water distribution systems for Legionella.* Semin Respir Infect, 1998. **13**(2): p. 147-59.

54. Lammertyn, E., et al., Evidence for the presence of Legionella bacteriophages in environmental water samples. Microb Ecol, 2008. **56**(1): p. 191-7.

55. Wright, A., et al., A controlled clinical trial of a therapeutic bacteriophage preparation in chronic otitis due to antibiotic-resistant Pseudomonas aeruginosa; a preliminary report of efficacy. Clinical otolaryngology : official journal of ENT-UK ; official journal of Netherlands Society for Oto-Rhino-Laryngology & Cervico-Facial Surgery, 2009. **34**(4): p. 349-57.

56. Coetser, S.E. and T.E. Cloete, *Biofouling and biocorrosion in industrial water systems.* Crit Rev Microbiol, 2005. **31**(4): p. 213-32.

57. Hall-Stoodley, L., J.W. Costerton, and P. Stoodley, *Bacterial biofilms: from the natural environment to infectious diseases.* Nat Rev Microbiol, 2004. **2**(2): p. 95-108.

58. Maukonen, J., et al., Methodologies for the characterization of microbes in industrial environments: a review. J Ind Microbiol Biotechnol, 2003. **30**(6): p. 327-56.

59. Gilbert, P., et al., The physiology and collective recalcitrance of microbial biofilm communities. Adv Microb Physiol, 2002. **46**: p. 202-56.

60. Donlan, R.M. and J.W. Costerton, *Biofilms: survival mechanisms of clinically relevant microorganisms.* Clinical Microbiology Reviews, 2002. **15**(2): p. 167-93.

61. Davey, M.E. and G.A. O'toole, *Microbial biofilms: from ecology to molecular genetics.* Microbiol Mol Biol Rev, 2000. **64**(4): p. 847-67.

62. Mittelman, M.W., Structure and functional characteristics of bacterial biofilms in fluid processing operations. J Dairy Sci, 1998. **81**(10): p. 2760-4.

63. Cloete, T.E., L. Jacobs, and V.S. Brözel, *The chemical control of biofouling in industrial water systems.* Biodegradation, 1998. **9**(1): p. 23-37.

64. Costerton, J.W., *Overview of microbial biofilms.* J Ind Microbiol, 1995. **15**(3): p. 137-40.

65. Shuren, J., Federal Register, ed US Food and Drug Administration, 2006. **71**: p. 47729-47732.

66. Labrie, S.J., J.E. Samson, and S. Moineau, *Bacteriophage resistance mechanisms*, in *Nat Rev Micro.* 2010. p. 1-11.

67. Ramanculov, E. and R. Young, Genetic analysis of the T4 holin: timing and topology, in Gene. 2001. p. 25-36.

68. Wang, I.-N., Lysis timing and bacteriophage fitness, in Genetics. 2006. p. 17-26.

69. Heineman, R.H. and J.J. Bull, Testing optimality with experimental evolution: lysis time in a bacteriophage, in Evolution. 2007. p. 1695-709.

70. Fischetti, V., *Bacteriophage lytic enzymes: novel anti-infectives.* Trends Microbiol, 2005. **13**(10): p. 491-6.

71. Fischetti, V., *Bacteriophage lysins as effective antibacterials.* Curr Opin Microbiol, 2008. **11**(5): p. 393-400.

72. Grandgirard, D., et al., Phage lytic enzyme Cpl-1 for antibacterial therapy in experimental pneumococcal meningitis. J INFECT DIS, 2008. **197**(11): p. 1519-22.

73. Merril, C.R., D. Scholl, and S.L. Adhya, The prospect for bacteriophage therapy in Western medicine, in Nat Rev Drug Discov. 2003. p. 489-97.

74. Hagens, S., et al., Therapy of experimental pseudomonas infections with a nonreplicating genetically modified phage, in Antimicrob Agents Chemother. 2004. p. 3817-22.

75. Schoofs, M., FDA Is Easing Way for Drug Cocktails, in Wall Street Journal. 2010.

76. Dai, W., et al., Three-dimensional structure of tropism-switching Bordetella bacteriophage. Proc Natl Acad Sci USA, 2010.

77. Liu, M., et al., Reverse transcriptase-mediated tropism switching in Bordetella bacteriophage. Science, 2002. **295**(5562): p. 2091-4.

78. Lederberg, J., *Smaller fleas ... ad infinitum: therapeutic bacteriophage redux.* Proc Natl Acad Sci USA, 1996. **93**(8): p. 3167-8.

79. Rabinovitch, A., et al., *Model for bacteriophage T4 development in Escherichia coli.* J Bacteriol, 1999. **181**(5): p. 1677-83.

80. Jensen, E.C., et al., Prevalence of broad-host-range lytic bacteriophages of Sphaerotilus natans, Escherichia coli, and Pseudomonas aeruginosa. Appl Environ Microbiol, 1998. **64**(2): p. 575-80.

81. Lu, T.K. and J.J. Collins, Engineered bacteriophage targeting gene networks as adjuvants for antibiotic therapy, in Proc Natl Acad Sci USA. 2009. p. 4629-34.

82. Hilpert, K., et al., High-throughput generation of small antibacterial peptides with improved activity. Nat Biotechnol, 2005. **23**(8): p. 1008-12.

83. Sambrook, J. and D. W. Russell, *Molecular Cloning: A Laboratory Manual.* 2001.

Chapter 4. Controlled release of AmPs from surfaces

4.1. Executive summary

The ability to eradicate and prevent the formation of bacterial biofilm on implantable medical devices provides an invaluable tool for the medical community. In this chapter, we present the fruits of a joint collaboration with the Hammond lab that led to the tunable release of antimicrobial peptides from degradable polymer coatings. We demonstrate the successful incorporation and release of three different antimicrobial peptides: melittin, dermaseptin, and ponericin G1. We developed techniques to alter the release profile and loading of AmPs by altering the number of film layers or by co-releasing of other therapeutic agents. Finally, we show that incorporation of the AmPs in the film did not affect their activity and that the release media was both non-toxic to mammalian cells, and effective at inhibiting the growth of bacteria and thus of biofilms.

4.2. Motivation for surface release of AmPs

One of the most serious complications with bacterial infections occurs with the formation of biofilms at the surface of medical devices and scar tissues. These bacteria colonies are difficult to eradicate because secrete an exopolysaccharide matrix that protects them against antimicrobial treatments and the host immune systems (*1*). These resistant bacteria give rise to planktonic cells that spread the infections and lead to implant failure (*2*). One approach to prevent biofilm formation is to prevent the initial attachment of the bacteria by coating antimicrobial agents on the surface of implantable surfaces (*3*). In the field of AmPs, Semprus Bioscience is developing novel chemistries to immobilize AmPs on polymer, membranes and device surfaces (*4*).

More recently, researchers are have been able to build layer-by-layer constructs to deliver in a controlled manner therapeutic agents (*6*). The layer-by-layer assembly allows for multiple agents to be incorporated and released sequentially, which would otherwise be difficult with single layer coatings. Novel antimicrobial agents, such as AmPs, are one particular agent of interest to coat and release from these LbL films. Thus, work has been done to incorporate AmPs but so far only in fixed, non degradable layer-by-layer polymer constructs (*5*). In this chapter, we describe a tuneable drug delivery technology for the controlled release of AmPs from LbL films. These films may serve as coatings of implantable medical surfaces to deliver AmPs locally and ensure the implant sterility. This work was performed in collaboration with Jeffrey Easly, Helen Chuang, and Anita Shukla from Paula Hammond's research group at MIT and the results were published in *Biomaterials* (*3*). Helen and the author conceptualized and designed the experiments together; the author measured the antimicrobial activity of AmPs towards *S. aureus* and guided the choice of active peptides; Helen built the LbL films independently; Helen, Jeffrey and the author collected sample release and measured AmP concentration together.

4.3. Layer-by-layer degradable polymer films

Layer-by-layer films are polymer films that can be applied as coatings to virtually any surface material. Their fabrication is based on alternate deposition of positively and negatively charged electrolytes one layer at a time, introducing the drug of choice in alternate layers. The drug delivery coating then erodes when placed under physiological conditions releasing the compounds of interest in inverse order (Figure 4-1).

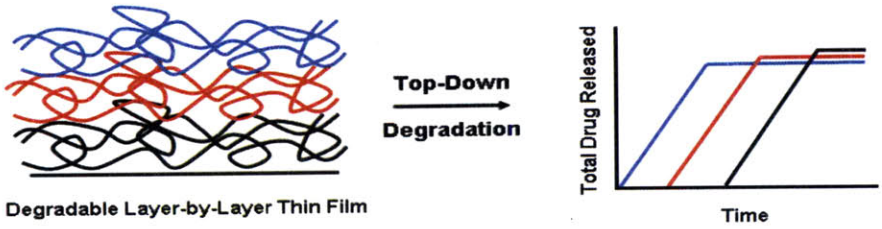

Figure 4-1: Schematic of layer-by-layer films and the time-release profile of therapeutic drugs. Figure adapted from Chuang 2007 (7).

The method by which these films are assembled is shown schematically in Figure 4-2. The process involves the formation of thin films through the alternating adsorption of positively and negatively charged polymer species at room conditions. Each adsorbed layer in the films can range from 1 to 20 nm or more in thickness (7). Total film thicknesses are anticipated to range from 100 nm to as much as 1 to 2 microns. Modulation of the film growth is achieved by changing adsorption conditions such as pH or salt content of the deposition solution. The LbL assembly technique is mild, versatile, low-cost and non-destructive, thereby allowing the incorporation of a broad range of functional polymers and therapeutic agents.

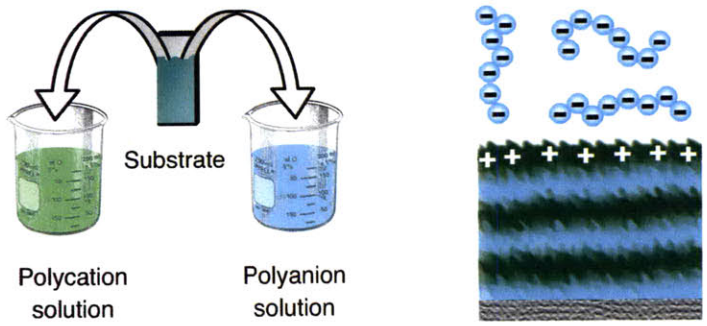

Figure 4-2: Schematic of alternating layer-by-layer assembly to create thin films. The substrate is dipped successively in a polycation and polyanion solution resulting in the build up of a film of alternating polymer layers. Figure adapted from Chuang 2007 (7).

AmPs being small natural polycations, they can easily be incorporated into LbL films as a structural and active component. Through sequential depositions of a biodegradable polycation (*e.g.* poly (β-amino ester)), AmPs, and a biocompatible polyanion (*e.g.* hyaluronic acid, heparin, chondroitin sulfate, and dextran), we have constructed LbL films that can release in a controlled manner therapeutically relevant amounts of AmPs.

4.4. Methods for the release of AmPs from LbL films

Experimental methods described in section 4.4 were reproduced from Helen Chuang's PhD thesis (*7*) with her consent.

4.4.1. Choice of bacterial target and AmPs

S. aureus is one of the most common bacteria colonizing implantable medical devices and is thus chosen as the pathogenic target in this work. We selected three antimicrobial peptides active against *S. aureus* or *E. coli*. These were melittin, dermaseptin and ponericin G1.

Table 4-1: AmPs incorporated in the LbL films

Name	Source	Sequence	$MIC_{S.aureus}$ (ug/ml)
Melittin	Honeybee venom	GIGAVLKVLTTGLPALISWIKRKRQQ	16
Dermaseptin	S. American frog	ALWKTLLKKVLKA	256
Ponericin G1	Ant venom	GWKDWAKKAGGWLKKKGPGMAKAALKAAMQ	8

4.4.2. Preparation for the AmP LbL films

Briefly, Poly(β-amino esters) (referred to as *Poly X, X* = 1, 2, and 6) were synthesized as previously described (*8*). Silicon wafers (test grade n-type) were purchased from Silicon Quest (Santa Clara, CA). Linear poly(ethylenimine) (LPEI, M_n = 25k) was received from Polysciences, Inc. Poly (sodium 4-styrenesulfonate) (PSS, M_n = 1M) and sodium alginate (or alginic acid) were purchased from Sigma-Aldrich (St. Louis, MO). Sodium hyaluronate (or hyaluronic acid (HA), M_n = 1.76 MDa) was purchased from Lifecore Biomedical, Inc. (Chaska, MN). Dipping solutions containing *Poly X* and HA were made at a concentration of 10 mM with respect to the polymer repeat unit in 100 mM sodium acetate buffer (pH 5.1 by glacial acetic acid). AmPs dipping solutions were prepared by dissolving the AmPs sample with sodium acetate buffer and glacial acetic acid. Nondegradable base layers were deposited from dipping solutions of LPEI and PSS in deionized water pH adjusted to 4.25 and 4.75, respectively. Deionized water used to prepare all solutions was obtained using a Milli-Q Plus (Bedford, MA) at 18.2 MΩ.

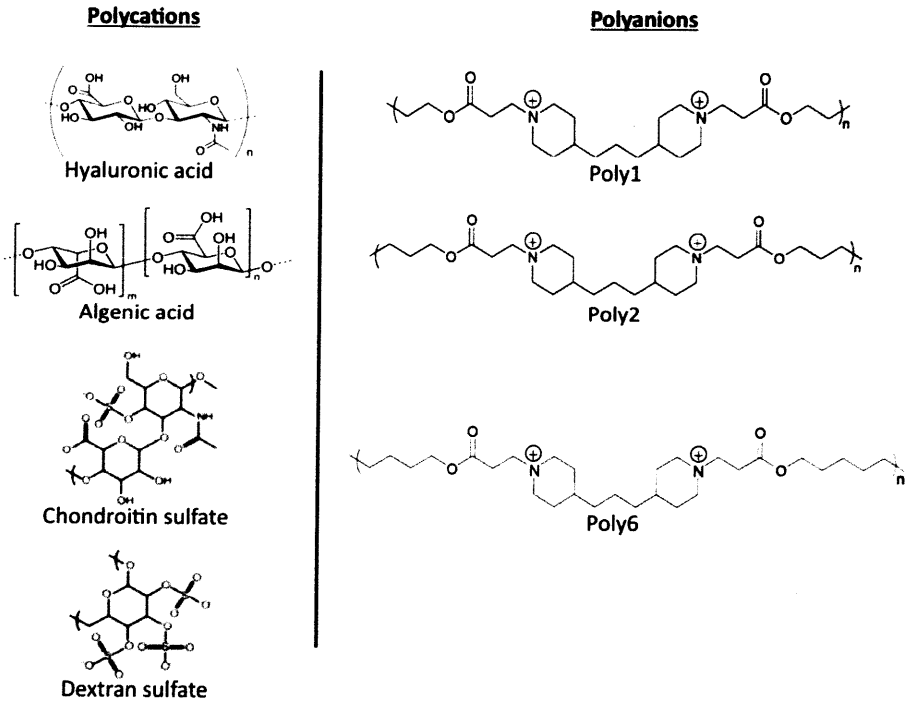

Figure 4-3: Structure of the polycations and polyanions used to build the LbL films. Three different polyanions and four polycations with carboxyl (hyaluronice acid and algenic acid) and sulfonate groups (chondroitin sulfate and dextran sulfate) were studied to obtain large diversity in the LbL films constructs and span a range of affinity for the AmPs. Figure adapted from Chuang 2007 (7)

All polyelectrolyte LBL thin films were constructed according to the alternate dipping method. A ten-bilayer nondegradable base film ($(LPEI/PSS)_{10}$) was deposited by submerging plasma treated silicon substrates in an LPEI dipping solution for 5 minutes, then a cascade rinse cycle consisting of three deionized water rinsing baths (15, 30, and 45 seconds, respectively). Substrates were then submerged in a PSS dipping solution for 5 minutes followed by the same cascade rinsing cycle, and the entire process was repeated ten times. Next, degradable films were deposited on the existing polyanion-terminated base layer by repeating the above procedure with the $[(Poly\ X/HA)_a(AmP/HA)_b]_n$ architecture, dipping for 10 min in each of the *Poly X*, HA, and AmPs solutions and repeating the $(Poly\ X/HA)_a(GS/HA)_b$ structure as many times (n) as desired. *Poly X* and HA dipping solutions were re-made every 24 hours. Following deposition, films were immediately removed from the final rinsing bath and air-dried.

4.4.3. Release experiment

The release experiments were carried out by placing a fixed size piece of silicon plate coated with the LbL coating containing the AmP in 1 ml of PBS and incubating at 37 °C. At different time points a 250ul aliquot of solution is withdrawn and replaced with fresh PBS. The aliquots are frozen at -20 °C until the end of the experiment. The AmP quantification assays are performed on the aliquots collected at different times to determine the time-release profile of AmPs from the LbL film.

4.4.4. Monitoring AmP release using BCA assay

Methods typically used to monitor the release of therapeutic agents from the LbL film are fluorescence tagging and micro bicinchoninic acid (BCA) protein assay. Fluorescence assay requires the attachment of fluorescein tag to the one end of the AmPs. It is unclear whether the attachment of such

functional group interferes with the release of the peptide from the LbL films and the peptide's antimicrobial activity; thus Micro BCA assay (Pierce, Rockford, IL) is preferred to monitor the release of AmPs.

In the BCA assay, the peptide bonds of the AmP reduce the Cu^{2+} ions from the BCA reaction mixture to Cu^{1+}, which then chelates with the bicinchoninic acid forming a purple product, which absorbs light at 562nm. The intensity of colorimetric absorption is proportional to the total level of the AmP in the solution and the is compared to dilut ions of known concentration of the peptide (*9*).

4.4.5. Osteoblast toxicity assay

Briefly, MC3T3-E1 Subclone 4 was maintained in minimum essential medium supplemented with 10% fetal bovine serum, 100 U/mL penicillin, and 100 mg/mL streptomycin. Cells were split 1:15 every 3-4 days, with the medium refreshed in between.

During the toxicity assays, cells were seeded at 10^4 cells/mL in a 96-well plate at 150 μL per well. Cells were monitored daily until they reached 50% confluence, at which point the medium in each well was replaced with the medium released from the AmP-LbL films, $[(PolyX/HA)(AmP/HA)]_n$, to be tested. For concentration of AmP above 64ug/ml, dilutions with known concentration of the natural AmP were used instead. All test media were sterile-filtered through 0.2um membranes prior to use. Three wells were left untreated as negative controls.

Cells were incubated with the test media for the defined test period. At the end of the test period, medium in each well was replaced with fresh untreated medium, and 15uL of alamarBlue was added to each well. Cells were incubated at 37°C for 4 hours, examined visually for color change then read at 570 nm and 600 nm using a microplate spectrophotometer. Cell metabolic activity was computed from the spectrophotomeric readings based on manufacturer's specifications.

4.5. Controlled release of AmPs from LbL films

4.5.1. Initial burst followed by continuous release of AmPs

Melittin was released from layer-by-layer films of $[(Poly1/HA)(Mel/HA)]_n$ with twenty and seventy layers (n=20, n=70) and monitored using a BCA assay. Figure 4-4 shows the release of melittin over a period of 8 days. The films exhibited an initial burst release of the AmPs during which ~80% of the total AmP content was released within the first 8 hours. This burst profile is associated with the rapid diffusion of the AmPs across the different layers of the LBL film to the AmPs' small molecular size. The burst release was then followed by a sustained linear release of the AmPs for a period of over 8 days. The slower linear profile is associated the gradual degradation of the LBL film and subsequent release of AmPs from the layers.

The initial burst followed by continuous released demonstrated here can be of great benefit in a therapeutic settings. The risks of infection are greatest immediately after surgery and the implant of medical devices. A larger dose of antimicrobial agent is necessary to prevent an initial infection and kill the pathogens not just at the surface but also in the direct vicinity of the implant, thus requiring an initial burst release of agent. The following continuous release of antimicrobial agent will then ensure the sterility over longer time period and prevent attachment of bacteria at the surface of the device.

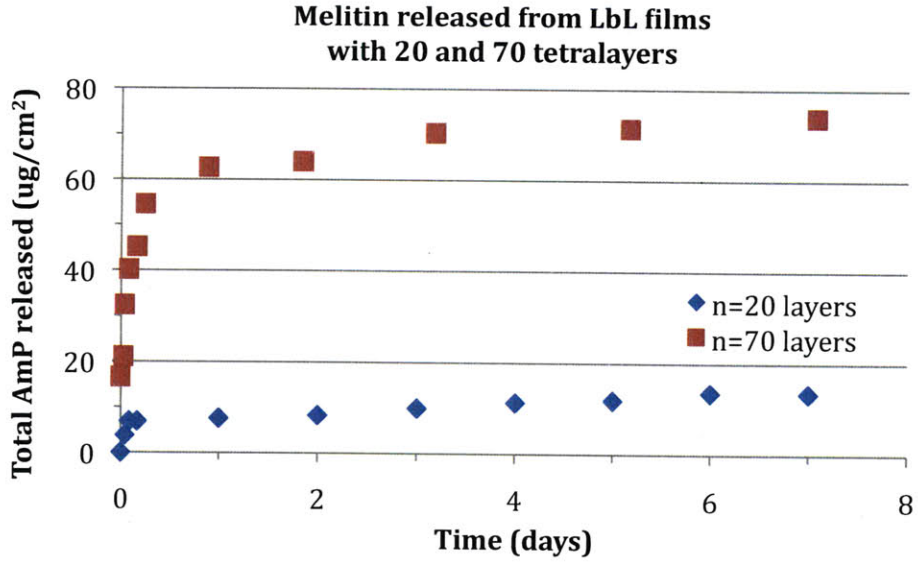

Figure 4-4: Melittin release from [(Poly1/HA)(Mel/HA)]$_n$ films (n= 20 or 70). Melittin release from the films follows a burst profile in the first 8 hours followed by a sustained linear release for the following 8 days. The amount of melittin released from the film constructed with 70 layers is 5-times higher than that released from the 20-layers film. Figure adapted from Chuang 2007 (7)

Several parameters can be altered during the films manufacturing process to alter the time-release profile of the AmPs. These parameters include increasing the number of layer, varying the nature and size of the AmPs, adding a co-release agents to slow down inter-layer diffusion of the AmPs and to change the nature of the polyanions to control the rate of degradation. The effect of these parameters will be explored individually in the following sections.

Increasing the number tetralayers from 20 to 70 tetralayers increased the film capacity for AmPs. However, the correlation between number of layers and capacity is not linear. While the number of layers was increased from 20 to 70 and thus by a factor of 3, the overall film capacity increased from 13ug/cm^2 to 73ug/cm^2, a 5-fold increase. This suggests that the outer layer have a higher capacity for AmPs than the inner ones. The tendency to have such a superlinear growth is supported by other authors as well

(*10*). The thicker outer layers is also the reason for the initial burst release as they incorporate and thus release a greater amount of AmP than thinner inner layers.

4.5.2. Similar surface loading for different AmPs

To investigate the surface loading of different AmPs, two identical hyaluronic acid-based LbL films with 70 tetralayers were constructed using a 1mg/ml solution of melittin in a first film and of dermaseptin in a second one. Figure 4-5 shows the 8-day release profile of two films. Both films feature an initial burst followed by continuous release as described in Section 4.5.1. However, the total amount incorporated in the dermaseptin film, 160ug/cm^2, is twice that incorporated in the melittin film, 73ug/cm^2. The difference is justified, as the dermaseptin stock concentration, 0.6mM, was twice that of melittin, 0.3mM due to its smaller peptide size. This suggests that regardless of the size or nature of the AmPs and their stock solution concentration, a constant AmP loading of 40-60nmol/cm^2 was achieved for the $[(Poly1/HA)(AmP/HA)]_{70}$ films.

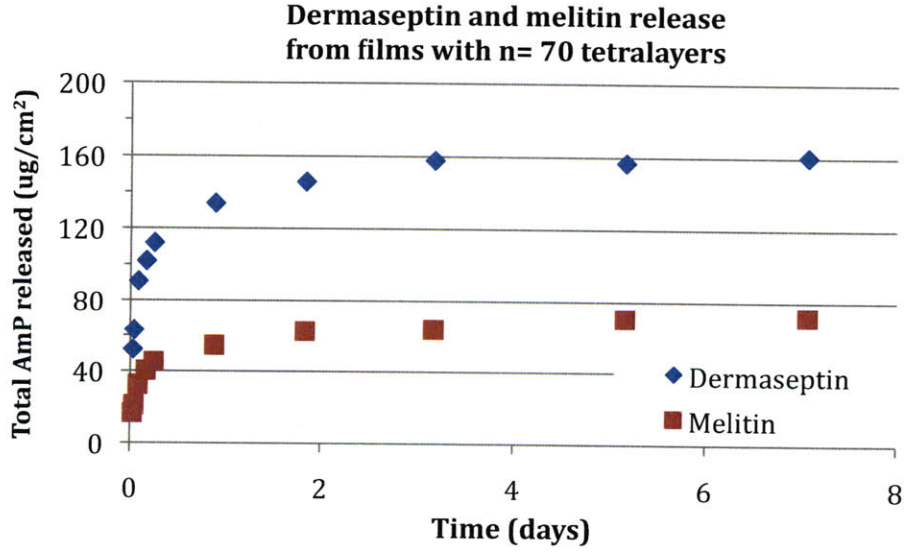

Figure 4-5: Dermaseptin and melittin release from $[(Poly1/HA)(Mel/HA)]_{70}$ films. The films were able to incorporate 160ug/cm^2 of dermaseptin and 73ug/cm^2 of melittin, which correspond to a constant AmP surface loading of 40-60nmol/cm^2. Figure adapted from Chuang 2007 (7)

4.5.3. Co-release of growth factors slows and extends release profile

In order to slow the release, we have tried to co-release large agents alongside with the therapeutic compound of interested. We used basic fibroblast growth factors (bFGF), large molecules of size 24kD, as co-release agent from the AmP LBL films. These factors promote wound healing and provide significant therapeutic benefit to patient recovery (*11*). Two types of films were built to study the effect of co-release on the release profile. The first films, $[(P1/HEB)(Derm/HEP)]_{100}$, with 100 tetralayers incorporating dermaseptin only. The second film, $[(P1/HEB)(bFGF/HEP)]_{20}[(P1/HEB)(Derm/HEP)]_{100}$, with 20 tetralayers incorporating bFGF on top of which 100 teralayers incorporating dermaseptin were deposited.

Figure 4-6 shows the release profile of dermaseptin measured using BCA with and without the bFGF underlayer. It appears that the bFGF slows down and extent the release profile of the AmP. Without the underlayer, all of the dermaseptin was release within 10 days while with the bFGF underlayer the release profile was extended beyond 17 days, thereby extending the length of the release and active life of the antimicrobial coating.

The underlayer also slowed down the release of the AmPs during the burst phase. Without the underlayer, 70% of the total dermaseptin content was released within the first 8 hours, while only 50% was released when the underlayer was present. Most importantly, the duration of the burst release phase was reduced from 1 day to 8 hours when the bFGF underlayer was added. These effects are explained by the inter-diffusion of dermaseptin into the bFGF underlayer, thereby lowering its effective concentration in the top layer and countering the rapid release due to diffusion of the AmP the media. A similar effect for the bFGF underlayers was observed and documented by Chuang for the release of gentamycin from similar LbL film (*7*).

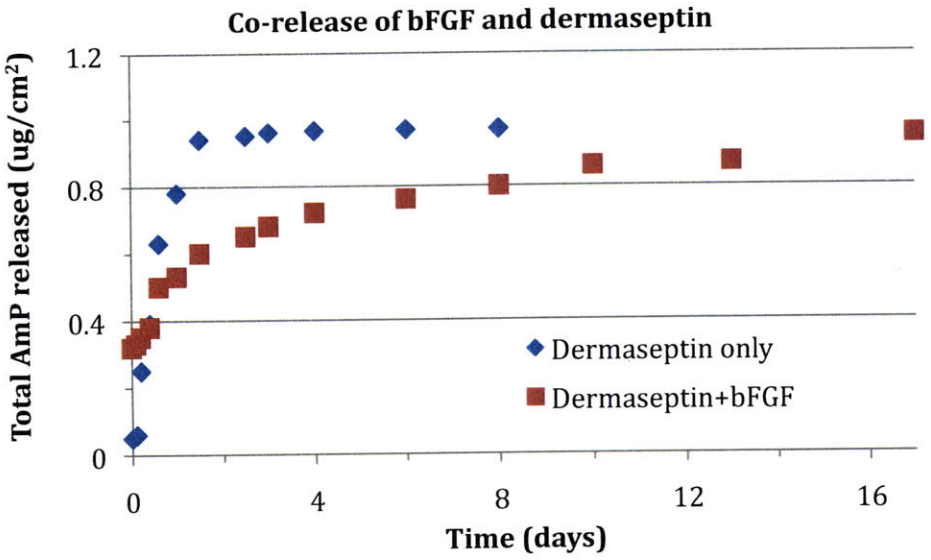

Figure 4-6: Co-release of dermaseptin with bFGF underlayer. The growth factor underlayer allows for diffusion of the AmP and slows down the burst release profile of the AmPs thereby extending the realease time from the LbL coating. Figure adapted from Chuang 2007 (7), films were built by Mara Macdonald.

4.6. Antimicrobial activity of the released media

The antimicrobial activity of the released solution was tested for films incorporating ponericin G1 using a micro dilution growth inhibition assay. Briefly, the ponericin content in the PBS-based release media was measured using the BCA assay. 160ul of the released media were then added to 40ul of 5X concentrated LB in a flat bottom 96 well plate seeded with 10^5 CFU/ml of *Staph. aureus* bacteria from a mid-log culture at OD=0.4. The plate was incubated at 37°C for 8 hours and the resulting OD was

measured with a plate spectrophotomer.

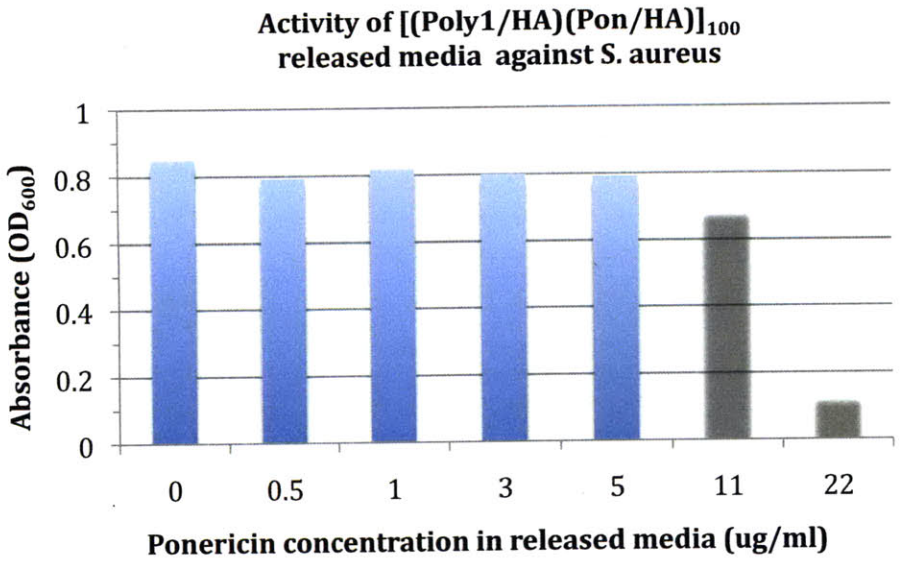

Figure 4-7: Antimicrobial activity of the released media. Ponericin G1 was released from [(Poly1/HA)(Pon/HA)]$_{100}$ and the ponericin content was estimated using BCA. The released media prevented the growth of S. aureus when the ponericin content reached 22 ug/ml. Figure adapted from Chuang 2007 (7)

The released media prevented the growth of *Staph. aureus* when the Ponericin concentration reached 22ug/ml. This is slightly higher but comparable to the 8ug/ml MIC of native ponericin G1. The discrepancy may be due by the presence of charged polyanions and polycations that interfere and somewhat shield the AmPs. Most importantly, Figure 4-7 shows the incorporation and release of ponericin from the films did not degrade the peptide antimicrobial activity thus validating the possible application of this technology for antimicrobial coatings.

4.7. Non-toxicity of released media towards mammalian cells

The non-toxicity of the LbL films release towards mammalian cells was assessed using the mouse osteoblast MC3T3 toxicity assay with alamarBlue. The toxicity assay measures the metabolic activity of MC3T3 cell after 2 days and 4 days of exposure to the media released from a [(PolyX/HA)(Pon/HA)]$_{70}$

film. Two-fold dilutions of natural ponericin were carried out to test mammalian toxicity to concentration as low as of 4ug/ml. The metabolic activity was normalized with respect to the negative control with no released media was added. After two days of incubation, no significant decrease in metabolic activity were observed for ponericin concentration up to 64ug/ml. Above that concentration, ponericin showed effect on mammalian cell growth and a >50% decrease in metabolic activity. After four days of exposure to ponericin, metabolic activity of the cells were decreased only by ~50%. In combination with Figure 4-1, these results show that ponericin at concentration above 20ug/ml is effective at preventing bacterial growth while little toxicity to mammalian cell is observe even after 2 or 4 days of exposure.

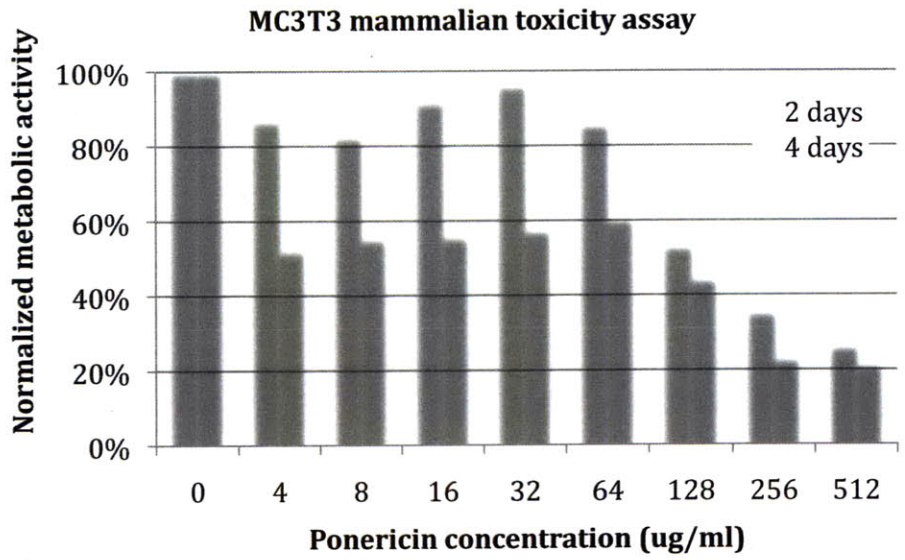

Figure 4-8: MC3T3 mammalian toxicity assay. Ponericin had little effect on metabolic activity of the MC3T3 cell up to 64ug/ml after 2 days of exposure. Metabolic activity was reduced to 50% after 4 days of exposure to ponericin concentrations up to 128ug/ml and reduced to 20% above for concentration up to 512ug/ml. Figure adapted from Chuang 2007 (7)

4.8. Chapter conclusion

In this chapter, we demonstrated the ability to integrate and release AmPs from degradable LbL films. We showed the ability to control the kinetics of the drug release by altering the loading of the film,

the nature of the polymers and by co-releasing large other therapeutic agents. We also showed that the incorporation process does not affect the antimicrobial activity of the AmPs and that the released media is non-toxic to mammalian cell. This technology is readily applicable to provide an antimicrobial coating for implantable devices and prevent the formation of bacterial biofilms and infections in patients. This work and its extension was also published in Helen Chuang's PhD Thesis (*7*) and in *Biomaterials* as *Controlling the release of peptide antimicrobial agents from surfaces* (3).

4.9. References

1. T. K. Lu, J. J. Collins, in *Proc Natl Acad Sci USA*. (2007), vol. 104, pp. 11197-202.
2. J. Costerton, P. Stewart, E. Greenberg, in *Science*. (1999).
3. A. Shukla *et al.*, in *Biomaterials*. (2009).
4. C. Loose, in *MIT PhD Archive*. (2007).
5. O. Etienne *et al.*, in *Antimicrob Agents Chemother*. (2004), vol. 48, pp. 3662-9.
6. K. C. Wood, S. R. Little, R. Langer, P. T. Hammond, in *Angew. Chem. Int. Ed.* (2005), vol. 44, pp. 6704-6708.
7. H. Chuang, R. Smith, P. Hammond, in *Biomacromolecules*. (2008).
8. D. M. Lynn, R. Langer, *J. Am. Chem. Soc.* **122**, 10761 (October 18, 2000, 2000).
9. B. RE, J. KL, H. KJ, in *Anal Biochem JO* -. (1989), vol. 180, pp. 136-139 DO -.
10. C. Porcel *et al.*, in *Langmuir*. (2006), vol. 22, pp. 4376-83.
11. Pasumarthi, Kardami, Cattini, in *Circ Res JO* -. (1996), vol. 78, pp. 126-136 DO -.
12. P. KB, K. E, C. PA, in *Circ Res JO* -. (1996), vol. 78, pp. 126-136 DO -.

Chapter 5. Rational Design of Antimicrobial Peptides

5.1. Executive summary

In this work, we improved the accuracy of our peptide design algorithm by accounting for the activity of the peptide from which the conserved motifs in amino acid sequence were derived and incorporating specific structural design criteria common to natural AmPs. We first measured the antimicrobial activity of the all 163 AmPs from which the motifs were derived against 4 different organisms. Using this activity information, we assigned the motifs to different antimicrobial activity zones. The motifs that best describe the activity of underlying peptides were then tiled together to form proto-peptide, which in turn filtered for strength in predicted activity. The instances of the parent peptides that best match structural criteria common to natural AmPs were selected, synthesized and its antimicrobial activity tested.

5.2. Natural AmPs-based therapeutics

The typical approach to developing AmPs as therapeutics agents relies on screening organisms for new AmPs or optimizing known natural sequences. For example, magainins (*113*), gaegurins (*114*) and pentadactylin (*115*) are all natural AmPs that were isolated from the skin secretions of amphibians. Piscidins (*116*) and hepcidin (*117*) were isolated from marine life, while cathelicidin and defensins from humans (*118*), and plectasin from fungi (*119*). Optimization of natural AmPs aims at increasing the activity of natural peptides. Typically optimization approaches increase the peptide's positive charge (*120*), hydrophobicity (*121, 122*), mutate selected amino acids (*123*), incorporate non-natural ones or modify the N-terminus (*124*) or C-terminus (*26*). While a few isolated or modified natural AmPs have gone through the therapeutic development process (*26*), the screening organisms and isolation and identification of active peptides is a slow and laborious process to producing therapeutic leads.

Additionally, the therapeutic leads are tightly confined to sequence space surrounding the starting AmP. Because of the great similarity between the optimized and native AmPs, the optimized peptides often have similar efficacies against the same microbes. A better approach is to produce AmPs candidates with little homology to existing natural peptides as these can display significant improvements in the breadth and potency of their antimicrobial properties.

5.3. Existing approaches to designing *de novo* AmPs

5.3.1. Undirected AmP design

One approach to producing *de novo* AmPs that is with the undirected high-throughput screening and selection of peptides expressed from combinatorial libraries *in vivo* (*125-128*). However, the large sequence space to explore posses formidable screening challenges and no peptide discovered with this approach have reached clinical trials (*129*).

5.3.2. Computational AmP design

Computational tools have also been used to guide the design of *de novo* peptides and predict peptide secondary structures (*130*), find highly charged regions (*131*) or identify peptide portions likely to form helices (*132*). More sophisticated tools includes quantitative structure activity relationship (QSAR) analysis and neutral network analysis (*133, 134*) have been used to model the peptide/membrane interactions. However, these methods are most applicable within a highly conserved set of sequences and focus on a known subset of natural peptides

5.3.3. Motif-based AmP design

An alternative approach is to base the design of *de novo* peptides on conserved structures across AmPs. Conserved amino-acid motifs (*135-137*) and conserved three dimensional structures (*138-140*) have been identified across a diversity of sequences across subclasses of AmPs and have been shown to play a role in converting antimicrobial activity to the peptides. These structures have persisted over

millions of years of evolution (*25*) and are now used as a basis for peptide design. In our previous work, we showed that the conserved motifs in amino acid sequence can be utilized to produce *de novo* antimicrobial peptides (*141*) that span a large sequence space diversity.

Because of their small size AmPs do not depend on their ternary structure for activity (*24*). Instead their activity is derived from their secondary structure, which is tightly correlated with their amino acid sequence. AmPs within the same family are known to share highly conserved patterns in their amino acid sequence (Figure 5-1). Some of these patterns can be recognized easily while more complex patterns require pattern discovery softwares, such as IBM's Teiresias, in order to be identified. The strong correlation between antimicrobial function and primary structure of AmPs suggests that these motifs encode in part for the antimicrobial activity of peptides.

Figure 5-1: Highly conserved patterns in cecropins. Alignment of cecropins from a variety of organisms reveals a highly conserved pattern. This pattern can be represented by a motif, the bottom sequence. In the motif, bracketed terms indicate a specific set of amino acids that may be selected at a position, and a period indicates that any amino acid may be selected at a position.

More loosely conserved motifs exist across the different classes of AmPs, and are utilized in the motif-based design algorithm. Figure adapted from Jensen 2006 (142).

Recent studies have confirmed that many more such motifs can be found throughout the entire space of known AmPs. These motifs can be recombined to design novel peptides that share little homology with natural peptides (*143*). The AmPs designed using the motifs populate a region of the sequence space that deviates significantly from the space of known peptides while maintaining a high probability of having antimicrobial function (Figure 5-2).

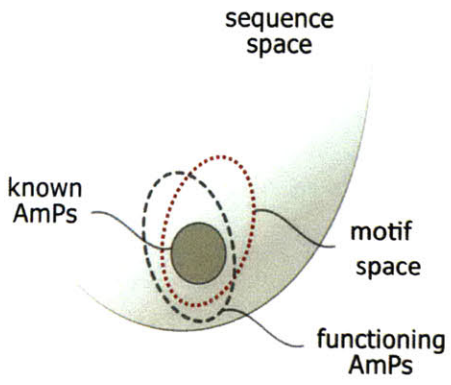

Figure 5-2: Representation of a motif based search space. Sequence space for a typical 20 amino acid AmP contains approximately 1026 sequences; only hundreds of these AmPs are known. The motif-based design of AmPs focuses on peptides inside the "motif space," while allowing deviation from natural AmP sequences. This allows the design peptides that show no significant homology to any naturally occurring sequences, but have the desired antimicrobial properties. Figure adapted from Jensen 2006.

5.4. Blind motif-based approach to AmP design

In order to understand the improved peptide design algorithm described in Section 5.5 of this thesis, it is important to first understand the structure and the limitations of the original motif-based design algorithm. A brief description of the original motif-based design algorithm is provided below while a more complete acount were already published (*26, 142, 143*). This original motif-based approach is «blind» because it performs without any knowledge of the actual activity of the natural AmPs from which the motifs are derived. Taking the activity of the natural AmPs in consideration to improve the efficacy and activity of the design algorithm is one of the improvements that will be describped in Section 5.5.

Teiresias is an algorithm that discovers patterns in any database of biological sequences including DNA and peptides (*144*). Patterns are discovered given the following parameters:

- Pattern length, L: Patterns must be at least L characters long.
- Pattern occurrence, K: Patterns must occur at least K times in the dataset.
- Window size, W: Patterns must have a minimum fraction of L/W non-wild card characters over any window of length W.

An example of patterns discovered using these parameters are shown in Figure 5-3. After pattern discovery is executed, the discovered patterns are filtered to ensure their statistical significance.

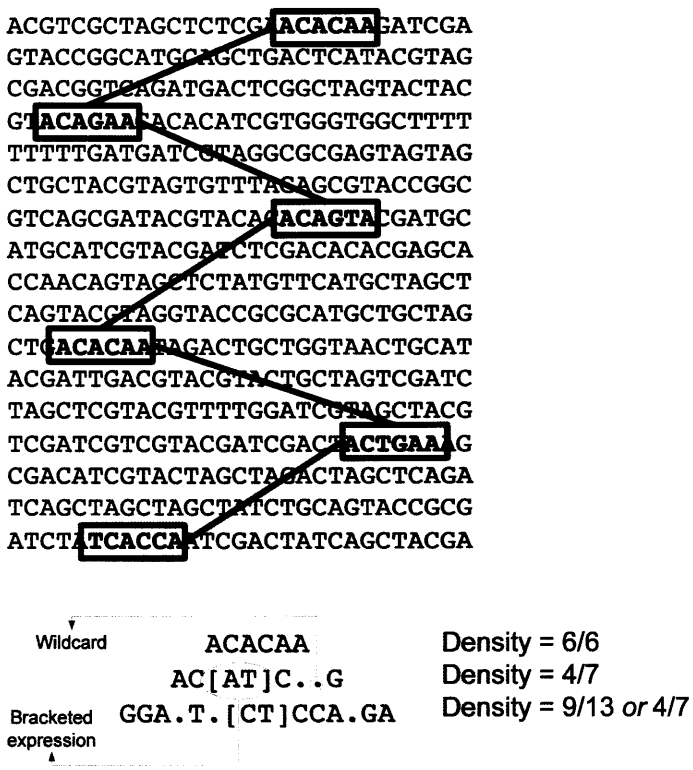

Figure 5-3: Sample results of a Teiresias search. Patterns which meet an L/W of 6/6, 4/7, and 9/13 are shown. An L/W of 4/7 means that in a sliding window of 7 characters, at least 4 must be uniquely specified (not brackets or wild card). Figure adapted from Jensen 2006.

Teiresias pattern discovery was applied to a database (University of Nebraska, Antimicrobial Peptide Database (*145*)) of 526 well characterized eukaryotic AmPs sequences to identify motifs encoding for antimicrobial activity. Peptides naturally contain short, highly conserved, and reoccurring sequences of amino acids, which may not necessarily convey antimicrobial activity. The first step in the discovery algorithm is to identify these short highly-conserved segments and hide them from the database to allow for the subsequent discovery of more loosely conserved sequences of peptides. Teiresias was run with the following settings: L = 6, W = 6, and K = 2 to identify these short, highly conserved sequences. The sequences identified were then masked from the input sequence database. The motifs, which were hypothesized, encode for antimicrobial activity are more loosely conserved. Discovery of these loosely conserved motifs across the natural AmP database was done by repeating the

Tereisias discovery using L = 7, W = 15, K = 5 and the following amino acid equivalency groups [[AG], [DE], [FYW], [KR], [ILMV], [QN], [ST]] (*144*). Teiresias identified 684 sequence motifs from this set of 526 natural peptides.

Teiresias outputs its motifs in regular expressions using wildcards, which are each displayed as a dot (Figure 5-3). According to Teiresias terminology, a wildcard can be replaced by any one amino acid. However in order to remain closer to the set of original peptides, the wildcards in these motifs were instead de-referenced. That is the wildcards were replaced by the set of possible amino acids observed in the peptides from the natural database. To facilitate the future reconstruction of a designed peptide, we divided each motif into sub-motifs using a sliding-window of size 10. This resulted in 1551 motifs of length ten.

The 1551 ten-amino acid motifs characterize conserved segments in the sequences obtained from the database. However, these motifs do not necessarily encode for the active portion of the antimicrobial peptides. To improve selectivity of the derived motifs, the motifs were searched for in a nearly exhaustive list of all known antimicrobial peptides, approximately 1000 sequences, compiled from the AMSdb database (http://www.bbcm.univ.trieste.it/~tossi/pag1.htm) and the AmP section of Swiss-Prot database (*146*). To identify motifs unlikely to encode for antimicrobial activity, the motifs were searched for in the list of non-AmPs sequences in Swiss-Prot. Based on these two searches, motifs that were not at least 80% selective for antimicrobial peptides were eliminated. The resulting final set contained 684 ten-amino acid motifs and was used to design novel AmPs.

5.5. Refined motif-based approach to AmP design

In this work, we improved the accuracy of the peptide design algorithm by accounting for the activity of the peptide from which the conserved motifs in amino acid sequence were derived and

incorporating specific structural design criteria common to natural AmPs. We first measured the antimicrobial activity of all 163 AmPs from which the motifs were derived against 4 different organisms. Using this activity information, we assigned the motifs to different zones of antimicrobial activity. The motifs with strong activity were then tiled together to form proto-peptide. The instances of the parent peptides that best matches structural criteria common to natural AmPs were selected, synthesized and its antimicrobial activity tested.

5.5.1. Selection and scoring of conserved motifs

5.5.1.1. Identifying motifs from existing AmPs

The Nebraska Antimicrobial Database (http://aps.unmc.edu/AP/) assembles a list of peptides with known antimicrobial characteristics. We used the database as published in 2004 with its 526 peptides to perform our motif discovery (*145*). An updated database was later published in 2009 with over 1500 peptides (*147*). Conserved motifs in the amino acid sequence of the antimicrobial peptides published in the Nebraska database were identified using the IBM's Teiresias pattern discovery algorithm (*144*). Details of the method to identify patterns were previously described (*26*). Briefly, a library of 380 conserved proto motifs was extracted from the database by enforcing 7 minimum literals, up to 8 wildcards and requiring a minimum of 5 motif occurrences in the database. These motifs were then cut into 10mer segments by a moving window of size 10 sequence positions to obtain 1551 motifs. After duplicate and redundant entries were removed, the library contained 894 unique 10-mers motifs (Figure 5-4:).

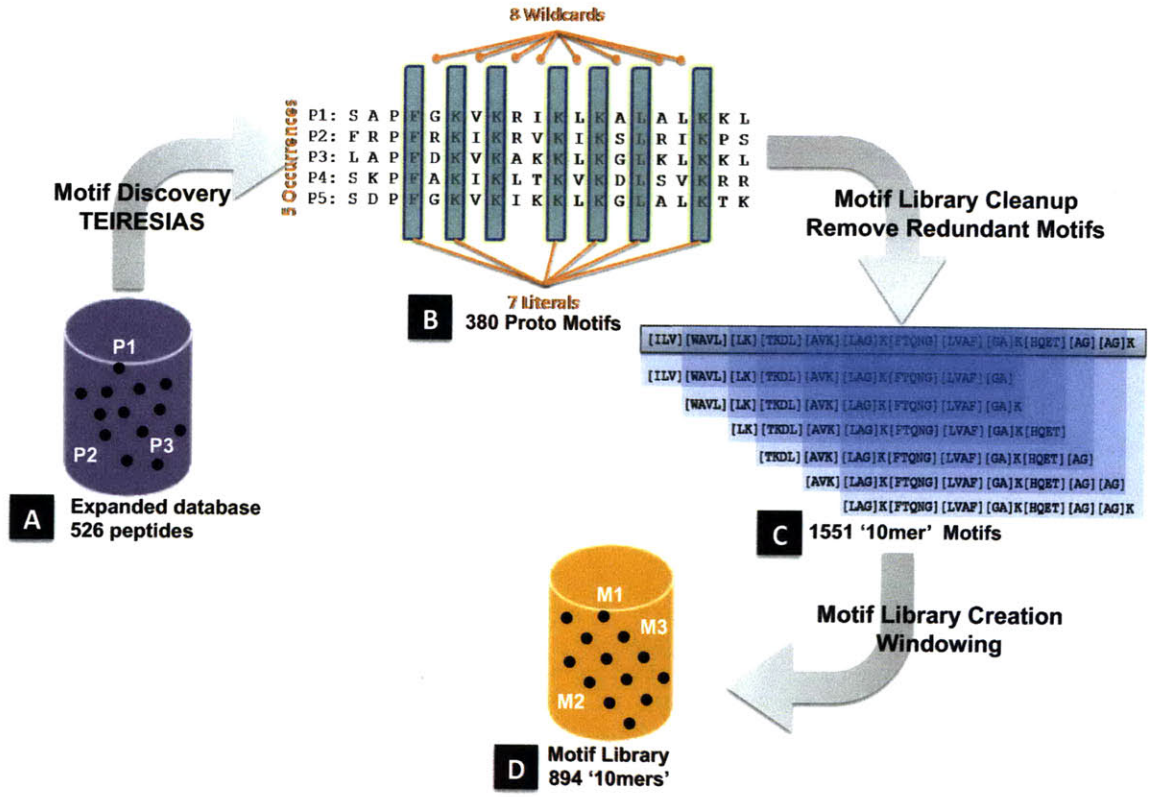

Figure 5-4: Creation the motifs library.

(A) TEIRESIAS motif discovery was applied to the Nebraska Antimicrobial Peptide Database containing 526 natural AmPs and other previous designed AmPs. (B) 380 proto-motifs with 5 occurrences in the database and containing a minimum of 7 literals and a maximum of 8 wildcards are identified. (C) The proto-motifs were then cut into 1551 motifs of size 10 amino acids using a sliding window. (D) Duplicate entries were removed to constitute the complete motif library of 894 10-mer motifs.

5.5.1.2. MIC of existing AmPs

The strong correlation between antimicrobial function and primary structure of AmPs (*141*) suggests that these highly conserved motifs may encode for antimicrobial activity of the peptides. To determine which motifs actually contribute antimicrobial activity, the activity of the originating peptides needs to be measured.

240 peptides from which these 894 unique motifs originated were identified in the Nebraska Database. We furthermore restricted the allowed length (shorter than 40AAs) and shape (short linear) of the peptides that need to be tested due to constraints on peptide synthesis using FMOC chemistry. Finally, a total of 163 peptides satisfied these requirements and were synthesized. These 163 peptides contained only 667 of the original 894 identified motifs. The antimicrobial activity of the peptides was determined using a standardized microdilution MIC determination assay (*49*) against clinical isolate of *E. coli* (ATCC 25922), *P. aeruginosa* (6294), *S. aureus* (ATCC 25923) and *S. epidermidis* (ATCC 14990). The MIC values of these 163 natural AmPs are reported in Table 5-2: . Since all of the tested peptides demonstrated antimicrobial activity against *E. coli*, the pepdides MIC value against *E. coli* served measurement criteria for antimicrobial activity.

5.5.1.3. Scoring motif's potential for antimicrobial activity

In order to project antimicrobial activity information to the motifs given which peptide they originated from, the content matrix T is defined. Each row of matrix T represents one of the 667 motifs identified and each column represents one of the 163 peptides tested. A value of 1 (represented by dot in Figure 5-5:) at location (m,n) indicates that motif Mm is present in peptide Pn, whereas a value of 0 indicates it is not present.

The columns of content matrix T are then sorted by decreasing activity level of the peptides against *E. coli*. Three zones of peptides activity are created namely strong activity peptides (S shown in green) where MIC values are less than 32ug/ml, medium peptides (M shown in yellow) where MIC values are between 32ug/ml and 128ug/ml and weak peptides (W shown in red) where MIC values above 128ug/ml.

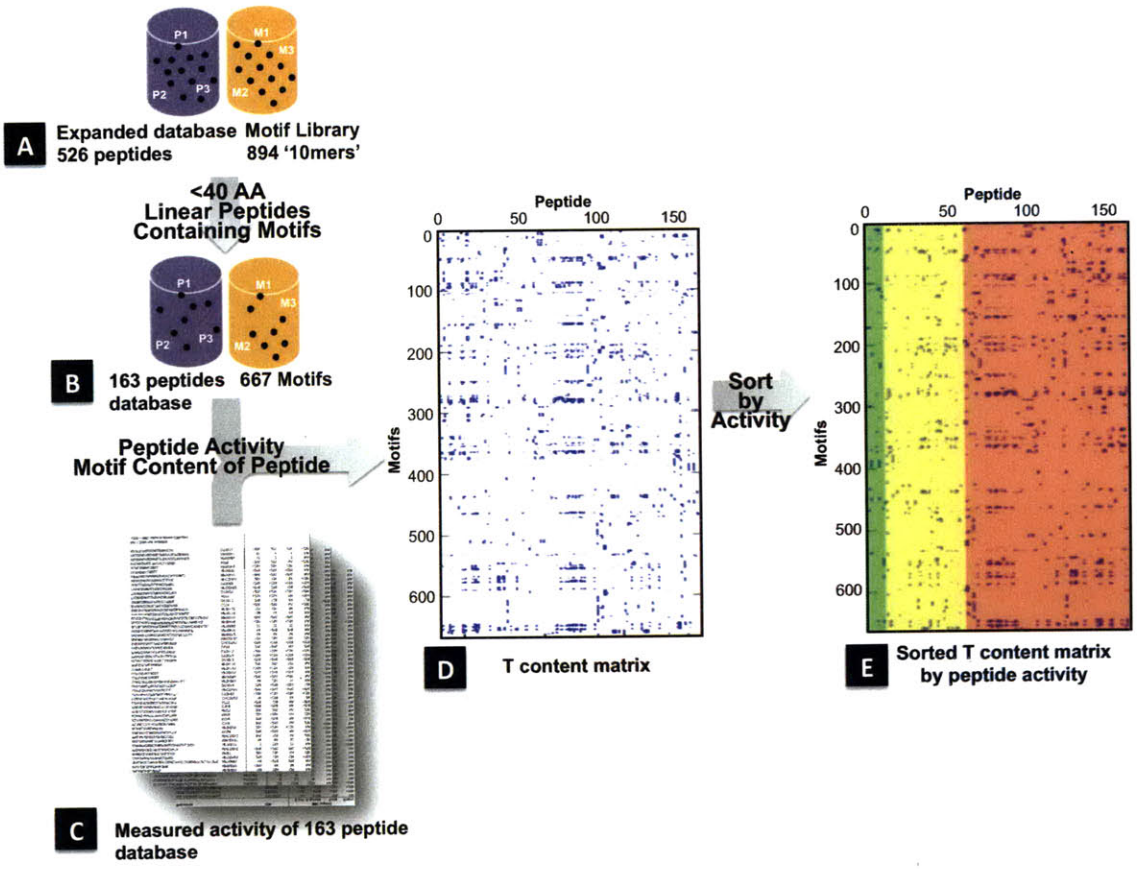

Figure 5-5: Assigning peptides activity to motifs. (A) The complete peptide and motif database was restricted to only short, linear peptides with less 40 amino acids to make up (B) the starting peptide database of 163 and motif library of 667. (C) each of these 163 peptides was synthesized and the antimicrobial activity measured against 4 different pathogenic organisms. (D) The content matrix T relates associates peptides from the database to motif from the library. Each rows of the matrix represents one of the 667 motifs identified and each column represents one of the 163 peptides tested. A blue dot indicates that the motif is present in peptide. (E) The peptides were then sorted by decreasing activity level and partitioned in three activity zones: strong peptides in green with MIC <32ug/ml, medium peptides in yellow with MIC between 32ug/ml and 128ug/ml, and weak peptides in red with MIC >128ug/ml.

As shown in Figure 5-5: , there are many more weak activity (W) peptides than there are medium (M) or strong (S) ones. The strong activity zone contains 7 peptides, the medium activity zone contains

39 peptides wide, while the weak activity zone contains 117 peptides. Therefore, any analysis on the motifs representation within the activity zones must account and correct the bias introduced by the difference in the total number of peptides contained in the activity zones.

Our ranking algorithm determines the putative activity of the motif based on its relative occurrence in each activity zone. For example, assume that a particular motif occurs in 4 of the 7 peptides present in the strong activity zone, and in 58 of the 117 weak peptides.

A simple comparison of the relative ratio may suggest that the motif is predominant in the strong zone (Strong activity zone: 4/7=0.57 > Weak activity zone: 58/117=0.49). However a more rigorous analysis should take into consideration the uncertainty associated with the difference in sample sizes of each activity zone. The mathematics for sorting by average rating while accounting for observation uncertainty were derived by Edwin B. Wilson in 1927 (Ref: Wilson, 1927). A lower bound requiring a 95% confidence interval is found for the adjusted ratio and defined as the the motif's score for the particular activity zone.

For the above example, the motif's score is thus 0.41 for the strong activity zone and is 0.45 for the weak activity zone. Therefore, adjusting for the sample size bias shows that the motif is in fact more characteristic of peptides in the weak zone since its score is highest for the weak zone. The motif is thus classified as a weak motif.

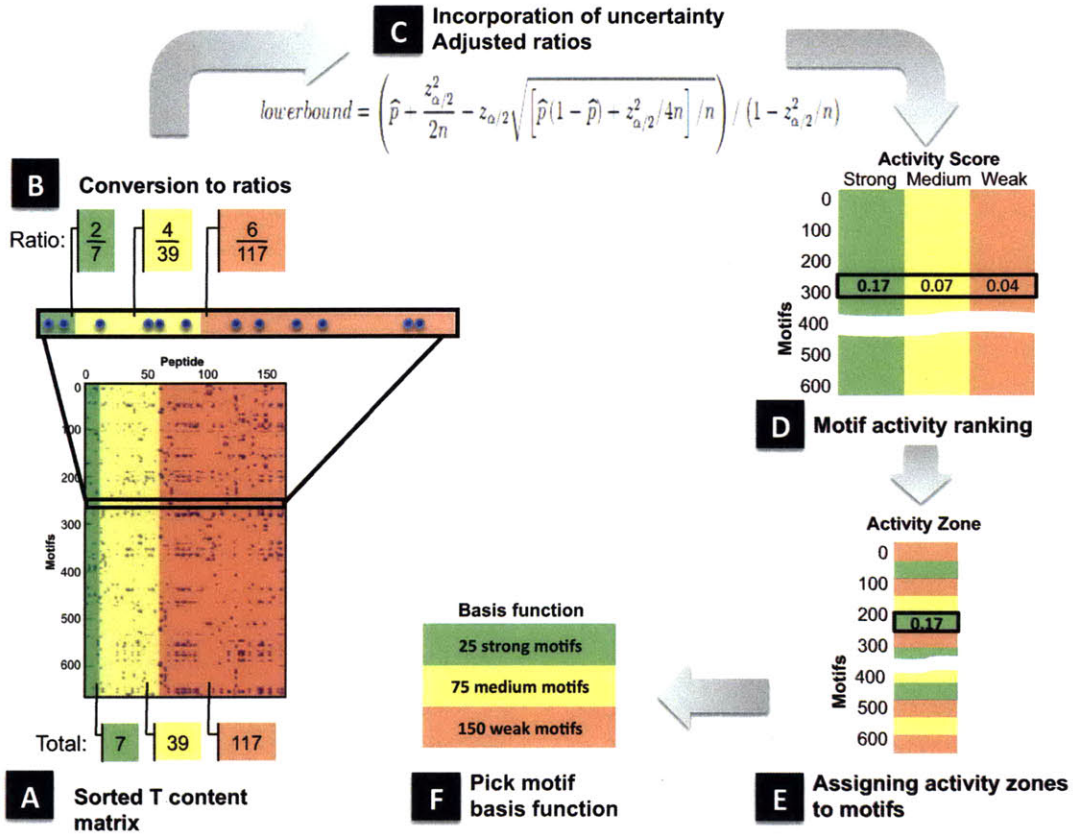

Figure 5-6: Motif scoring and activity zone assignment. (A) The sorted T matrix contains a total of 7 strong, 39 medium and 117 weak peptides. (B) Motif M_{234} for example is found in 2 of the 7 strong, 4 of the 39 medium and 6 of the 117 weak peptides. The motif's respective representation is given by the ration where it is found. (C) The score of the motif is the adjusted ratio computed to account for the uncertainty introduced by the different size of each activity zone. The adjusted ratio accounts for sample size uncertainty in the motif score. p is the observed unadjusted ratio, $z_{\alpha/2}$ is the (1-α/2) quantile of the standard normal distribution, and n is the total number of observations. (D) The score of the motif for each activity zone is computed and (E) the motif is assigned to the activity zone with the highest score. The motifs are then ranked according to their activity scores and the highest-ranking motifs are selected to form the motif basis function to design new peptides. 25, 75, and 150 motifs were selected to form the basis function for the strong, medium and weak zone respectively.

This motif-scoring algorithm is repeated for each of the 667 motifs. Motifs are assigned to their appropriate activity zone and sorted by ascending score. 71 motifs were assigned to the strong activity zone, 146 to the medium activity zone and 359 to the weak zone. The remaining 91 motifs were omitted for lack of stastical accuracy as they were present in less than two peptides either the medium or weak zones and thus had activity scores is close to zero.

The highest scoring motifs from each activity zone form a motif basis function used to designing new peptides. For the validation of this algorithm and for the actual design of new peptides, we selected the 25 highest scoring motifs from strong activity zone, 75 from the medium activity zone and 150 from the weak zone.

5.5.2. Algorithm validation

5.5.2.1. Training and testing set of peptides

Before using the selected set of motifs as basis to design new antimicrobial peptides, we validated our motif selection algorithm using the measured activities of the 163 naturally occurring antimicrobial peptides from the Nebraska Database. The dataset is divided into two groups (Figure 5-7): a training set of 83 AmPs from which motifs are selected, and a testing set of 80 AmPs, whose activity zone is predicted using the motifs selected from the training set. The original dataset was divided such that the training and testing set had similar motif content for a more accurate assessment of our activity predictions. Applying the motif selection and scoring algorithm to the training set, a total of 250 motifs were selected and assigned to an actity zone. These motifs were then used to predict the antimicrobial activity of the peptides in the testing set.

5.5.2.2. Activity prediction of test peptides

The activity of peptides is determined from its motif content and by assinging the peptide to the activity zone with the highest representation based on the motif content. That is for a peptide containing

2 strong motifs and 5 weak ones, the activity is weak. The algorithm validation is done by comparing the activity prediction of the peptide in the test set with their actual measured MIC values.

We define over-prediction as a successful event given the overall goal to design peptides, which will ultimately be screened experimentally. Thus over-predictions are false-positive assignment. On the other hand, lower-prediction than the activity are false-negative assignment and would result in the incorrect dismissal of potentially strong peptide sequences. Our validation algorithm is able to exactly predict or over-predict the activity of 84% the peptide in the test set. Only 5% of the predictions made inaccurate false-negative assignments. If several activity zones are equally represented in the peptide then the algorithm makes no prediction on the actual activity of the peptides. This was the case for 11% of peptides present in the testing set.

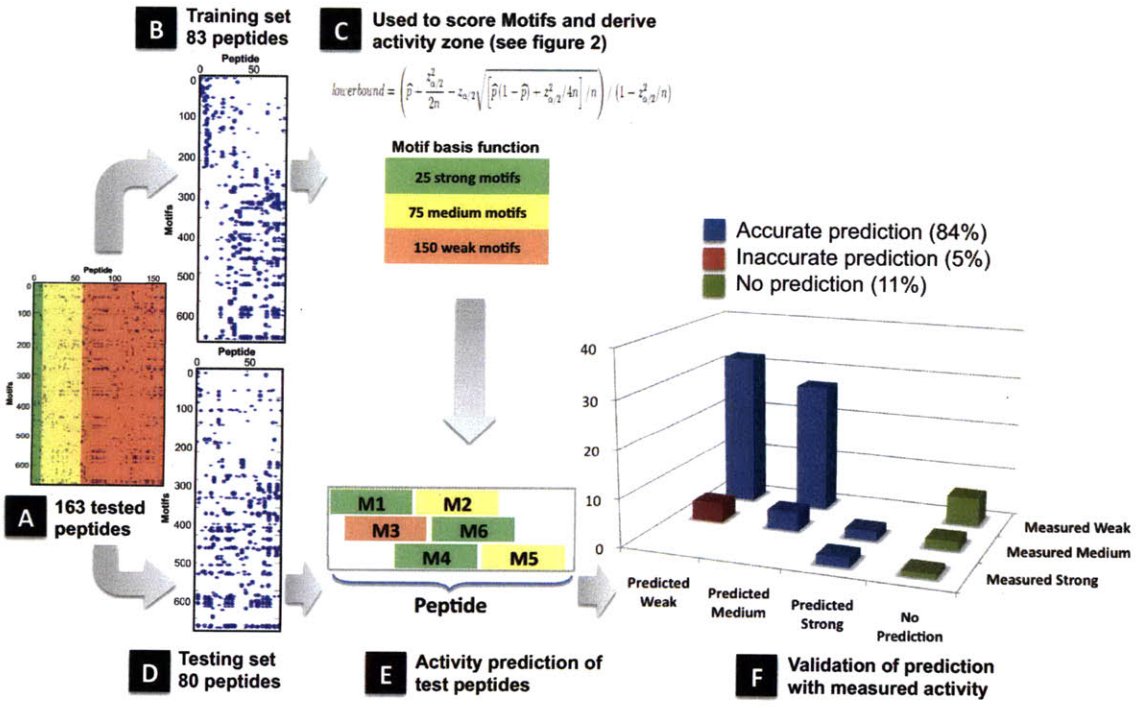

Figure 5-7: Algorithm validation. (A) The database of 163 tested peptides is divided into (B) a training set of 83 peptides used to train the algorithm and (C) assign motifs to a particular activity zone as described in Figure 5-5: . The remaining peptides constitute (D) a testing set of 80 peptides.

(E) The activity of the testing set is predicted based on the peptide's motif content. (F) The algorithm is able to accurately predict the activity of 84% of the peptides in the testing set. Accurate prediction is defined at predicting the exact or a higher activity zone, which allows for false negative. Only 5% were incorrect false-positive predictions while 11% could not be predicted due to equal motif representation in the peptide.

5.5.3. Designing de novo AmPs

5.5.3.1. Tiling motifs to create parent peptides

Given our working hypothesis that motifs play a role confining antimicrobial activity, we use these motifs as building blocks to design de novo peptides. Since both strong and weak motifs are found in activity peptides, we replicate the same behavior in our peptide design strategy and incorporate motifs of various activity zones. We tile motifs together to design new peptides and incorporated as many motifs as possible to increase the chances of creating peptides with antimicrobial activity. For practical reasons including peptide synthesis limitations, therapeutic applications and manufacturing cost, the size of the designed peptides is limited to exactly 20 amino acids, an common peptide size for natural AmPs.

The tiling algorithm overlaps 9 amino acid locations at each tiling step and thus increasing the size of the motif by one amino acid. The algorithm creates a 20 positions long motif that we will call a parent peptide (Figure 5-8:). Using the 250 motifs identified above (25 strong, 75 medium and 150 weak), the tiling process creates 5,579 unique parent peptides. Each parent peptides can be enumerated to create individual of peptides instances by choosing one amino acid for each position from the set of allowable options. Thus, each parent peptide encodes for millions of possible peptides instances.

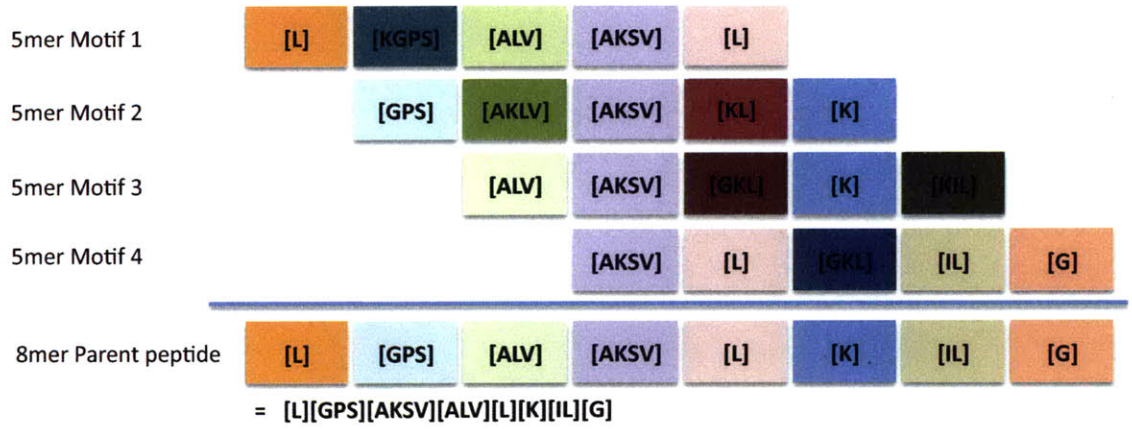

Figure 5-8: Tiling of motifs to created parent peptide.

In this example, four 6-mer motifs are tiled to form an 8-mer parent peptide. All 72 instances of the 8-mer parent peptide are enumerated by picking one amino acid from the choice in the brackets for each location.

5.5.3.2. Scoring parent peptides

Given our assumption that motif content plays a role in the determining the bioactivity of peptides and since all instances of a parent peptide contain the same motifs, it is possible to predict the activity to parent peptides without enumerating all of its instances. This does not however mean that all instances have the same activity since certain amino acid choices will be better than others for certain locations. These issues will be addressed by implementing specific peptide design criteria.

Ranking of the parent peptides is done by counting the number of Strong, Medium and Weak motifs represented in each parent peptide. The parent peptide is then assigned the activity zone most represented by the motifs content. Since we aim at creating peptides with strong bioactivity, only parent peptides assigned to the strong activity zone are maintained and medium and weak parent peptides are eliminated. This reduces the size of the parent peptide library to 2,255 strong parent peptides.

The parent peptides are then ranked with peptides and preference is given to peptides containing more of the strong motifs. Starting from the strongest candidate a set of 15 parent peptides that share the least amount of common motifs are selected such that the resulting set of candidate have a diverse motif

content to eliminate biases that a similar motif content might introduce. This selection is done by starting from the highest ranking parent peptide (highest number of strong motifs), then comparing its motif content to that of the other 2,255 strong parent peptides and then selecting the next strongest one with the least amount of common motifs. The third candidate is then the strongest parent peptide with the least common motifs from the combined list of motifs from the first two candidates. This process is repeated until the desired number of parent peptides, fifteen, are selected. This selection results in the following 15 parent peptides.

Table 5-1: Final parent peptide

Parent Peptide	Position 1	2	3	4	5	6	7	8	9	10	11	12	13	14	15	16	17	18	19	20
#1	L	GPS	AKSV	ALV	L	K	IL	G	A	K	L	L	P	KS	LV	V	CG	AKLM	AFIV	QT
#2	KLMW	S	GIKL	AILV	K	FK	V	A	K	L	A	A	K	V	FLV	P	AS	ILV	FIV	CG
#3	AG	K	FKS	ILV	AG	K	F	LV	AG	K	F	LV	AG	K	FT	LV	AG	K	DEFNQT	AGLQVY
#4	AG	K	EFKT	IV	AG	K	ET	V	A	K	ET	V	A	K	EHQT	AV	A	K	AEGHQT	AGLQV
#5	ST	AG	L	K	GK	L	A	K	G	V	AG	K	H	V	AG	K	GHN	L	ALMY	K
#6	AFGILV	AG	K	FKS	ILV	AG	K	F	LV	AG	K	F	LV	AG	K	FT	LV	AG	K	DEFNQT
#7	ILV	AG	K	EFKT	IV	AG	K	ET	V	A	K	ET	V	A	K	EHQT	AV	A	K	AEGHQT
#8	KLMW	S	GIKL	AILV	K	DE	IV	AG	K	E	V	AG	K	EN	A	AG	K	AELNT	A	AG
#9	ST	AG	L	K	GK	L	V	K	G	V	A	K	HLN	AIV	AG	K	AEGH	ALQ	ALMY	K
#10	AFKLQS	AFGILV	AG	K	FKS	ILV	AG	K	F	LV	AG	K	FT	LV	AG	K	DEFNQT	AGLQVY	AGILMY	K
#11	DEFGKST	ILV	AG	K	EFKT	IV	AG	K	ET	V	A	K	EHQT	AV	A	K	AEGHQT	AGLQV	AM	K
#12	ILM	KLMW	S	GIKL	AILV	K	F	V	A	K	L	A	A	K	LV	FLV	P	AS	ILV	FIKY
#13	KR	AFKLQS	AFGILV	AG	K	FKS	ILV	AG	K	F	LV	AG	K	FT	LV	AG	K	DEFNQT	AGLQVY	AGILMY
#14	K	DEFGKST	ILV	AG	K	EFKT	IV	AG	K	ET	V	A	K	EHQT	AV	A	K	AEGHQT	AGLQV	AM
#15	G	ILV	K	S	L	A	K	K	V	A	K	L	A	A	K	V	LV	CP	AGHS	ILV

5.5.3.3. Applying specific design criteria to guide the choice of amino acid

Each of the 15 parent peptides in Table 5-1 above yields millions of unique peptides sequences, not all of them may be active. Factors such as amino acid content, distribution and motif location will have an effect on the activity of the peptides. A review of literature reveals that common features of natural antimicrobial peptides include distribution of hydrophobic and hydrophilic amino acids, high content of cationic amino acids and cationic N-terminus (*148-154*). We then take into account these natural characteristics of AmPs to guide our choice of amino acid selection at each position from the parent peptide. The three different selection criteria utilized are:

- *Maximize Hydrophobicity:* At each position select the most hydrophobic amino acid. If there are more than one with the same hydrophobicity value then select one of them randomly.
- *Maximize Cationic Charge:* At each location select an amino acid with cationic charge. If there are more than one options select one of them randomly.
- *Mixed – Cationic Tail, Maximum Hydrophobicity:* For the first 5 positions apply maximim cationic charge and for the rest of 15 positions maximize hydrophobicity.

Applying these rules and counting how many times they are satisfied them (i.e. there are 20 positions but some of them are fixed with no choice of amino acids) we generated 3 sets of 15 peptides for each rule and then selected from each the top 5 sorted by highest number of rule satisfied. In total, 15 designed peptides, 5 satisfying different design criteria, were synthesized and tested for activity. To ensure that the bioactivity of the designed peptides is a direct result of their motif content, we created a negative control by shuffling their amino acid sequence and ensured that the shuffled control did not contain any of the motifs from the 667 large motif libraries.

The activity of the designed and shuffled peptides was measure against *E. coli, S. aureus, S. epidermidis,* and *P. aeruginosa.* We also tested the peptides' activity against a methicillin resistant strain of S. aureus (ATCC 700698, Mu3 designation) and measured their hemolytic activity as a measured of toxicity towards human cells.

5.5.4. Results and Discussion

5.5.4.1. Methods for the synthesis of peptides

The antimicrobial peptides are synthesized using solid phase Fmoc chemistry by the MIT Biopolymers Laboratory on the Intavis Multistep Synthesizer (San Marcos, CA). Briefly, the peptides are built backwards starting with tentagel resin, from the C-terminus to the N-terminus. After synthesis, the peptides are cleaved from the resin, yielding the crude form of the peptides. The peptides are provided as a dry powder and are used in their crude form (non-desalted). Mass spectrometry is used to confirm the

accuracy of the synthesis. Typical purities obtained in prior work with the synthesizer were greater than 85%.

5.5.4.2. Methods for MIC determination

A microdilution growth inhibition assay was used to determine the minimum inhibitory concentration of the peptides against 4 strains of bacteria *Escherichia coli,* Staphylococcus aureus, Staphylococcus epidermidis, and Pseudomonas aeruginosa. The microdilution assay is particularly suited to determine the MIC of our peptide library because the assay can test for a large number of peptides in a high-throughput manner. The assay proposed here was developed as a modification of the method described in NCCLS M-26A (Ref: NCCLS 1999) and by the Hancock laboratory.

Briefly, 10ul of serial dilutions of peptides in 0.2% Bovine Serum Albumin and 0.01% acetic acid are made at 10x the desired testing concentration, which ranges from 2 to 256ug/ml, in sterile polypropylene microtiter plates (Ref. 3790, Corning Inc., Corning, NY). Next, 90ul of $2x10^5$ to $7x10^5$ CFU/ml of bacterial suspension in Cation Adjusted Mueller Hinton II Broth (CMHB, Ref. 212322, BD, Franklin Lakes, NJ) are added. The cultures are incubated under mild shaking at 37 ^oC for 18 to 24 h. Cultures without the peptides are used as a negative control. The tests are carried out in duplicates. The MIC is determined based on visual inspection of optical density and is defined as the minimum peptide concentration that prevents growth.

5.5.4.3. Activity of existing AmPs

A total of 163 natural AmPs and designed peptides were used to identify a library of 667 motifs. The MIC of these peptides against the four pathogens, *E. coli, P. aeruginosa, S. epidermidis, S. aureus* is reported in Table 5-3. The activity distribution of those peptides is reported in Figure 5-9A. 29% of the tested peptides were ineffective at preventing growth of any of the four pathogens, even at concentrations up to 256ug/ml. This shows that the AmPs in listed in the antimicrobial peptide database are in fact not necessarily active. Other authors have showed that peptides classified as AmPs may in fact

act not be antimicrobial under physiological conditions but rather recruit and direct the response of the innate immune system (*148*). 71% of the peptides in the database demonstrated growth inhibition properties against one or more of the tested pathogens. Of those, 22% showed weak activity (256≥MIC>128ug/ml), 23% medium (128≥MIC>32ug/ml) and 25% showed strong activity (32ug/ml≥MIC).

Table 5-2: Activity table of the 163 tested natural AmPs.

Sequence	ID#	MIC [ug/ml]			
		E.coli	S.aureus	S.epi	P.aeru
AALKIGAKLLPKLVCKFKKK	CACD002	64	>256	128	128
AGKVLPSIFGLAAKLFPSVF	DT0007	>256	>256	>256	>256
AGLGKKVLPSIAGLAAKVFP	DT0002	>256	>256	>256	>256
AIKVLPSIFGLAAKVLPSII	HPCD005	>256	>256	>256	>256
ALWKDILKNVGKAAGKAVLNTVTDMVNQ	AP00163	256	>256	>256	NA
ALWKNMLKGIGKLAGKAALGAVKKLVGAES	AP00159	8	32	16	NA
ALWKNMLKGIGKLAGQAALGAVKTLVGAE	AP00165	32	64	128	NA
ALWKTIIKGAGKMIGSLAKNLLGSQAQPES	AP00164	64	64	128	NA
ALWKTLLKKVLKA-NH2	Dermaseptin	16	256	8	NA
ALWKTMLKKLGTMALHAGKAALGAAADTISQGTQ	AP00157	128	>256	>256	NA
ALWMTLLKKVLKAAAKALNAVLVGANA	AP00160	64	32	16	NA
AMWKDVLKKIGTVALHAGKAALGAVADTISQ	AP00293	256	256	>256	NA
APSIAKLAAKLFPSIAKAAA	CACD005	>256	>256	>256	>256
AVLKVGAKLLPAVICAISKK	A392	>256	>256	NA	>256
FFPIVAGVAGQVLKKIYCTISKKC	AP00455	256	32	32	NA
FGLPMLSILPKALCILLKRKC	AP00358	256	64	32	NA
FILKIGAKLVPAVFCKVTKR	C321	>256	>256	NA	>256
FLFPLITSFLSKVL	AP00408	>256	128	>256	NA
FLFRVASKVFPAIFCKLTKR	DT0001	64	32	16	64
FLFRVASKVFPALIGKFKKK	D51	128	32	16	NA
FLGGLIKIVPAMICAVTKKC	AP00513	256	32	32	NA
FLGGLMKAFPAIICAVTKKC	AP00515	>256	32	32	NA
FLGVVFKLASKVFPAVFGKV	D28	128	8	16	128
FLPAIAGVAAKFLPKIFCAISKKC	AP00466	256	32	64	NA
FLPAIFRMAAKVVPTIICSITKKC	AP00071	256	8	16	NA
FLPAIVGAAAKFLPKIFCVISKKC	AP00467	>256	16	32	NA
FLPAIVGAAGKFLPKIFCAISKKC	AP00454	256	16	32	NA
FLPFIAGMAAKFLPKIFCAISKKC	AP00463	128	16	32	NA
FLPFIAGVAAKFLPKIFCAISKKC	AP00465	128	8	16	NA
FLPFIARLAAKVFPSIICSVTKKC	AP00117	128	4	8	NA
FLPIIAGVAAKVFPKIFCAISKKC	AP00469	256	8	16	NA
FLPIIASVAAKVFPKIFCAISKKC	AP00472	256	8	16	NA
FLPIIASVAAKVFSKIFCAISKKC	AP00470	>256	16	16	NA
FLPIIASVAANVFSKIFCAISKKC	AP00471	>256	128	128	NA
FLPILINLIHKGLL	AP00111	>256	>256	>256	NA
FLPIVGKLLSGLL	AP00112	>256	>256	>256	NA
FLPLFASLIGKLL	AP00105	>256	64	256	NA
FLPLIGKVLSGIL	AP00098	>256	256	256	NA

FLPLLAGLAANFLPKIFCKITRKC	AP00073	128	8	16	NA
FLPLLAGLAANFLPTIICKISYKC	AP00090	>256	>256	>256	NA
FLPMLAGLAASMVPKLVCLITKKC	AP00461	>256	8	32	NA
FVLKIGAKLLPSVVCLVTRK	A046	>256	128	NA	>256
FWGALIKGAAKLIPSVVGLFKKKQ	AP00390	64	4	8	NA
GAAAKIAAKVLPAIFCKIKK	CACD004	128	>256	>256	128
GCWSTVLGGLKKFAKGGLEAIVNPK	AP00425	256	>256	256	NA
GEKLKKIGQKIKNFFQKL	AP00499	256	>256	64	NA
GFLGPLLKLAAKGVAKVIPHLIPSRQQ	AP00424	64	16	16	NA
GFVDFLKKVAGTIANVVT	AP00262	>256	>256	>256	NA
GFVDLAKKVVGGIRNALGI	AP00317	>256	>256	>256	NA
GGLKKLGKKLEGVGKRVFKASEKALPVLTGYKAIG	AP00133	2	>256	>256	NA
GIGAAILSAGKSIIKGLANGLAEHF	AP00053	>256	256	>256	NA
GIGALSAKGALKGLAKGLAEHFAN	AP00049	>256	>256	>256	NA
GIGASILSAGKSALKGFAKGLAEHFAN	AP00419	256	>256	>256	NA
GIGASILSAGKSALKGLAKGLAEHFAN	AP00050	256	>256	>256	NA
GIGGALLSAGKSALKGLAKGLAEHFAN	AP00054	256	>256	>256	NA
GIGGKILSGLKTALKGAAKELASTYLH	AP00060	32	32	16	NA
GIGGVLLSAGKAALKGLAKVLAEKYAN	AP00061	128	16	32	NA
GIGTKILGGVKTALKGALKELASTYAN	AP00058	32	256	64	NA
GILDFAKTVVGGIRNALGI	AP00319	>256	>256	>256	NA
GILDSFKGVAKGVAKDLAGKLLDKLKCKITGC	AP00118	128	>256	>256	NA
GILDSFKQFAKGVGKDLIKGAAQGVLSTMSCKLAKTC	AP00093	256	>256	>256	NA
GILDTLKQFAKGVGKDLVKGAAQGVLSTVSCKLAKTC	AP00088	256	>256	>256	NA
GILDVAKTLVGKLRNVLGI	AP00322	256	256	128	NA
GILLDKLKNFAKTAGKGVLQSLLNTASCKLSGQC	AP00078	256	>256	>256	NA
GIVDFAKKVVGGIRNALGI	AP00316	256	>256	>256	NA
GIWGTALKWGVKLLPKLVGMAQTKKQ	AP00389	64	8	8	NA
GKAAKIAAKVVPAIICLILK	MXCD004	256	128	64	256
GKKVLPTVAKLAAKLLPSIF	DT0008	>256	>256	>256	>256
GKLLPSIFGLAAKLVPSVYA	DT0009	>256	>256	>256	>256
GLFDIAKKVIGVIGSL	AP00019	>256	>256	256	NA
GLFDIIKKIAESI	AP00012	>256	>256	>256	NA
GLFDIIKKVASVIGGL	AP00353	>256	>256	>256	NA
GLFDIVKKIAGHIAGSI	AP00020	256	>256	>256	NA
GLFDIVKKIAGHIVSSI	AP00022	256	256	128	NA
GLFDIVKKVVGTIAGL	AP00017	>256	>256	>256	NA
GLFDVIKKVASVIGGL	AP00351	256	256	256	NA
GLFGVLGSIAKHVLPHVVPVIAEK	AP00248	>256	>256	>256	NA
GLFKVLGSVAKHLLPHVVPVIAEK	AP00247	>256	256	>256	NA
GLFLDTLKGAAKDVAGKLEGLKCKITGCKLP	AP00115	>256	>256	>256	NA
GLFSVLGAVAKHVLPHVVPVIAEK	AP00245	>256	>256	>256	NA
GLKIGAKLVPSIFCAITRKC	DT0006	>256	>256	>256	>256
GLLDIVKKVVGAFGSL	AP00014	>256	>256	256	NA
GLLDSIKGMAISAGKGALQNLLKVASCKLDKTC	AP00508	>256	>256	>256	NA
GLLDSLKGFAATAGKGVLQSLLSTASCKLAKTC	AP00075	>256	>256	>256	NA
GLLDTIKGVAKTVAASMLDKLKCKISGC	AP00120	256	>256	>256	NA
GLLGVLGSVAKHVLPHVVPVIAEHL	AP00241	>256	256	>256	NA
GLLRKGGEKIGEKLKKIGQKIKNFFQKLVPQPEQ	AP00281	64	>256	>256	NA
GLLNTFKDWAISIAKGAGKGVLTTLSCKLDKSC	AP00091	256	>256	>256	NA
GLLQTIKEKLESLESLAKGIVSGIQA	AP00263	>256	>256	>256	NA
GLLSKVLGVGKKVLCGVSGLC	AP00507	32	256	32	NA
GLLSSLSSVAKHVLPHVVPVIAEHL	AP00243	>256	>256	>256	NA
GLLSVLGSVAKHVLPHVVPVIAEHL	AP00240	>256	128	256	NA
GLLSVLGSVAKHVLPHVVPVIAEKL	AP00345	>256	128	256	NA
GLLSVLGSVAQHVLPHVVPVIAEHL	AP00242	>256	>256	>256	NA
GLLSVLGSVVKHVIPHVVPVIAEHL	AP00244	>256	256	>256	NA
GLMSVLGHAVGNVLGGLFKS	AP00434	>256	128	128	NA
GLVSSIGKALGGLLADVVKTKEQPA	AP00251	>256	>256	>256	NA
GTLAGLASKVLPSVFCMFQT	DT0017	>256	256	64	>256
GVFLDALKKFAKGGMNAVLNPK	AP00426	>256	>256	>256	NA
GVIDAAKKVVNVLKNLP	AP00325	>256	>256	>256	NA
GVLSNVIGYLKKLGTGALNAVLKQ	AP00209	128	256	256	NA
GWASKIGQTLGKIAKVGLKELIQPK	AP00239	64	>256	256	NA
GWGSFFKKAAHVGKHVGKAALHTYL	AP00166	64	>256	128	NA
GWGSFFKKAAHVGKHVGKAALTHYL	AP00493	32	256	256	NA
GWLRKAAKSVGKFYYKHKYYIKAAWQIGKHAL	AP00330	2	32	4	NA
HRRRHILGHIAKGAHIAGKILWGFF	AP00339-Rev	8	16	16	NA
ILGPVLGLVGNALGGLIKKI	AP00526	>256	256	>256	NA
ILGPVLSLVGNALGGLLKNE	AP00065	>256	>256	>256	NA

ILQKAVLDCLKAAGSSLSKAAITAIYNKIT	AP00510	>256	NA	256	>256
INLKAIAALAKKLL	AP00448	128	NA	128	256
INLKALAALAKKIL	AP00201	128	NA	128	256
INVLGILGLLGKALSHL	AP00070	>256	NA	64	64
ISRLAGLLRKGGEKIGEKLKKIGQKIKNFFQKLVPQPE	AP00498	64	NA	256	>256
IVAKVAAKVVPAIICLITKD	HPCD003	256	>256	128	128
KIAKVGAKVLPSVICLILKR	M587	256	256	NA	256
KIGAKVLPSVFGLAAKVVCA	MXCD005	>256	>256	256	>256
KIKWFKTMKSIAKFIAKEQMKKHLGGE	AP00517	2	NA	32	256
KKLAKVAAKVVPAIICLILK	MXCD001	64	128	32	64
KKLAKVAAKVVPAIICLITT	MXCD003	256	256	64	128
KKLAKVGAKVVPSIICAVTK	M724	256	>256	NA	>256
KLAKLAKKLAKLAK	AP00506	256	NA	>256	>256
KLAKLGAKVLPAIICKLKKK	C706	256	256	NA	>256
KLFGIGSKVVPAVVCAVTKR	M386	256	>256	NA	>256
KVAKLAAKVVPAVICAVTKR	M600	256	256	NA	>256
KVFGLGSKVLPSIVCLILKR	M375	256	256	NA	256
KVLGLAAKVVPAVYCKATRK	C568	>256	>256	NA	>256
LGAVLKVASKVLPSVFCAIA	A725	>256	>256	NA	128
LGKALKIGAKLLPKLVCKFK	CACD003	16	64	64	>256
LGVASKVLPSVAGLAAKVFC	DT0003	>256	>256	>256	>256
LGVILGIAAKVVPAIICLIL	HPCD001	>256	>256	>256	>256
LKNVAKLGAKVLPSLFCKIL	DT0018	256	128	>256	>256
LLKELWTKIKGAGKAVLGKIKGLL	AP00384	64	NA	16	256
LLPILGNLLNGLL	AP00096	>256	NA	>256	>256
LLPIVGNLLKSLL	AP00095	>256	NA	>256	>256
LLPNLLKSLL	AP00100	>256	NA	256	>256
NFLGTLINLAKKIM	AP00110	256	NA	128	256
NLAKLAAKVLPSIFCAFQKK	DT0013	>256	>256	>256	>256
PKAFKLGSKVLPSIFCKVTK	DT0016	>256	>256	>256	>256
PVAFGIAAKVLPAIYCSATR	DT0015	>256	>256	>256	>256
SALKIAAKVLPAVICKIKKK	C618	256	256	NA	>256
SALKKGAKLLPKLVGKFKKK	CACD001	>256	>256	>256	>256
SALKKVAKVAAKVVPAIICL	MXCD002	128	256	128	256
SIGAKILGGVKTFFKGALKELASTYLQ	AP00062	64	NA	64	64
SIGSALKKALPVAKKIGKIALPIAKAALP	AP00414	64	NA	256	>256
SLFSLIKAGAKFLGKNLLKQGACYAACKASKQC	AP00085	32	NA	32	32
SLGGVISGAKKVAKVAIPIGKAVLPVVAKLVG	AP00416	>256	NA	>256	>256
SLGSFLKGVGTTLASVGKVVSDQFGKLLQAGQ	AP00315	>256	NA	>256	>256
SMLSVLKNLGKVGLGFVACKINKQC	AP00114	128	NA	64	64
SMLSVLKNLGKVGLGLVACKINKQC	AP00122	128	NA	64	128
SVVKKGGKVLPKLVGKLKKK	C724	>256	>256	NA	>256
TAFKLGKKVLPSIFCLITRK	DT0012	256	128	64	128
TVLKIGAKLLPSIVCAVTRK	A012	>256	>256	NA	>256
TVLKNGAKVLPKVVCKITKR	DT0020	>256	>256	>256	>256
TVVKIGAKVLPSIICAITKK	HPCD002	>256	>256	128	256
VAKLLPSVFGLAAKLVPAIF	DT0005	>256	>256	>256	>256
VILKIGAKVVPSVVCLILKK	HPCD004	256	>256	64	128
VIPFVASVAAEMQHVYCAASRKC	AP00072	>256	NA	>256	>256
VLPIIGNLLNSLL	AP00097	>256	NA	>256	>256
VLPLISMALGKLL	AP00109	>256	NA	256	256
VVLKIGAKLLPKLVCLVSKD	A076	>256	>256	NA	256
WLGSALKIGAKLLPSVVGLFKKKKQ	AP00386	32	NA	2	2
WLGSALKIGAKLLPSVVGLFQKKKK	AP00387	32	NA	4	4
WLPTLFGIGSKLLPAVICKI	DT0014	>256	>256	256	256

NA = data not available

>256 = MIC value is above 256 ug/ml and could not be measured

5.5.4.4. Activity of the designed peptides

The activity of fifteen *de novo* AmPs designed in section 5.5.3.3 was measured using the standard MIC protocols against found pathogens (Table 5-2). Their activity distribution is reported in Figure 5-9B. 27% of the designed peptides did not show any activity against any of the four pathogens. 13% of the designed peptides show strong activity against a least one of the peptide with MIC <32ug/ml, and 53% had medium activity while only 7% of the designed peptides had weak activity.

The addition of peptide activity information and design criteria to the algorithm resulted in significantly higher success in designing active peptides. We used the peptides designed in previous work (*143*) as point of comparison. Only 45% of those designed peptides were active when the "blind" design algorithm was used (Figure 5-9D). A higher portion of those peptides had weak activity (18%) and only 5% showed strong activity. Thus, factoring in peptide activity information and design criteria had a strong positive impact on increasing the success rate of the design algorithm.

It appears that the current algorithm is successful at designing peptides with at least medium activity (66%) but it not yet optimized to exclusively design peptides with strong activity. While strong, medium and weak motifs were incorporated in the design of parent peptides, using strong motifs only would not necessarily increase the activity of our designed peptides. That is because the algorithm already selected for fifteen parent peptides with the strongest motifs content (Table 5-1). One approach to further increase the activity of our designed peptides is to refine the peptide leads using the optimizing techniques described in section 5.3.1. This second tier optimization strategy to peptide design has already been demonstrated by other authors (*26*). Thus the value of the improvements made to the peptide design algorithm lie in the ability to design diverse therapeutic leads with a higher rate of success (73% versus 45%) in with higher levels of antimicrobial activity (66% medium and strong peptides versus only 27%).

5.5.4.5. *Activity of the shuffled peptides*

To demonstrate that the activity of the peptide lies in the conserved motifs, we measured the MIC of shuffled versions of those peptides. The shuffled peptides have the same amino acid content and bulk physical and chemical properties as their unshuffled counterparts except that they do not contain any conserved motifs in their amino acid sequence. The MIC of the shuffled peptides is shown in Table 5-1 and their activity distribution in Figure 5-9C. 73% of the shuffled peptides show no activity against any of the four tested pathogens, while only 7% and 20% had weak and medium activity. None of the shuffled peptides had strong activity. These results show that elimination of the conserved sequences by shuffling the amino acid sequence destroys the activity of the peptides. As a result, we infer that the conserved motifs encode for antimicrobial activity since we demonstrate that simple alignment of these motifs predominantly leads to peptides with antimicrobial activity and that shuffling of the sequences.

Table 5-3: Hemolytic activity and MIC of designed and shuffled peptides against E. coli, P. aeruginosa, S. epidermidis, S. aureus and MRSA.

ID#	Sequence	MIC (ug/ml)					HC_{50}
		EC	PA	SE	SA	MRSA	(ug/ml)
Designed Peptide							
J9072.C2	KKLGKKIGKTVAKHVAKHGA	+	+	+	+	+	512
J9072.C3	KVGKKIGKTVAKHAAKHLMK	+	+	+	+	+	512
J9072.C4	TGLKKLVKGVAKHAAKHLLK	256	256	256	+	+	64
J9072.C5	IGKKVGKTVAKTVAKHVAKH	+	+	+	+	+	512
J9072.C6	TALKKLAKGVAKHVAKHLYK	128	256	256	+	+	256
J9072.C7	KLVGKFVGKFLGKTLGKFVI	128	256	128	+	256	8
J9072.C8	IMSLIKFVAKLAAKLLPSVI	256	+	64	64	64	8
J9072.C9	FIGKFIAKFLGKTVGKTLLK	64	128	64	64	256	4
J9072.C10	IGKFVGKFLGKFLAKTVGKT	256	256	128	128	+	32
J9072.C11	AKFIAKFVAKFLAKTLGKFV	+	+	256	+	+	4
J9072.C12	KKFAKFIAKFVGKFLGKFLI	16	16	16	16	16	4
J9072.D1	KSKVKFVAKLAAKVVPSIVC	128	256	128	+	+	512
J9072.D2	KVGKKVGKFLAKTVGKTLLK	128	128	128	+	+	512
J9072.D3	KKIAKTVAKTVAKHAAKAVA	+	+	+	+	+	512
J9072.D4	IKSKLKFVAKLAAKLVPSII	32	64	32	128	+	256
Shuffled Peptide							
J9098.E5	AKHIAKKGLVKGHTAVKGKK	+	+	+	+	+	512
J9098.E6	VKAAKLHVMKHTIKAKKGGK	+	+	+	+	+	512
J9098.E7	GKHKVLVKKAHALTKALLGK	+	+	+	+	+	256
J9098.E8	VGVKTGVAKHKKTIKAVAKH	+	+	+	+	+	512

J9098.E10	VFGKLFLVKGGGTVKLKFIK	+	+	256	+	+	512
J9098.E11	VIIMALPLSVKILSAKLKAF	+	+	+	+	+	512
J9098.E12	ATFKFLKTLGFLIKIKVGGK	64	256	256	64	+	8
J9098.F1	VLFIGKFGTFGKKKLKVGAT	+	+	+	+	+	512
J9098.F2	VVKLKLKAGFFKIFAFATAK	128	+	+	+	128	4
J9098.F3	AKKKIIVFGFFFLAKKKGLF	64	256	+	64	+	4
J9098.F4	ACKLFIVASKVSPVAKKVVK	+	+	+	+	+	512
J9098.F5	KTGVGAKFKKKKLVLGVLKT	+	+	+	+	+	512
J9098.F6	AKAKVKATVKHKATVAKIAA	+	+	+	+	+	512
J9098.F7	KKLIISAVPKAKFLASIVLK	+	+	+	+	+	512

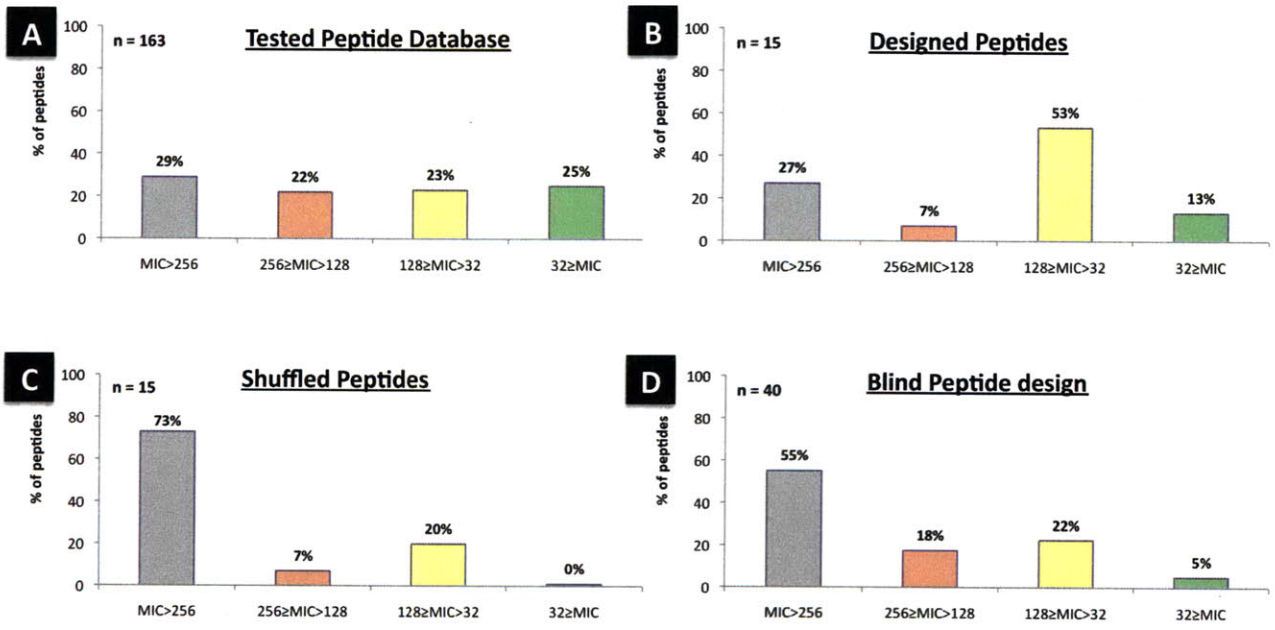

Figure 5-9: MIC activity distribution for (A) database of existing peptide, (B) designed peptides, (C) their shuffled peptides equivalent; and (D) the blind peptide designs from (143).

5.5.4.6. Specificity of the designed peptides

Two of the 15 designed peptides (J9072.C12, J9072.D4) showed strong activity against three or more pathogens. J9072.C12 is particularly strong and has an unusually broad activity spectrum with MIC values of 16ug/ml across all four tested organism, both gram positive and gram negative (Figure 5-10). The design algorithm here uses *E. coli* MIC values to rank the motif strength (see Figure 5-5:). As a result the designed peptides tend towards higher activity against *E. coli* with ten active peptides (Figure 5-10).

Also, the designed peptides are also slightly more active against gram-negative pathogens (EC and PA) then against gram-positive pathogens (SE, SA).

The algorithm allows changing the motif ranking criteria from the $MIC_{E.\ coli}$ to any other kind of activity measurement. For example, the motifs could be ranked to maximize their activity on *S. aureus* or gram-positive pathogens, or to minimize mammalian toxicity. The incorporation of activity information could thus enable us to control the selectivity and targeting of the designed peptides via the selection and ranking of the conserved motifs used by the algorithm.

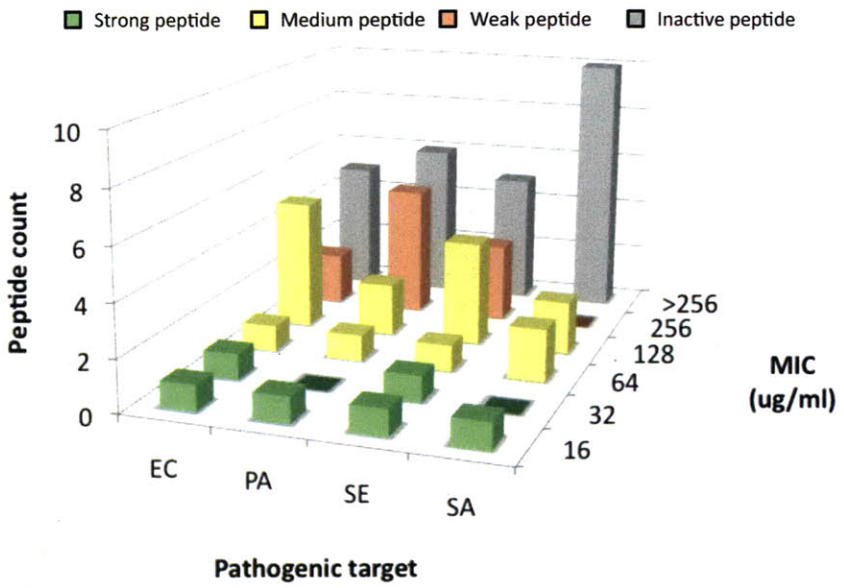

Figure 5-10: MIC activity distribution for the designed peptides against the different pathogens tested. In green are strong peptides with MIC≤32ug/ml, in yellow medium peptides with 32<MIC≤128ug/ml and in red 128ug/ml<MIC≤256ug/ml. The peptides were designed using an algorithm that favors activity against E. coli. Thus, the designed peptides tend to have slightly higher activity towards E. coli and gram-negative pathogens.

Controlling the motifs used by the algorithm via an activity ranking is one of two parameters to control selectivity of the designed peptides (Figure 5-6:). The second parameter lies in enforcement of specific design parameters to guide the choice of amino acid in parent peptides (section 5.5.3.3). In this

iteration of the algorithm, we enforced general design criteria but one can imagine a different choice of different amino to modify the specificity of the peptides for example.

5.5.4.7. Methods for measuring the hemolytic toxicity

Systemic antibiotics require a large drug dosage to maintain therapeutic concentration throughout the body. At such therapeutic concentrations, many peptides could impart significant toxicity to human hosts. The first toxicity screen typically carried out is used to look for hemolytic activity. Hemolytic activity is defined as the maximum peptide concentration at which less than 50% hemolysis of Human Red Blood Cells (HC_{50}) occurs as measured using standard high-throughput methods. A high value for HC_{50} thus implies that the peptide is less toxic.

Briefly, 20 ul of serial dilutions of peptides in 0.2% Bovine Serum Albumin and 0.01% acetic acid are made at 5x the desired testing concentration, which ranges from 4 to 512 ug/ml, in sterile microtiter plates. A stock of human red blood cells (Ref. R407-0050, Rockland, Gilbertsville, PA) is diluted by 40x with a buffer of 150 mM NaCl and 10 mM Tris at pH 7.0. Next, 80 ul of the red blood cell solution is added to the peptides and incubated for 1 hour at 37 °C after which the cells are centrifuged and spun down at 6000 G. The tests are carried out in duplicates. The HC_{50} is determined based on visual inspection of optical density and is defined as the maximum peptide concentration at which less than 50% hemolysis occurs.

5.5.4.8. Toxicity of the designed peptides

The 50% hemolytic concentration of the designed peptides was measured and is reported in Table 5-3. The balance between antimicrobial agents activity towards bacterial cells and their toxicity is measured by computing the therapeutic index.

Therapeutic Index = Hemolysis concentration (HC_{50}) / Antimicrobial concentration (MIC)

We used the lowest MIC value against the four pathogens as antimicrobial concentration to calculate the therapeutic index for active designed peptides in Table 5-3. The therapeutic index of the designed peptides is reported in Table 5-4. The therapeutic index ranges from a value of 0.06 for J9072.C9 to a value of 8 for J9072.D4. The therapeutic index indicated the range of peptide concentration for which antimicrobial activity is achieved and before hemolysis occurs. Seven of the ten designed peptides have therapeutic indexes <1 indicating that they may also induce hemolysis at their active concentration. The other peptides had a therapeutic range >1, which implies the peptides has higher affinity toward bacterial cells. J9072.D4 is particularly interesting because it is both strong activity (32 ug/ml) and extremely low toxicity (254ug/ml). Several optimization strategies could be implement to reduce the hemolytic activity of the designed peptides. The current design algorithm does currently account peptide toxicity. One approach would be to incorporate toxicity information in the design algorithm to select for motifs that are associated with peptides of lower toxicity. Another approach would be to increase the therapeutic index by modification of the peptide terminus as reported previously other authors (*26*). These is methods would help reduce toxicity concerns and design peptides that specifically target bacterial cells.

Table 5-4: Therapeutic index (TI) of active designed peptides. The therapeutic index is calculated as the ratio between the MIC antimicrobial concentration and HC_{50} hemolytic concentration.

ID#	Sequence	MIC	HC_{50}	TI
J9072.C4	TGLKKLVKGVAKHAAKHLLK	256	64	0.25
J9072.C6	TALKKLAKGVAKHVAKHLYK	128	256	2
J9072.C7	KLVGKFVGKFLGKTLGKFVI	128	8	0.06
J9072.C8	IMSLIKFVAKLAAKLLPSVI	64	8	0.12
J9072.C9	FIGKFIAKFLGKTVGKTLLK	64	4	0.06
J9072.C10	IGKFVGKFLGKFLAKTVGKT	128	32	0.25
J9072.C11	AKFIAKFVAKFLAKTLGKFV	16	4	0.25
J9072.C12	KKFAKFIAKFVGKFLGKFLI	128	4	0.03
J9072.D2	KVGKKVGKFLAKTVGKTLLK	128	512	4
J9072.D4	IKSKLKFVAKLAAKLVPSII	32	256	8

5.6. Chapter conclusion

In this chapter, we present a method to combine conserved motifs in the sequence of AmPs to create novel peptides with antimicrobial activity. We first measured the antimicrobial activity of starting database of 163 peptides and assigned the identified motifs to different zones of antimicrobial activity. We then tile the motifs to form 20-mer parent peptides and selected the fifteen parents peptide with the highest representation of the motifs belonging to the strong antimicrobial activity zone. We applied specific design criteria to guide the selection of amino acid in the parent peptide. These specific criteria tried to mimic naturally occurring peptides and maximized hydophobicity or cationic charge. One major benefit of the methodology presented is the low cost of computations to design the peptides with desired properties. Instead of enumerating all possible outcomes and clustering them, we rank the parent peptides. The specific design step further reduces the number actual peptide instances to those that are more likely to be active. Finally, the incorporation of the antimicrobial activity information and specific design criteria resulted in an algorithm that was significantly more successful at designing active peptides (73% success rate instead of 45%).

5.7. References

1. M. Zasloff, B. Martin, H. C. Chen, in *Proc Natl Acad Sci USA.* (1988), vol. 85, pp. 910-3.
2. J. M. Park, J. E. Jung, B. J. Lee, in *Biochem Biophys Res Commun.* (1994), vol. 205, pp. 948-54.
3. J. D. King *et al.*, in *Comp Biochem Physiol C Toxicol Pharmacol.* (2005), vol. 141, pp. 393-7.
4. U. Silphaduang, E. J. Noga, in *Nature.* (2001), vol. 414, pp. 268-9.
5. H. Shike *et al.*, in *Eur J Biochem.* (2002), vol. 269, pp. 2232-7.
6. M. Zasloff, in *Nature.* (2002), vol. 415, pp. 389-95.
7. P. H. Mygind *et al.*, in *Nature.* (2005), vol. 437, pp. 975-80.
8. T. J. Falla, R. E. Hancock, in *Antimicrob Agents Chemother.* (1997), vol. 41, pp. 771-5.
9. M. Wu, R. E. Hancock, in *Antimicrob Agents Chemother.* (1999), vol. 43, pp. 1274-6.
10. Y. Park *et al.*, in *Biochem Biophys Res Commun.* (2004), vol. 321, pp. 631-7.
11. K. Hilpert, R. Volkmer-Engert, T. Walter, in *Nat Biotechnol.* (2005).
12. H. Wakabayashi *et al.*, in *Antimicrob Agents Chemother.* (1999), vol. 43, pp. 1267-9.
13. C. Loose, in *MIT PhD Archive.* (2007).
14. J. R. Walker, J. R. Roth, E. Altman, in *J Pept Res.* (2001), vol. 58, pp. 380-8.
15. D. Raventós *et al.*, in *Comb Chem High Throughput Screen.* (2005), vol. 8, pp. 219-233.
16. R. A. Houghten *et al.*, in *Nature.* (1991), vol. 354, pp. 84-6.
17. D. Raventos *et al., Comb Chem High Throughput Screen* **8**, 219 (2005).
18. A. R. Koczulla, R. Bals, *Drugs* **63**, 389 (2003).
19. A. Tossi, M. Scocchi, B. Skerlavaj, R. Gennaro, in *FEBS Lett.* (1994), vol. 339, pp. 108-12.
20. I. Zelezetsky, U. Pag, N. Antcheva, H.-G. Sahl, A. Tossi, in *Arch Biochem Biophys.* (2005), vol. 434, pp. 358-64.
21. T. Sigurdardottir *et al.*, in *Antimicrob Agents Chemother.* (2006), vol. 50, pp. 2983-2989.
22. O. Taboureau, O. Olsen, J. Nielsen, in *Chemical Biology and Drug Design.* (2006).
23. A. Cherkasov *et al.*, in *ACS Chem Biol.* (2009), vol. 4, pp. 65-74.
24. T. Ganz, in *Nat Rev Immunol.* (2003), vol. 3, pp. 710-20.
25. M. E. Selsted, A. J. Ouellette, in *Nat Immunol.* (2005), vol. 6, pp. 551-7.

26. J. Orivel, in *Journal of Biological Chemistry*. (2001), vol. 276, pp. 17823-17829.

27. N. Y. Yount, in *Proceedings of the National Academy of Sciences*. (2004), vol. 101, pp. 7363-7368.

28. A. Guder, I. Wiedemann, H. G. Sahl, in *Biopolymers*. (2000), vol. 55, pp. 62-73.

29. N. Mandard, P. Bulet, A. Caille, S. Daffre, F. Vovelle, in *Eur J Biochem*. (2002), vol. 269, pp. 1190-8.

30. R. E. W. Hancock, H.-G. Sahl, in *Nat Biotechnol*. (2006), vol. 24, pp. 1551-1557.

31. C. Loose, K. Jensen, I. Rigoutsos, G. Stephanopoulos, in *Nature*. (2006), vol. 443, pp. 867-869.

32. H. G. Boman, in *Jounral of Internal Medicine*. (2003), pp. 197-215.

33. K. Jensen, in *MIT PhD Thesis*. (2006), pp. 1-490.

34. C. Loose, K. Jensen, I. Rigoutsos, in *Nature*. (2006).

35. I. Rigoutsos, A. Floratos, in *Bioinformatics*. (1998), vol. 14, pp. 55-67.

36. Z. Wang, G. Wang, in *Nucleic Acids Res*. (2004), vol. 32, pp. D590-2.

37. A. Bairoch, *Bioinformatics* **16**, 48 (2000).

38. G. Wang, X. Li, Z. Wang, in *Nucleic Acids Res*. (2009), vol. 37, pp. D933-D937.

39. A. Barry *et al.*, in *Clinical and Laboratory Standards Institute*. (1999), vol. 19, pp. M26-A.

40. R. E. Hancock, *Lancet Infect Dis* **1**, 156 (2001).

41. T. Ganz, *C R Biol* **327**, 539 (2004).

42. R. E. Hancock, *Expert Opin Investig Drugs* **9**, 1723 (2000).

43. M. Zasloff, *Nature* **415**, 389 (2002).

44. R. E. Hancock, A. Rozek, **206**, 143 (2002).

45. N. Sitaram, R. Nagaraj, *Curr Pharm Des* **8**, 727 (2002).

46. M. Papagianni, *Biotechnol Adv* **21**, 465 (2003).

Chapter 6. Mechanism and resistance to Ponericin antimicrobial peptides

6.1. Executive summary

The development of new AmP-based therapeutics requires an understanding of the targets and mode of action of the peptides. These issues are addressed in this chapter by studying the AmP family of ponericins, and focusing specifically on ponericin G1.

- In section 6.2, we argue that the MIC is an incomplete determinant for the antimicrobial potential as AmPs and that cell viability is more a representative measurement for bactericidal activity.
- In section 6.3, we screen a panel of AmPs for bactericidal activity against *E.coli* and *S.aureus* We selected a series of four AmPs with strong growth inhibition and bactericidal activity for further mechanistic studies – ponericin G5, ponericin W3 and the natural and amidated versions of ponericin G1.
- In section 6.4, we study the stress response caused by these AmPs on the membrane of *E.coli* using a novel high speed AFM and a microfluidic device to visualize the cellular membrane disruption.
- In section 6.5, we identify two sensing pathways that play an important role in allowing the cell to resist the cidal activity of these AmPs. We also show that cells who are enable to engage the SOS response through recA were more susceptible in section 6.6.
- In section 6.3.2, we explore in greater details the effect of C-terminal amidation of ponericin G1 and show that C-terminal amidation results in a change in the mode of action and cidal activity.
- In section 6.7, we correlate using DNA micro arrays these changes in cidal activity with differences in the gene regulation that the cell undergo when stressed with natural and amidated version of ponericin G1. We concluded that the bacteriostatic amidated ponericin G1 acts on the

iron import system and subsequently slows down the TCA cycle while the bactericidal natural ponericin G1 targets tRNAs synthetases in the ribosome.

- In section 6.8, we apply this newly gained mechanistic knowledge to design a synergistic therapeutic treatment using natural ponericin G1 as adjuvant to kanamycin, antibiotic also targeting the ribosome. The combination treatment results in a 10-fold increase in bacterial killing over kanamycin treatment alone.

The work described in this chapter was performed in close collaboration with Dr. Michael Koeris and Dr. Timothy Lu from the laboratory of James Collins at Boston University. The results of this collaboration particular regarding the differences in mechanism between the natural and the amidated versions of ponericin G1 constitute a manuscript in progress.

6.2. Current understanding of AmP mechanism

Albeit the growing interest in developing AmPs as novel therapeutics, relatively little is know as to their mechanism of action. This is because there are many different families and classes of AmP and each have different targets and mode of action. Some AmP cause disruption of the cell membrane (*1, 2*), others acts on intracellular targets (*1*), or act by recruiting and boosting the host innate immune system (*3*). Before AmPs can be developed as therapeutics, there is thus a need for a clearer understanding of their mechanism of action. The work described in this chapter offers some understanding particularly focusing on the family of ponericins isolated from ant venom (*4*).

6.2.1. MIC incomplete determinant for antimicrobial activity

The scientific community typically compares the therapeutic potential of AmPs using minimum inhibitory concentration assays (MIC) (*5*). The MIC is the lowest concentration at which the peptide prevents growth of an inoculum of 10^5 cells/ml of exponentially growing bacteria. Using the MIC as determinant for antimicrobial activity provides many benefits:

- the MIC determination can be performed in a fast high throughput manner using micro-dilution assays, thereby testing large libraries of peptides is feasible.
- MIC determination is can be standardized such that the MIC obtained by different researchers can easily be compared to one another – at least, theoretically as the community still needs to decide which protocol to use.
- the MIC is a familiar notion in the field of antimicrobial discovery and development since many small molecule antibiotics also compared using this standard.
- finally, MIC values do provide useful information regarding the peptides antimicrobial ability to inhibition growth.

Thus, the MIC provides a single quantifiable and easily measurable point of comparison among different peptides. However, there are also many drawbacks to using MIC as sole determinant for antimicrobial activity:

- lack of information on actual killing of the bacterial cells, which is the true criteria for determining antimicrobial activity.
- lack of differentiation between bacteriostatic and bactericidal activity.
- lack of any kinetics consideration considerations

Based on this understanding, the MIC measurements were thus used as a first screening method that was complement with in-depth studies to evaluate the peptides bactericidal and kinetics properties.

6.3. Bactericidal activity of antimicrobial peptides

While growth inhibition properties in AmPs are necessary characteristics, they are not sufficient to assess the full antimicrobial potential of the peptides. The family of ponericin AmPs was selected for further studies based on its generally low MIC values against *E. coli* (EC) and *S. aureus* (SA) (Table 2-1).

Table 6-1: MIC (ug/ml) and bactericidal activity of natural and amidated ponericins against E. coli (EC) and S. aureus (SA)

Name	Sequence	MIC		Cidality	
		EC	SA	EC	SA
PonG1	**GWKDWAKKAGGWLKKKGPGMAKAALKAAMQ**	**2**	**8**	**Rebound**	**Cidal**
PonG1-NH2	**GWKDWAKKAGGWLKKKGPGMAKAALKAAMQ-NH2**	**2**	**4**	**Static**	**Cidal**
PonG5	GLKDWVKIAGGWLKKKGPGILKAAMAAATQ	16	64	Rebound	Reboun
PonG7-NH2	GLVDVLGKVGGLIKKLLPG-NH2	16	8	Rebound	Static
PonW2	WLGSALKIGAKLLPSVVGLFQKKKK	32	4	Static	Static
PonW3	GIWGTLAKIGIKAVPRVISMLKKKKQ	8	4	Cidal	Cidal
PonW3-NH2	GIWGTLAKIGIKAVPRVISMLKKKKQ-NH2	64	8	Cidal	Cidal
PonW4	GIWGTALKWGVKLLPKLVGMAQTKKQ	64	4	Cidal	Cidal
PonW5	FWGALIKGAAKLIPSVVGLFKKKQ	+	256	Cidal	Cidal
PonW6	FIGTALGIASAIPAIVKLFK	+	16	Static	Static
PonW6-NH2	FIGTALGIASAIPAIVKLFK-NH2	25	+	Rebound	Cidal

6.3.1. Study of the ponericin family

The kinetic and bactericidal properties of ponericins was assessed by exposing a exponentially growing bacterial culture at 10^8CFU/ml (OD_{600}=0.4) to 10-fold excess of the peptide's MIC reported in Table 2-1. A sample of the treated culture was removed at desired time points and the number of viable cells was counted by plating ten-fold dilutions on growth agar overnight. The kill curve for each AmP is shown in Figure 2-2. Three distinct bactericidal behaviors are observed: static AmPs, rebounding AmPs, and cidal AmPs.

PonW2, PonW6 and PonG1-NH2 are all static AmPs (Figure 2-2A). With an MIC value above >512ug/ml, PonW6 is barely effective against *E. coli*. On the other hand, PonG1-NH2 has a very low MIC against *E. coli* of 2ug/ml (and against staph. aureus 4ug/ml) but does not show any cidal activity against *E. coli* even at concentrations 10-fold above its $MIC_{E.coli}$, which is 40ug/ml. PonG1-NH2 's action on *E. coli* is thus purely bacteriostatic. However when tested against *Staph. aureus* (Figure 2-2D), PonG1-NH2 shows very strong bactericidal properties also 10-fold its $MIC_{S.aureus}$, which is 40ug/ml. The difference in cidal activity against *E. coli* and *S. aureus* is rationalized by the large difference in membrane structure

and composition between gram-negative and gram-positive bacterial kingdom, of which *E. coli* and *S. aureus* are two representative of respectively.

Rebounding AmPs (Figure 2-2B) kill the bacteria through cell lysis and reduce the viability count from 10^8 CFU/ml to as low as 10^3 CFU/ml within 2 hours post treatment. However, the bacterial cells are able to adapt to the presence of the peptides and start regrowing, typically after 3 hours and reach similar cell counts as the untreated cell control 6 hours after treatment (~10^8 CFU/ml). Possible causes for this adaptation include resistance due to changes in the cell membrane structure, degradation of exogenous AmPs by proteases, excretion of AmPs acting intracellularly, etc. (*6*). In all, the cells adapt rapidly to the challenge posed by the AmPs. Ponericins for which this rebounding effect was observed, even at 10-fold their $MIC_{E.coli}$ value, include PonG1, PonG5, PonW6-NH2 and PonG7-NH2, all of which do in fact demonstrate favorable growth inhibition qualities and low MIC.

Cidal AmPs (Figure 2-2C) show a strong, rapid and permanent killing effect on the cells and reduced to the CFU count from 10^8 CFU/ml to below the minimum detection level of 200 CFU/ml (corresponds to 1 viable bacteria per 5ml plated). Four ponericins were identified with such strong bactericidal activities –PonW3, PonW3-NH2, PonW4, PonW5– all of which also posses medium to strong growth inhibition behaviors

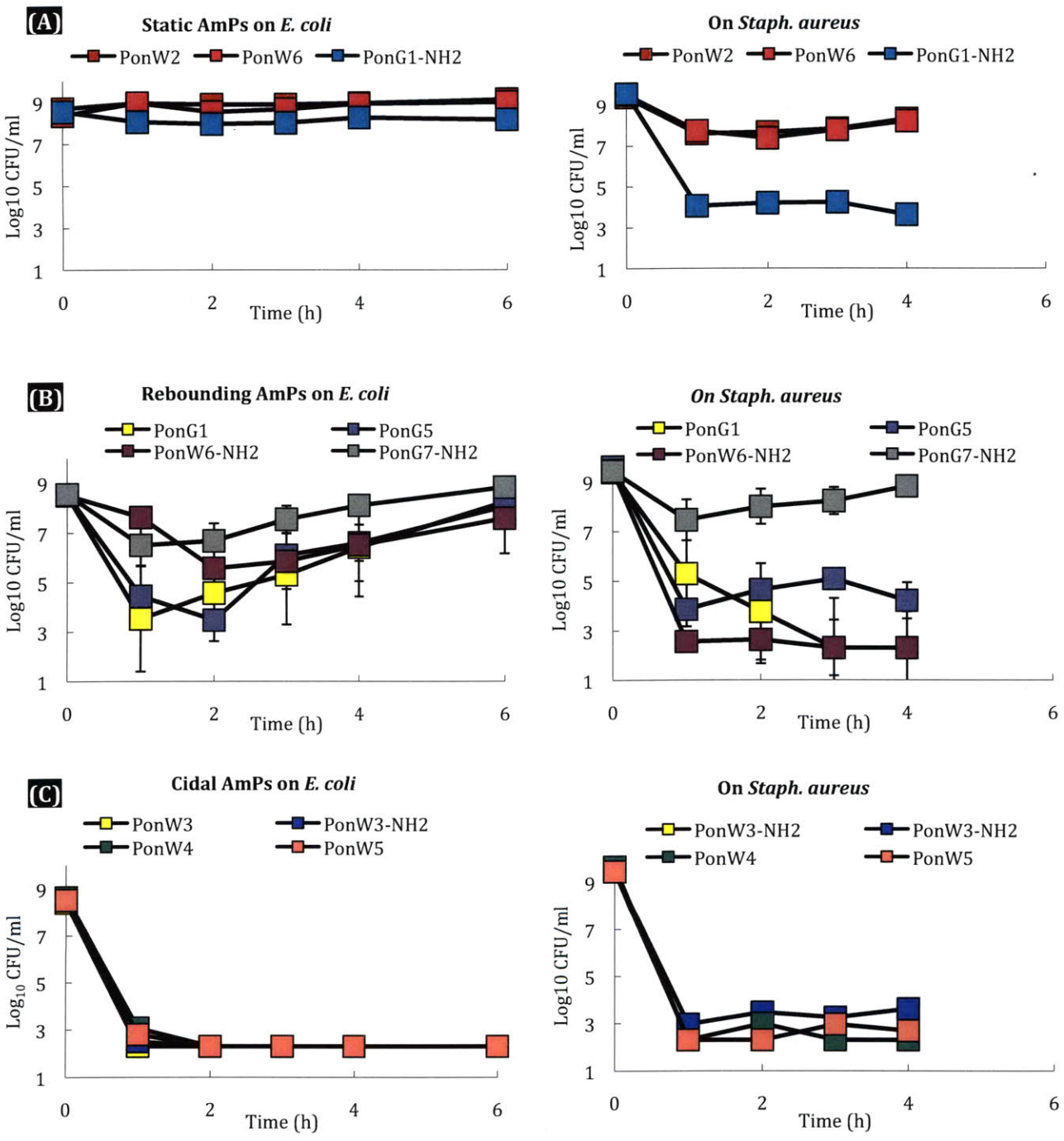

Figure 6-1: Kill curve for (A) bacteriostatic, (B) rebounding and (C) bactericidal ponericins against E. coli and S. aureus.

As demonstrated in Figure 2-2, classification of AmPs based on their organism of origin appears debatable. Small differences in the amino acid sequence have drastic effects on the peptide's cidal activity and mode of action. Instead a classification based on the peptide's cidal activity is preferred. This reclassification enabled us to identify a series of cidal AmPs that possess excellent growth inhibition properties as well as strong bactericidal behaviors against *E.coli* making them more likely candidates for drug development.

6.3.2. C-terminal amidation significantly alters cidal activity of ponericins

The previous section (Figure 2-2) included bactericidal activity of several natural and amidated ponericins such as ponericin G1, ponericin W3 and ponericin W6. The kill curve for these peptides was rearranged in Figure 6-2 to compare the cidal activity between the natural and amidated version of these peptides.

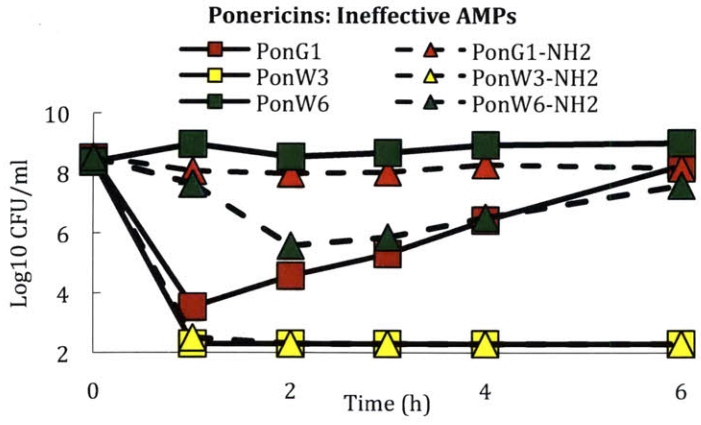

Figure 6-2: Kill curve for natural and amidated ponericin G1, W3 and W6.

Amidation at the C-terminus has been reported to increase activity and reduce the MIC of AmPs because it shields the negative charge of the C-terminus of the peptide. However, this understanding is simplistic and fails to understand the complete impact of the C-terminus amidation. Figure 6-2 instead suggests that the simple change from a C-carboxyl group to a C-amide group has much broader implication and directly affect the cidal activity and the mode of action of the peptide. While C-terminal

amidation may reduce the MIC of some peptides, it is however not necessarily beneficial for the peptides cidal activity. For example, C-terminal amidation can turn a cidal peptide in to a static one (PonG1) or a static one into a cidal AmP (PonW6). The natural version of Ponericin G1 has shows cidal activity and suppresses *E. coli* culture from 10^8CFU/ml to 10^3CFU/ml in the first hour post treatment (Figure 2-2). On the other hand, its amidated version, PonG1-NH2, does not show any bactericidal activity. Thus, C-terminal amidation can be both detrimental, or positive. Such sharp contrast in the peptides cidal activity hints at different targets and mode of action although these two peptides are identical except for the C-terminus modification. We elaborate in greater details the difference in the peptide's mechanism in section 6.7.

6.4. Visualization of the membrane disruption action of AmPs

6.4.1. Microscopic visualization using high speed atomic force microscopy

Our effort to understand the different mechanisms and cidal activity of AmPs starts by visualizing the stress they impose on cellular membrane. To that extent, we collaborated with Georg Fantner from the laboratory of Angela Belcher at MIT and utilized a homemade high-speed atomic force microscope to follow in real time the deformation of live *E. coli* cells subjected the antimicrobial peptide, Cecropin A Melittin. Cecropin A Melittin (CAM) was selected as AmP for this study because it has been reported to have strong membrane disruption membrane ability (*7*) and was available in quantities necessary for this experiment.

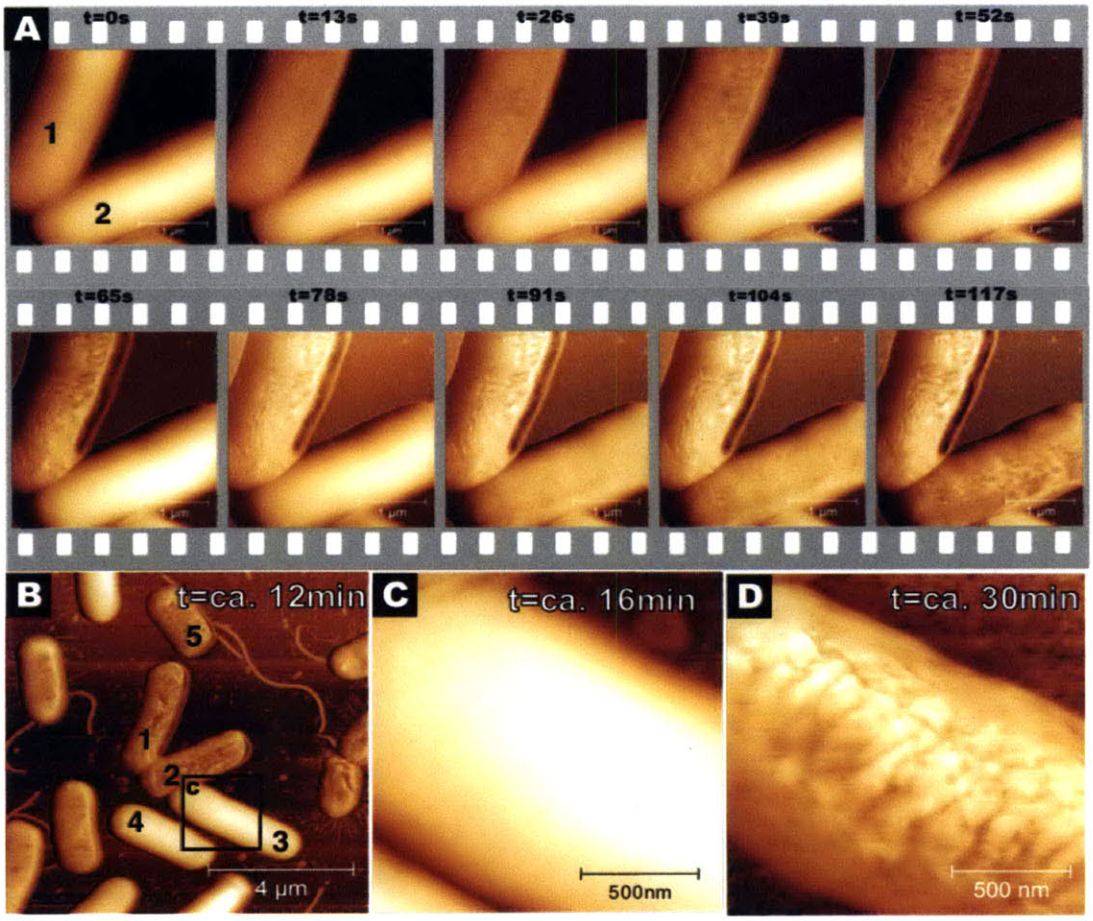

Figure 6-3: Imaging using high-speed atomic force microscopy shows E. coli cell disruption induced by the AmP CAM.

The addition of CAM induces change the morphology and surface roughness of the bacterium cell membrane. Prior to the addition of CAM, the cells were smooth. However after addition of CAM the cells become corrugated (Figure 6-3A). Changes in cell morphology occurred within 13 seconds for the upper bacterium #1 while the lower bacterium #2 was able to resist the action CAM for over 78 seconds. A larger view was taken after 12 minutes and shows that most, but not all bacteria, had become corrugated (Figure 6-3B). Bacterium #3 for example was still smooth after 16 minutes (Figure 6-3C) but became corrugated after 30 minutes (Figure 6-3D). These results demonstrate that the membrane disruption action of the AmPs is very rapid, on the order of a few seconds only. Such rapid killing action have been

hypothesized for other AmPs (*8*) however this work is the first report of a direct visualization on the killing for CAM using AFM imaging.

However, there appears to be a large spread in the time required killing as some cells are able to resists the action of the AmP for up to 30 minutes before a morphological change to the membrane is observed. Given the AmP concentration was made homogenous through the sample by pipette mixing, the timing difference is not due to differences in the local AmP concentration. Instead, some cells appear to have the ability to resist the action of the AmP for extended time period.

Gaining a true understanding of the mechanism that allows these cells to resist the action of AmP requires the cells to be placed in an environment in which they are able to divide and growth. These growth conditions cannot be achieved in the high speed AFM because of technical limitation on the apparatus and thus these studies were carried out using a microfluidic device (section 6.4.3). The kinetic results obtained with the AFM instrument were published by Dr. Georg Fantner in *Nature Nanotech* (*9*) where our contribution was also acknowledged.

6.4.2. Macroscopic validation of the time scale for the membrane disruptive action of AmPs

The short time frame for membrane disruption observed at a microscopic level with the AFM was validated on a macroscopic level using a luminescent variant of E. coli. The strain, *E.coli-Xen14* was donated by Calipers, CA and contained a stable copy of the *Photorhabdus luminescens* lux operon on the bacterial chromosome (Xen14 strain from CALIPERS). Xen14 cells were grown to a mid-log phase at 10^8 CFU/ml (OD600= 0.4) from an overnight culture and the luminescence intensity was measured in a 96 well plate reader.

Cecropin A melitin (CAM) was added to *E.coli-Xen14* culture to a final concentration of 128ug/ml. A complete and immediate drop in luminescence of the bacterial culture was detected within one-minute

(Figure 6-4) post CAM addition. The quenching of luminescence suggests a loss of the proton gradient due to a disruption of the cell membrane and leakage of intracellular ATP. These experiment confirm the rapid membrane disruption and killing observed on a microscopic level to macroscopic level applied to a whole batch culture. The luminescence cause by the few individual cells that resisted the action of the AmP could not be detected, as it was likely below the minimum level of detection of the reader.

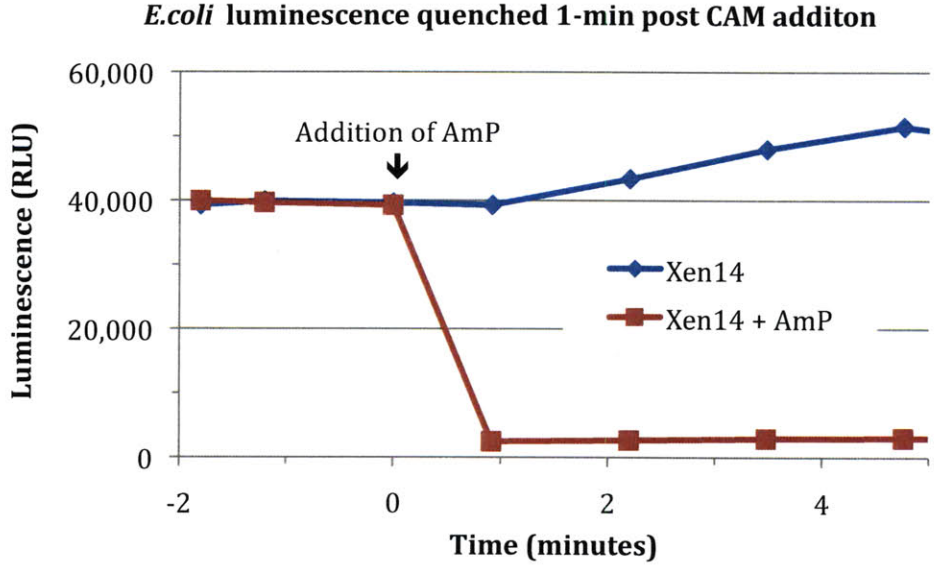

Figure 6-4: Luminscence reading of Xen14 luminescent E.coli subjected to XXug/ml of cecropin A melitin. The immediate drop in luminescence caused by disruption of the cell membrane Effect on intracellular ATP concentration and preventing the ATP driven cell luminescence.

6.4.3. Microscopic visualization using microfluidic device

In order to properly study the cell's stress and adaptation to AmPs in a potential therapeutic setting, they should be maintained in normal growth and division conditions. However, AFM imaging described in section 6.4.1 does not allow such growth condition to be replicated – instead the cells are kept alive in PBS but in a non-dividing state. Therefore, we continued our microscopic visualization studies using a specially constructed microfluidic device developed by Dr. Ahmad Khalil from the laboratory of James Collins at Boston University.

The microfluidic device is made from PDMS using standard soft lithography techniques and is composed of a 1 um high culture chamber that enable monolayer of *E.coli* cells to grow and through which growth media, nutrient, drugs, etc are perfused in a controlled manner. A microscope is mounted on top of the chamber to visualize and follow cell growth. The microfluidic device offers several advantages over visualization with the AFM; namely

- it is more representative of actually physiological condition in patients in terms of temperature, growth environment, etc
- bacterial cells are maintained in pseudo-exponential phase state, i.e. alive and dividing
- the control of the local concentration of antimicrobial agent is more accurate
- it allows for the formation of bacterial biofilms with long term cultures, which are harder to kill
- it provides a more challenging assay and more clinical relevant target for the design of antibiotics

We studied the effect of two AmPs – bactericidal PonW3 and rebounding PonG1 – on *E.coli* cells using the device. The sequence and MIC of these peptides is provided in Table 2-1 and their cidal activity profile in Figure 2-2. Figure 6-5 shows time profile of cell growth in under microfluidic device after 5X MIC of AmP (8ug/ml for PonW3 and 2ug/ml for PonG1) is perfused continuously starting at 0 seconds.

A change in the membrane morphology is observed within the first 12 minutes of continuous perfusion of the bactericidal peptide ponericin W3 through the chamber (Figure 6-5A). The cells membrane appears corrugated, and collapsed. The cells that displayed this collapse were also no longer able to divide. This change in cell morphology is indicative of a disruption of the cell membrane and a dead state of the bacteria. After 25 minutes of perfusion, all the bacteria in the view area underwent cell membrane collapsed. One possible future experiment would be to stop flow of AmP at a given time point and perfuse straight growth media to observed if the cells can be rescued. However, since none of the

cells that underwent the experiment were able to regrow after being plated overnight, this suggest that the change in membrane morphology indicates a strong bactericidal behavior for PonW3 at the concentration used.

When the rebounding peptide ponericin G1 was perfused through the chamber at 5X MIC, a similar changes in membrane morphology was observed for some cells within the first 10 minutes (Figure 6-5B). However, the PonG1 does not affect all the cells equally. In fact, some cells are able to resist the membrane disruption action of the peptide and continue to multiply in the chamber. This indicates that PonG1 is not as effective an antimicrobial as PonW3 and that some cells are able to resist PonG1 and regrow, which is also seen in the kill curve in Figure 2-2. It should also be noted that because of the particular chamber conditions – media perfusion, low partial pressure – cell growth occurs about 25% slower in the microfluidic device and the E.coli cell divide every 25 minutes instead of the 20 min doubling time under optimal conditions. As cells continue to grow, some channeling effect may be observed temporarily and some cells may be exposed to higher local concentration of AmPs. After 30 minutes, the cells colonized the entire width of the device resulting in a more homogenous distribution of the media. It also appears that only the cell that were not affected by the AmP are able to divide and grow; while the cells that are corrugated stay in place and do not divide, thus indicating the cells are in fact dead.

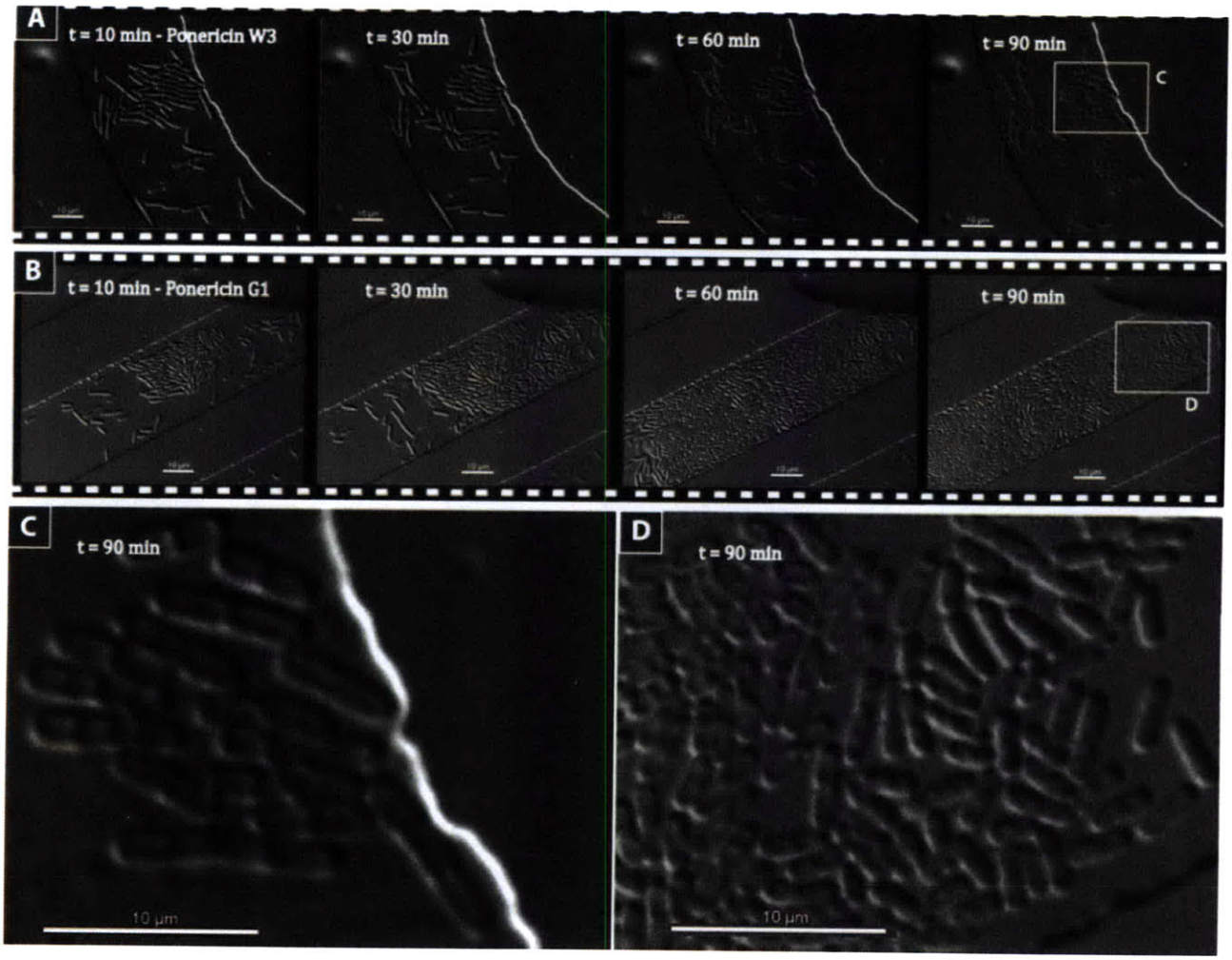

Figure 6-5: Imaging using a microfluidic flow chamber shows resistance to Ponericin G1 and cidal action of Ponericin W3. Treatment with Ponericin W3 at 10X MIC induces a membrane disruption manifested by a morphological change starting within 10min and affecting all the cells in the reactor. The cells are no longer able to divide and multiply resulting in the cidal effect of the peptide (Panel A). The morphology change is manifested through deflation of the cells and surface corrugation at the cell membrane. For cells disrupted during division, the septal ring at the centerline is even visible (Panel C). Treatment with Ponericin W3 affect some cells that become corrugated and cannot grow while others appear not affected and colonized the entire microfluidic chamber (Panel B and D).

6.4.4. Correlating visual observations with gene regulation response for PonG1, G5, W3

Both the AFM and the microfluidic device indicate that stress with cidal AmPs lead to a change in the cell membrane morphology and result in corrugated bacterial cells with permeabilized cell membrane. The microfluidic device shows that some cells gain the ability to resist the action of the AmPs. Understanding the mechanisms by which those cells derive resistance to AmPs is invaluable for the development of AmPs-based therapeutics. It is thus necessary to correlate these visual observations with changes on the gene regulation level to identify the pathways involved in activating and leading to AmP resistance.

Having observed significant perturbation to the cell membrane, we first study membrane stress sensors systems by the cells in section 6.5. Two separate systems were studied, the cpxAR system and the dpiAB system. These two component cell sensory pathways were studied for the action of AmP LL-37 and PG-1 against *B. subtilis* (10) but this is the first report of such study for the family of ponericins.

6.5. Membrane stress sensors induce cellular resistance to ponericins

6.5.1. CpxAR senses and corrects for misfolded envelope protein due to AmP membrane action

Based on our AFM and microfluidics observation, we hypothesize that AmPs lead to an alteration in membrane structure and the misfolding of envelope proteins. The CpxAR two-component system is responsible for sensing misfolded envelope protein and for regulating the cell response. Misfolded protein in the cell envelop protein stimulate CpxA autokinase, which in turns phosphorylates CpxR causing the upregulation of genes involved with the degradation and synthesis of membrane proteins, and transcription regulation (*11*). The CpxAR system has thus the ability to restore the cell membrane after the disruptive action of the AmP. Additionally, CpxAR activation has been shown to induce

expression of intrinsic multidrug exporter genes and lead to resistance to antimicrobials such as carbenicilin. Therefore, CpxAR system is a regarded as a potential target to overcome drug resistance mechanism (*12*). We studied the viability of a CpxA knockout mutant (CpxA-) subjected to treatment with 10X MIC of PonG1, PonG5 and PonW3 and compared it with the viability of the wild type cells (wt). CpxR- knockouts show strong negative growth defect and are not amenable to comparison and thus were not studied.

PonG1 is a rebounder AmP to which wild type cells are able to adapt and derive resistance against. However, when the cell's ability to sense and correct for membrane protein misfolding (CpxA-), the cells are unable to adapt and resist the action of PonG1 (Figure 6-6A). This suggests that the CpxAR mediated cellular sensing and response is uniquely necessary to evolve resistance to PonG1.

A similar detrimental effect is observed for CpxA- mutants treated with PonG5, another rebounder AmP (Figure 6-6B). However, the CpxA- knockouts were able to derive resistance to the AmP after 10 hours of treatment and the culture starts to regrow slowly. This indicated that while CpxAR sensing is important in the evolution of resistance but not crucially and that its knock out significantly delays the activation of the resistance mechanism. This suggests several input are present to the transcription program involved in resistance to PnG5, CpxAR being one of them.

Finally, PonW3 (Figure 6-6C) is a strong bactericidal AmP and remains so for CpxA- knockout mutants. The PonW3 lead to cell lysis indicated by a drop in optical density and completely sterilized the culture as no viable cells were detected after overnight plating. Thus, the cells ability to sense and respond to misfolded proteins via the CpxAR two-component systems plays an important role in enabling the cells to gain to the AmPs.

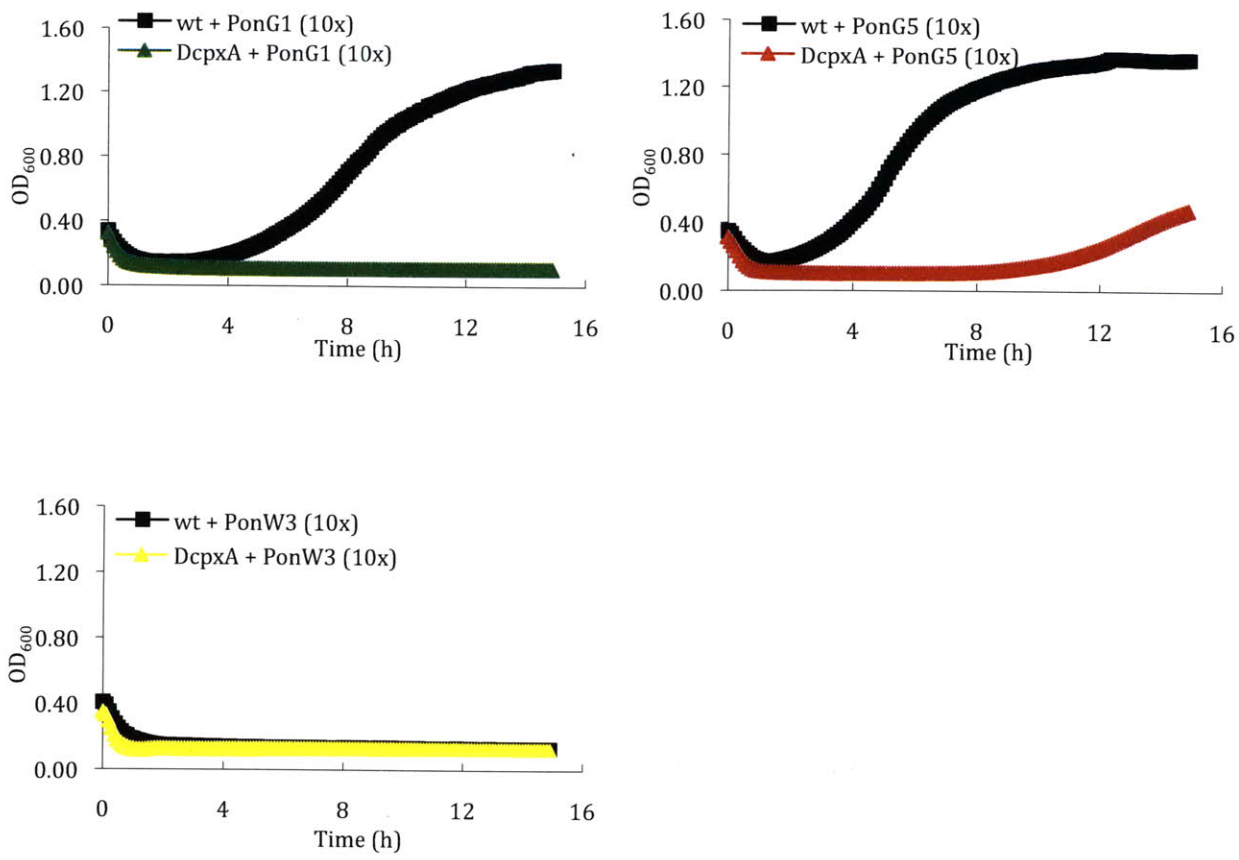

Figure 6-6: Optical density of culture of CpxA- knockouts challenged with 10X MIC of PonG1, PonG5 and PonW3. CpxA- knockouts show CpxAR system play an important role in the cell's ability to adapt and derive resistance to AmPs.

6.5.2. DpiAB sensing plays a role in bacteria resistance to PonG1

We tested the action of a second membrane stress sensor, the DpiAB system. DpiAB is a dual transcriptional regulator involved in anaerobic citrate catabolism. It also serves as a defense mechanism that utilizes bacterial two-component signal transduction system to induce the SOS response and temporarily inhibit cell division during exposure to antimicrobials, consequently limiting their bactericidal effects of these drugs (*13*). DpiAB thus regulates transcription but also binds to A/T-rich sequences in the replication origins of the *E. coli* chromosome thereby affecting DNA replication and inhibiting cell division. Since the DpiAB is involved evolution of resistance to commonly used

antimicrobials b-lactams, which act on the cell membrane, we decided to study whether the system also played a role in resistance to AmPs. We studied the viability of DpiA- and DpiB- gene knockouts mutants exposed to 10X MIC concentrations of PonG1 (MIC= 2 ug/ml), PonG5 (MIC= 16 ug/ml) and PonW3 (MIC= 8ug/ml) and compared it to viability of the wild type E.coli (Figure 6-7).

Wild type E.coli cells are able to adapt to the action of rebounder peptide Ponericin G1 and start regrowing typically after 1 hour of treatment. The DpiA- and DpiB- knockouts (Figure 6-7A, B) show 2.5 fold increased susceptibility to the PonG1 and 2 hours delay in the adaptation and regrowth to AmPs for both knockouts. Once AmP resistance was acquired, the growth rate of wild type and the knockout mutants was similar. This suggests that, while not essential for the evolution of PonG1 resistance, DpiAB sensing allows for earlier detection and faster response to the membrane stress caused by PonG1.

On the other hand, when exposed to rebounder peptide PonG5, deficiency in DpiAB sensing, either through DpiA- or DpiB- knockout (Figure 6-7C, D), results in a slight protective effect in the first three hours of treatment as the AmP kills more wild type cells. Past 3 hours, the wild type cells adapt better to the AmP and are able to adapt and regrow faster as the wild type viable trajectory at 4 hours overtakes that of both DpiA- or DpiB- knockouts.

Changes in viability due to DpiA- or DpiB- knockout could not be detected when the cells were exposed to the strong bactericidal PonW3 because the number of remaining viable cells was below the detection limit of the assay (Figure 6-7E, F)

DpiAB mediated membrane stress sensing thus plays a mixed but non-essential role in the cell's ability to adapt to the presence of different AmPs. Activation of the system is beneficial when the cells are exposed to PonG1 but is unfavorable when the cells are exposed to PonG5. These observations are internally consistent for both DpiA and DpiB knockouts and were validated with 2 independent experimental repeats.

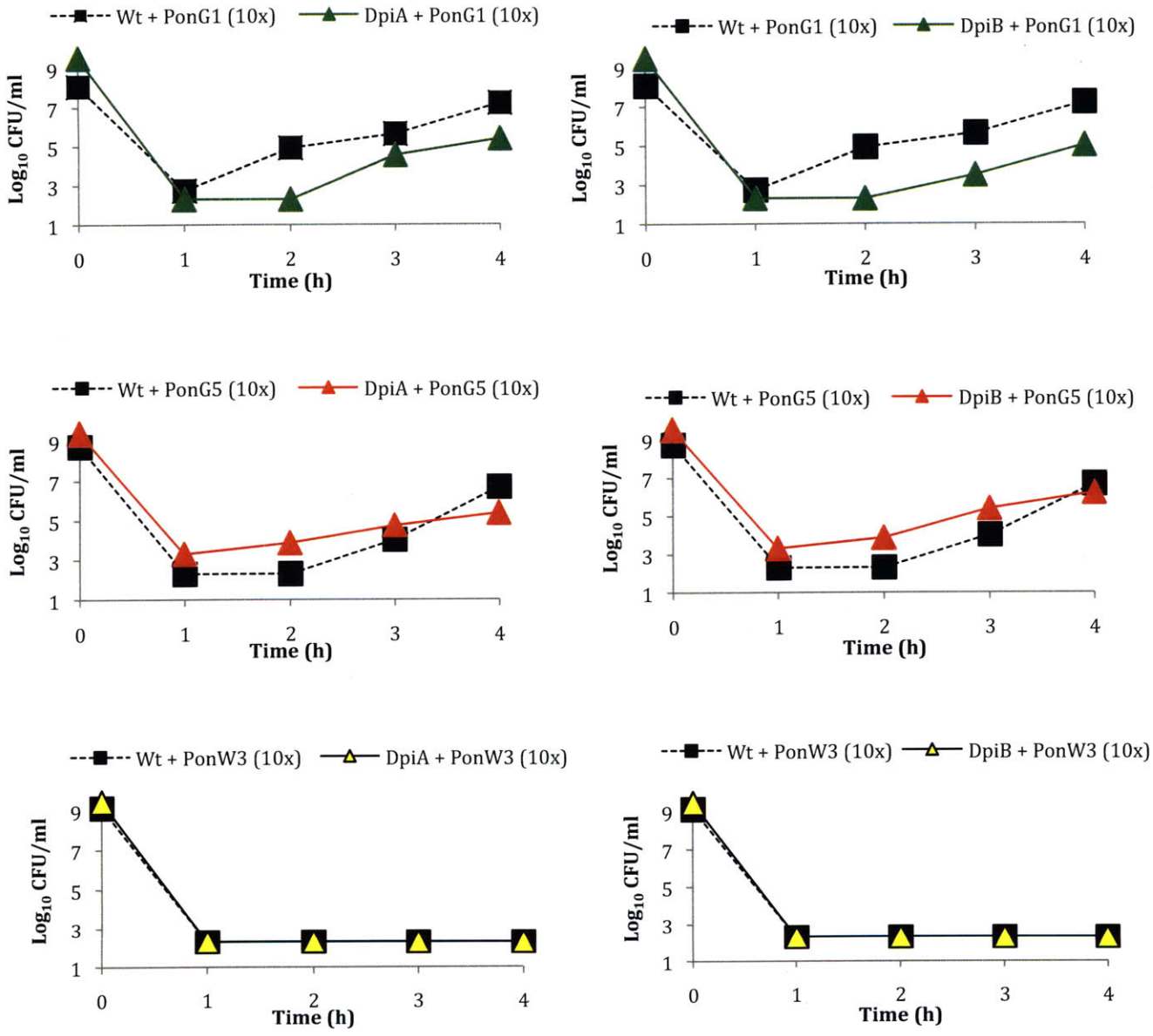

Figure 6-7: Survival of DpiA and DpiB knockouts challenged with 10X MIC of PonG1, PonG5 and PonW3.

6.6. Cellular resistance involves RecA data

Section 6.5.2 establishes that the cell's ability to sense AmP stress on the membrane the DpiAB system is beneficial to the cells and leads to the early development of adaptation and resistance to Amp

action such as that of PonG1. One of the gene targets of DpiAB is induction of the cell's SOS response to repair DNA. Thus, we hypothesize that PonG1 mode of action leads to DNA damage and that the cell adaptation and resistance is mediated by the SOS response. This hypothesis is reasonable given other peptides have been shown to block DNA replication and induce SOS response (B17 Blocks DNA Replication and Induces the SOS System in Escherichia coli). However, these studies have never been shown for any of the ponericins nor have they correlated the SOS activation with two-component stress membrane and bactericidal activity.

Two proteins play key roles in the regulation of the SOS response: the repressor LexA and the inducer RecA. The SOS response is activated with increasing level of DNA damaged after the DNA polymerase is blocked by intracellular antimicrobials resulting in accumulation of single stranded (ssDNA) regions at replication forks. RecA forms a filament around these ssDNA regions and becomes activated. The activated form of RecA promotes the self-cleavage of the LexA repressor from the operator and the gradual induction of the various SOS genes. The first repair mechanism to be induced is nucleotide excision repair, whose aim is to fix DNA damage without commitment to a full-fledged SOS response. If that does not suffice, later SOS genes will stop cell division, cause cell filamentation, and induce mutagenic repair (*14*). Since many antibiotics lead to DNA damage, and all bacteria rely on RecA to fix this damage, one strategy to enhance the toxicity of antibiotics – or to create new oness – is to block RecA function and preclude the induction of the SOS repair in the cell (*15, 16*). Thus, RecA activity is synonymous with the development of antibiotic resistance, and inhibitors serve to delay or prevent the appearance of resistance (*17*). Here, we challenged recA- knockout mutants that are unable to activate the SOS system and repair DNA damage with 10X MIC of PonG1, PonG5 and PonW3.

While wild type *E.coli* starts regrowing after 2 hours of treatment with Ponericin G1, the recA-knockout mutants lose the ability to adapt and resist to the action of peptide and no regrowth is observed. Even after 4 hours of treatment, the count of viable cells was still below the assay detection

level of 200 CFU/ml and no regrowth is observed. These observations imply that first the action of PonG1 leads, directly or indirectly, to extensive DNA damage in the cell and second that the cells ability to repair this DNA damage is absolutely necessary for the evolution of bacterial resistance to PonG1.

On the other hand, recA- knockout mutants are still able to adapt and resist to PonG5, a rebounding AmP. Since DNA repair is not essential for resistance, the initial cidal action of PonG5 does not center or cause lethal DNA damage. The recA- mutants are however more sensitive to the peptide and the lack of SOS response delays regrowth by ~1 hour. Thus, the activation of the SOS response is somewhat beneficial but not necessary for cell adaptation to PonG5.

Finally, PonW3 is has a strongly cidal activity regardless of whether the cell are able to repair DNA. This suggests that either the DNA damage is so extensive that even SOS cannot rescue the cell or that the mechanism causing cidality does not center on DNA damage.

In order to gain a holistic approach to put into perspective our finding as part of a grander understanding of the networks involved in resistance, we next performed a complete study of gene regulation using microarray. We chose PonG1 and its amidated version PonG1-NH2 as subject of our in-depth studies.

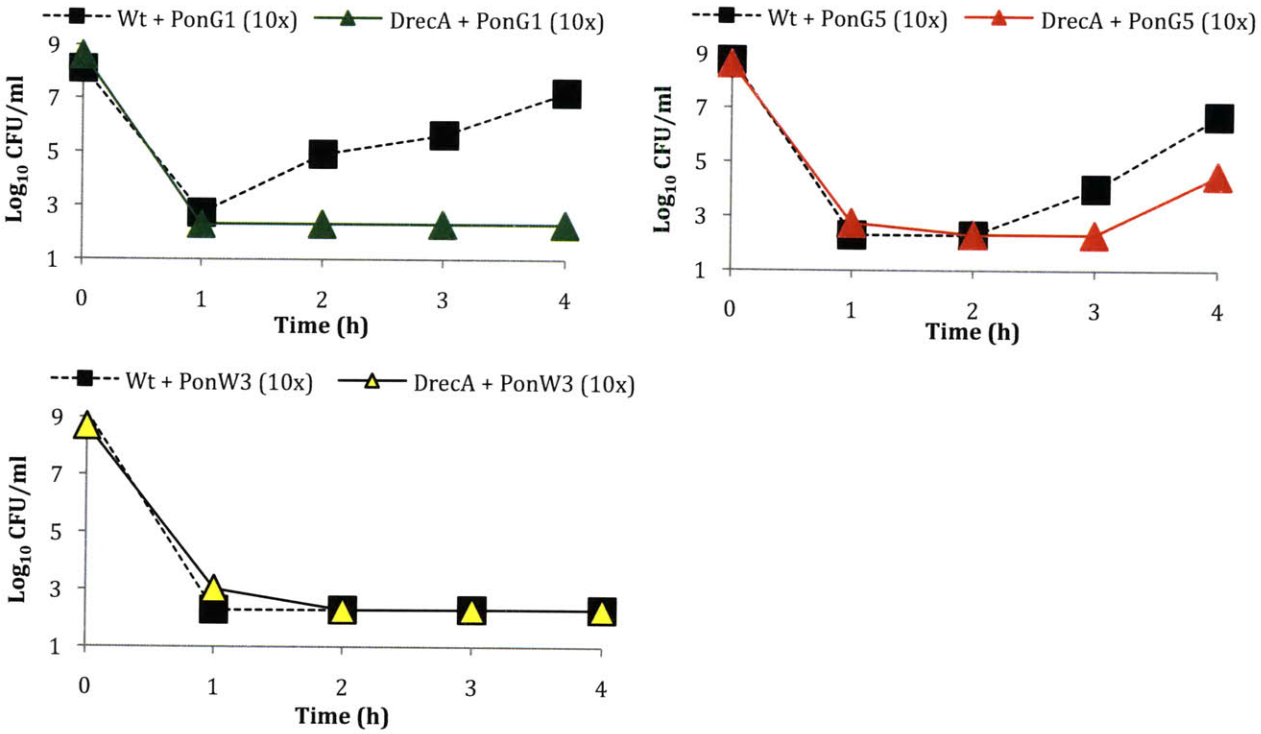

Figure 6-8: Survival of RecA knockouts mutants challenged with 10X MIC of PonG1, PonG5 and PonW3.

6.7. Microarray validation of the cellular targets of Ponericin G1

To gain a holistic understanding of the evolution mechanisms of bacterial resistance, we complement our previous findings with a study of the gene regulation using DNA microarray. The microarray enables us to identify the activated gene networks leading to resistance to PonG1 and infer the peptide's intracellular targets. Additionally, since sharp differences in cidal activity were observed between the natural and amidated version of PonG1 (Figure 6-2), we compare the cellular gene response upon treatment with these two peptides to understand the difference in target and mechanism resulting from the C-terminal amidation of PonG1. Section 6.7.1 describe the generalized experimental and analysis methods of the microarray study and was reproduced from Dr. Köris's PhD Thesis with the author's consent (*18*).

6.7.1. mRNA isolation and microarray hybridization

To elucidate the differences between the mode of action of the two AMPs, we ran an 8h microarray time course following the treatment of an exponentially growing culture with either AMP. We compared the microarray-determined mRNA profiles (GeneChip® E. coli Genome 2.0 Array, Affymetrix, Santa Clara, CA) of untreated wild-type E. coli K12 EMG2 cultures with cultures treated with 10x MIC of PonG1 and PonG1-NH2. For both samples, overnight cultures were diluted 1:1000 into 5 mL LB medium in a 14mL flask for collection of total RNA. Initial, untreated samples for microarray analysis were taken at an $OD_{600} \sim 0.6$ and then 1h, 2h, 3h, 6h, 7h and 8h post treatment with the AMPs. Treatment with the cidal natural PonG1 resulted in a significant cell lysis and not mRNA could be collected for the 1h, 2h, 3h time point.

Total RNA was obtained using the RNeasy Protect Bacteria Mini Kit (Qiagen) according to manufacturer's instructions. RNAprotect (Qiagen) was added to culture samples at a 2:1 volume:volume ratio, which were then incubated at room temperature for 5 minutes prior to pelleting by centrifugation at 3,000xg for 15 minutes and stored overnight at -80°C. Total RNA was then extracted using the RNeasy kit, and samples were DNase treated using the DNAfree kit (Ambion, Austin, TX). Sample concentration was measured using the ND-1000 spectrophotometer (NanoDrop, Wilmington, DE). cDNA was prepared from 10 μg total RNA by random primed reverse transcription using SuperScript II (Invitrogen, Carlsbad, CA). The RNA was digested by adding 1 M NaOH and then incubating at 65°C for 30 min. The mixture was neutralized by the addition of 1 M HCl. The cDNA was purified using a QIAquick PCR purification column (Qiagen) following the manufacturer's protocol. The cDNA was fragmented to a size range of 50–200 bases with DNase I (0.6 U/μg cDNA) at 37°C for 10 min, followed by inactivation of the enzyme at 98°C for 10 min. Subsequently, the fragmented cDNA was biotin labeled using an Enzo BioArray Terminal Labeling kit with Biotin-ddUTP (Enzo Scientific). Fragmented, biotinylated cDNA was hybridized to the arrays for 16 h at 45°C and 60 r.p.m.

Following hybridization, arrays were washed and stained according to the standard Antibody Amplification for Prokaryotic Targets protocol (Affymetrix). This consisted of a wash with non-stringent buffer, followed by a wash with stringent buffer, a stain with strepavidin, a wash with non-stringent buffer, a stain with biotinylated anti-strepavidin antibody, a stain with strepavidin–phycoerythrin and a final wash with non-stringent buffer. The stained GeneChip arrays were scanned at 532 nm using an Affymetrix GeneChip Scanner 3000. The scanned images were scaled and quantified using GCOS v1.2 software.

6.7.2. Differential gene expression analysis

We added the microarrays to the E. coli compendium used (E_coli_v3_Build_3 – download at http://m3d.bu.edu) and normalized all the CEL files together (*19*) using the robust multichip average (RMA) method (*20-22*). The normalization is necessary to reduce the experimental variability across different array spots while maintaining biological variability (*23*). Briefly, the RMA algorithm performs a probe-level quantile normalization only on perfect-match (PM) probes of an Affymetrix chip and quantifies a $\log_2$-transformed expression value for each gene based on a median polish algorithm that down weighs outlier probes, yielding a normalized expression for each gene. The mean normalized expression for each gene was subtracted from the respective normalized expression for each individual experiment and then divided by the respective standard deviation (calculated across all experiments) of that gene. A Z-score for each gene i was computed as follows where X is the $\log_2$-normalized expression value of gene i, $\overline{X}$ is mean expression of gene i and σ_i standard deviation of gene i across all experiments. The Z-score normalization of microarray expression values is calculated with the following equation:

$$Z_i = \frac{X_i - \overline{X}}{\sigma_i}$$

We compared the expression level of each gene in the chips of interest with the respective level in the rest of the compendium. For that purpose, the average of expression across the compendium was calculated for each gene. Furthermore, to assess how each gene's expression level changes upon

treatment with the AMPs, we determined if there are significant changes in the expression levels between the treated versus the untreated chips. Performing this analysis we identified the genes that have a statistically significant fold-change in expression value when the Amps are added. Expression changes and the associate P-value were recorded for the genes in the biochemical network of interest and are reported in Table 6-2 where a negative Z-score reflects a down regulation of the gene of interest while a positive Z-score reflects up-regulation of the gene.

Table 6-2: Z-score change for amidated PonG1-NH2

Amidated PonG1-NH2 treatement

1h		2h		3h		6h						7h				8h	
gudP	3.8	garP	3.7	garP	3.5	yffP	5.8	gutQ	2.4	ychS	2.0	yqeA	2.5	accC	2.5	recE	2.0	ymgF	2.1	accC	2.0	rsxD	2.5
garP	3.6	gudP	3.5	gudP	3.5	glnB	4.8	rsxC	2.4	iscA	2.0	pphA	2.5	aceB	2.7	recO	2.1	ymgJ	2.6	aceA	2.1	secA	2.5
cyoE	3.5	feoB	3.4	tdcA	3.3	yffM	4.7	yfhB	2.4	pspF	2.0	yeaX	2.5	acs	2.3	rfaE	3.2	ynbE	2.2	aceB	2.8	serS	3.2
cdaR	3.2	cdaR	3.1	garD	3.3	yffN	4.5	mokC	2.4	rsxG	2.0	ynaK	2.5	actP	3.0	rfaI	2.1	yneK	2.0	acrF	2.3	sgbE	2.1
feoB	3.1	garD	3.1	sodA	2.8	yffQ	4.3	amiA	2.4	nrdG	2.0	ninE	2.5	ahpF	2.0	rfbX	2.1	yoeA	2.8	acs	2.8	sgcR	2.5
cyoD	3.0	tdcA	3.0	ykgE	2.8	garP	4.1	plA	2.4	nirD	2.0	yeeO	2.5	aldB	2.7	rffA	2.1	yojO	2.2	actP	3.7	sgrS	2.0
sodA	2.9	feoA	3.0	feoB	2.7	feoB	4.1	degS	2.4	fieF	2.0	ygcJ	2.5	argR	2.4	rffH	2.1	ypdB	2.1	aldB	2.5	smpB	2.7
feoA	2.8	sodA	3.0	cspA	2.7	garD	4.1	rplI	2.4	narQ	2.0	pgaC	2.5	argT	2.7	ribA	2.4	ypfJ	3.0	amiA	2.1	srlR	2.2
cyoC	2.7	ykgE	2.9	ykgF	2.6	rfaE	4.0	trmI	2.4	accC	2.0	ydiN	2.5	aroE	2.1	rihC	2.3	yqcE	2.4	argR	2.4	sseB	2.5
garL	2.7	feoC	2.8	nirB	2.6	cdaR	4.0	rffH	2.4	moeB	2.0	ydaC	2.5	bcsG	2.1	rpe	2.4	yqeB	2.9	argT	3.7	sstT	3.0
nth	2.7	nirB	2.8	garL	2.6	pfkA	3.9	lptA	2.4	zipA	2.0	hyfJ	2.5	btuF	2.5	rplI	2.1	yqgA	3.1	aroE	2.1	tdcA	2.0
feoC	2.6	ykgG	2.7	feoC	2.5	yfeC	3.9	ecnA	2.4	rhlE	2.0	xylH	2.5	cdaR	3.9	rplJ	2.1	yqjI	2.9	astA	2.7	tfaD	2.3
cyoA	2.6	yoeA	2.6	nikA	2.5	gudP	3.8	ypeB	2.4	yejL	2.0	argT	2.5	cpxP	2.7	rplS	2.2	yraJ	2.5	astB	2.8	thrV	3.3
exbD	2.6	nikB	2.6	cdaR	2.5	ykgG	3.8	ung	2.4	srlR	2.0	katG	2.6	csdE	2.2	rplT	2.2	yrbC	2.3	astC	2.7	tldD	2.7
cobC	2.5	garL	2.6	ykgG	2.5	yqgA	3.7	hda	2.4	zwf	2.0	ygeX	2.6	cycA	3.4	rpmE	2.3	ysaA	2.9	astD	2.8	torY	2.1
cyoB	2.5	nikA	2.6	narK	2.5	ykgF	3.6	modE	2.4	ligT	2.0	gspJ	2.6	cydD	2.2	rpmF	2.5	ysaC	2.7	atoB	2.1	tppB	2.8
yfcL	2.4	cspA	2.6	feoA	2.5	nagB	3.5	queF	2.4	pnp	2.0	guaD	2.6	cysB	2.2	rpmG	2.6	ytfF	2.6	bax	3.5	treB	2.7
yoeA	2.4	narK	2.5	rsxE	2.4	smpB	3.5	menD	2.4	secB	2.0	ygfQ	2.6	dadA	2.2	rpoC	2.2	ytfI	2.0	blr	2.8	treC	2.0
cspA	2.4	ykgF	2.5	leuW	2.3	uvrC	3.5	yrbB	2.4	gcvP	2.0	ygeW	2.6	dadX	2.4	rpsO	2.3	zraS	3.6	btuF	2.5	trpR	2.5
yehS	2.4	nth	2.4	carB	2.3	der	3.5	rssA	2.3	torS	2.0	pinH	2.6	damX	2.2	rraB	2.1			cdaR	2.2	ugpE	2.3
arsR	2.4	nikC	2.4	yoeA	2.3	yjgQ	3.4	treB	2.3	hyuA	2.0	alpA	2.6	dcuR	2.8	rseA	2.1			cpxP	2.7	upp	2.3
artM	2.4	fhuB	2.3	mqo	2.2	ribA	3.3	yfeD	2.3	ytfI	2.0	yhfT	2.6	ddlA	2.2	rsmE	2.6			cyaR	2.0	uvrC	2.4
gudX	2.4	nikE	2.3	nikE	2.2	exbB	3.3	ybdZ	2.3	feaR	2.0	rspB	2.6	degP	3.0	rsxC	2.2			cycA	4.6	xylE	2.2
yhgN	2.3	fecE	2.2	nikB	2.2	rsxD	3.3	nrdD	2.3	ytfA	2.0	yaeF	2.6	degS	2.2	rsxD	3.0			dadA	2.3	xylF	4.0
garR	2.3	rsxE	2.2	yfcL	2.2	feoA	3.3	mngR	2.3	yfgI	2.0	ybdD	2.6	der	3.2	rsxG	2.2			dadX	2.5	xylG	2.4
garD	2.3	nirD	2.2	tppB	2.2	lpp	3.3	yfbB	2.3	hcaD	2.0	ybhD	2.6	dgsA	2.4	sapD	2.1			damX	2.2	xylH	3.4
mrcA	2.3	exbD	2.2	nth	2.2	kbaZ	3.3	yjhU	2.3	ydeR	2.0	ygeG	2.6	dipZ	2.2	secA	2.4			dcrB	2.3	yaiY	2.8
nikC	2.3	garR	2.2	nirC	2.2	yfgJ	3.3	rraB	2.3	ycfJ	2.0	ybfQ	2.6	djlC	2.0	serS	2.2			dctA	2.0	ybaB	3.3
coaD	2.3	nirC	2.1	fecE	2.2	intZ	3.2	feoC	2.3	dadA	2.0	atoE	2.6	dppA	2.2	sgcR	3.0			degP	5.5	ybaL	2.4
ycgF	2.3	fecB	2.1	infA	2.2	ybiH	3.2	fhuF	2.3	alsE	2.0	ybcV	2.6	dppB	2.5	sgrR	2.6			der	2.1	ybbM	2.1
yncE	2.3	dcuC	2.1	gudX	2.1	yehS	3.2	pdxJ	2.3	yhdZ	2.0	yedN	2.6	ebgA	3.4	slyD	2.4			dgsA	4.0	ybdD	2.8
nikB	2.3	fecC	2.1	dcuC	2.1	rpmF	3.2	dcrB	2.3	yibI	2.0	frc	2.6	ebgC	2.4	smpB	2.8			dppA	2.7	ybfI	2.8
rsxE	2.2	garK	2.1	nikC	2.1	gudX	3.1	yeiP	2.3	yfeN	2.0	aceB	2.6	ebgR	3.8	sodA	2.5			dppB	2.6	ybiH	2.6
garK	2.2	fecA	2.1	ompX	2.1	tdcA	3.1	pykF	2.3	yibV	2.0	yfbM	2.7	ecpD	2.0	speA	2.3			dppC	2.3	ycaC	2.3
fecC	2.2	ydiU	2.1	yfiH	2.1	exbD	3.1	yfdG	2.3	yadD	2.0	yadK	2.7	efp	2.2	srlR	2.1			dppD	2.2	ycbK	2.2
mreD	2.2	gudX	2.0	garR	2.1	ydiU	3.1	ryfC	2.3	yidK	2.0	xdhA	2.7	eno	2.1	sstT	2.7			dppF	2.0	ycbZ	2.6
yhhL	2.2	yncE	2.0	ydiU	2.1	nudK	3.1	yfiH	2.3	rhaT	2.1	yghW	2.7	era	2.2	tdcA	3.4			eamB	2.1	yceJ	2.7
nirB	2.2	suhB	2.0	suhB	2.1	manX	3.1	gnd	2.3	ygcH	2.1	mhpR	2.7	eutQ	2.1	tfaD	3.0			ebgR	2.1	yceK	2.1
mreC	2.2	uspG	2.0	fecA	2.0	ypfJ	3.0	ompX	2.3	yfjV	2.1	yfgH	2.7	exbB	3.0	thrV	2.2			era	2.1	ycgE	2.1
kup	2.1	hcaR	2.0	fecB	2.0	yfiB	3.0	guaC	2.3	gfcE	2.1	ybcI	2.7	exbD	2.8	tig	2.1			eutP	2.0	yciX	2.4
fecB	2.1	ydhU	2.0	entB	2.0	gpmM	3.0	hofN	2.3	ydaY	2.1	glnP	2.7	exoD	3.1	tonB	2.4			eutQ	2.4	ycjD	2.1
exbB	2.1	nlpD	2.0	fecC	2.0	narX	3.0	btuF	2.3	emrK	2.1	hybD	2.7	fadI	2.1	tppB	2.5			exbB	2.1	ydaE	2.7
fecE	2.1	rsd	2.0	dadA	2.0	slyD	3.0	lipB	2.3	degP	2.1	yjfC	2.7	feaR	2.3	treB	2.4			exbD	2.2	ydcI	2.1

fecD	2.1	glnQ	2.1	fucR	2.0	yeiW	3.0	fhuD	2.3	yfdF	2.1	yjiE	2.7	fecA	2.2	treC	2.6	exoD	2.3	ydcV	2.1
rsmD	2.1	yeeD	2.1	slt	2.0	ysaA	3.0	rlpA	2.3	bax	2.1	ybeU	2.7	fecB	2.3	trmI	2.5	exuR	2.6	ydcW	2.1
yqcC	2.1	cysH	2.1	hcaE	2.0	ybhT	3.0	murI	2.3	uhpC	2.1	yneK	2.7	feoA	3.0	trpR	2.7	fabB	2.0	ydeH	3.3
nikA	2.1	glnP	2.1	chiA	2.0	nirB	2.9	ppiD	2.3	bssR	2.1	ycfT	2.8	feoB	4.0	tsf	2.3	fadA	3.5	ydiU	2.1
nirD	2.1	fucA	2.1	glgC	2.0	rsmC	2.9	yihA	2.3	ykfN	2.1	cpxP	2.8	feoC	2.3	ulaE	2.3	fadB	2.9	yebE	3.1
yejL	2.0	narP	2.1	eptB	2.0	manZ	2.9	yciN	2.3	rhsA	2.1	yfgF	2.8	fhuA	2.8	ung	2.3	fadD	3.3	yehS	3.1
ycaO	2.0	yhhJ	2.1	dppD	2.0	yidF	2.9	mdoH	2.3	bglJ	2.1	yfjY	2.8	fhuD	2.4	upp	2.1	fadI	2.5	yehT	2.7
narK	2.0	glnH	2.1	gltI	2.0	ppa	2.9	serS	2.3	ycjD	2.1	yehR	2.8	fhuF	2.2	uvrC	2.4	feaR	3.0	yehU	2.9
uxaC	2.0	lsrD	2.1	xylH	2.1	garL	2.9	fabD	2.3	yehI	2.1	yqeB	2.8	focB	2.0	wcaD	2.2	fecA	2.4	yejB	2.4
fdhD	2.0	ycgK	2.1	ydcA	2.1	ybaB	2.9	yagF	2.3	yaaU	2.1	ymgF	2.8	folD	2.4	wcaM	2.3	fecB	2.8	yejO	2.7
ansB	2.0	eutQ	2.1	ulaF	2.1	nikA	2.9	metY	2.3	yjbS	2.1	ygdT	2.8	frc	2.4	xapB	2.0	fecE	2.3	yfcM	2.7
ompW	2.0	hybB	2.1	yhhM	2.1	gntR	2.9	nhaB	2.2	yjgH	2.1	prpR	2.8	frvB	2.1	xdhA	2.5	feoA	2.5	yfdE	2.3
slp	2.1	dadX	2.2	fabB	2.1	sodA	2.9	grxC	2.2	sfmH	2.1	eamB	2.8	garD	4.0	xylF	3.2	feoB	2.5	yfdI	2.3
yqeB	2.1	yjcH	2.2	yfgC	2.1	yqaB	2.9	valV	2.2	ykgH	2.1	xapB	2.8	garK	2.8	yaiY	2.5	feoC	2.4	yfeC	2.2
yjiT	2.1	hybG	2.2	ssnA	2.1	garK	2.9	guaA	2.2	cstA	2.1	ykgC	2.8	garL	2.9	yajL	2.0	fieF	3.5	yfeD	2.4
ydfZ	2.1	lsrA	2.2	aceA	2.1	yhfA	2.9	yfbT	2.2	yfdR	2.1	sfmA	2.8	garP	4.2	yajQ	2.3	fimZ	2.0	yffN	2.1
yahN	2.1	hybD	2.2	acs	2.1	yieP	2.8	melR	2.2	yidI	2.1	cycA	2.8	garR	2.6	ybaB	2.6	focA	2.2	yffP	2.3
mdtM	2.1	glcC	2.3	grxB	2.1	leuS	2.8	gyrA	2.2	uidC	2.1	perR	2.8	gcvP	2.1	ybaL	2.3	focB	2.1	yfgJ	2.2
nrfD	2.1	ynfG	2.3	spy	2.2	yoeA	2.8	fadR	2.2	glnH	2.1	ecpD	2.9	glcC	2.9	ybaP	2.2	gabD	2.2	yfiB	2.3
ftnA	2.1	aceB	2.3	hybB	2.2	yehT	2.8	yijO	2.2	yidJ	2.1	xylF	2.9	glnB	3.8	ybbA	2.8	gabP	2.1	yfjU	3.6
yjcO	2.1	yhjA	2.4	nupG	2.2	yjjK	2.8	rplS	2.2	yfcV	2.1	ysaC	2.9	glnH	2.0	ybbD	2.3	gabT	2.4	ygaF	2.3
ycgK	2.1	hybF	2.4	ydhU	2.2	rpe	2.8	serT	2.2	creD	2.1	yfbN	2.9	glnP	2.5	ybbL	2.1	gapA	2.5	ygdB	2.6
yqjI	2.1	xylH	2.4	cyaR	2.2	garR	2.8	rfbD	2.2	yfaH	2.1	yiaT	2.9	gloA	2.1	ybdD	2.9	garD	2.7	yggD	2.4
ydcA	2.2	ydhW	2.4	clpB	2.2	ykgE	2.8	yfdI	2.2	allS	2.1	yjiL	2.9	gnd	2.2	ybfF	2.8	garK	2.5	yggN	2.3
yjiY	2.2	lsrR	2.4	ycgK	2.2	rsmE	2.8	dgsA	2.2	chbG	2.1	yfbO	2.9	gntX	2.3	ybfI	3.2	garL	2.4	yggP	2.1
uspG	2.2	allC	2.4	hybG	2.2	yheV	2.8	bamA	2.2	yghD	2.1	yaiV	2.9	gor	2.2	ybfQ	2.6	garP	2.2	yghW	2.6
uspD	2.2	yfjU	2.4	ydeH	2.2	yffL	2.8	eno	2.2	wcaA	2.1	atoB	2.9	gpmM	3.0	ybhN	2.1	garR	2.4	ygiZ	2.4
pheL	2.2	allD	2.4	yfeK	2.2	pmbA	2.8	tig	2.2	yojO	2.1	yfjJ	3.0	grxC	2.3	ybhT	2.6	gcvP	3.3	ygjV	2.1
hybA	2.2	xylG	2.5	ulaB	2.2	nadC	2.8	miaB	2.2	fixC	2.1	sgcR	3.0	guaA	2.2	ybiH	3.3	gfcE	2.1	yhfA	2.5
elbB	2.2	mglC	2.5	yfjU	2.2	rplT	2.8	nadK	2.2	yehB	2.1	yehX	3.0	guaC	2.4	ycaO	2.6	glcC	3.6	yhfK	2.0
hdeA	2.2	yjcO	2.5	dppF	2.2	ybaL	2.8	rdgB	2.2	djlC	2.1	yjiS	3.0	gudD	2.6	ycbZ	2.0	glnB	3.1	yhfT	2.2
yfbM	2.3	lsrF	2.5	ygeW	2.2	damX	2.8	yfeH	2.2	yiiG	2.1	gspA	3.0	gudP	4.3	ycjD	2.1	glnH	2.2	yidA	2.4
hdeB	2.3	cpdB	2.5	xdhA	2.2	argR	2.8	blr	2.2	yjjQ	2.2	yjgN	3.0	gudX	2.9	ydaE	3.3	glnP	2.9	yidH	2.1
hybB	2.3	degP	2.5	glnP	2.2	thrV	2.7	ycgE	2.2	rhaD	2.2	ybbD	3.0	gutQ	2.3	ydcI	2.3	glnQ	2.3	yieP	2.0
yafC	2.3	htrG	2.5	yqeB	2.2	sgrR	2.7	rffA	2.2	yafT	2.2	cmtB	3.1	hcaR	3.6	ydeH	3.2	gor	2.5	yigM	2.4
nrfC	2.5	ydhV	2.6	uspG	2.3	yobA	2.7	cydD	2.2	ygaQ	2.2	hcaT	3.1	hcaT	2.8	ydhC	2.9	gpmM	2.3	yijP	2.1
tdcD	2.5	cycA	2.6	yphF	2.3	leuW	2.7	iscU	2.2	hybC	2.2	focB	3.1	hda	2.4	ydiU	2.5	gudD	2.1	yjaG	2.1
hybF	2.5	rbbA	2.6	nlpD	2.3	insA	2.7	hinT	2.2	folK	2.2	ymgJ	3.2	hemE	2.1	ydjH	2.2	gudP	2.2	yjcH	3.1
hybG	2.5	ynfF	2.6	dppA	2.3	iscS	2.7	hokD	2.2	msyB	2.2	yoaE	3.2	hofO	2.1	yebE	2.5	gudX	2.4	yjgQ	2.5
ydhX	2.6	actP	2.7	yjiK	2.3	zraS	2.7	rluD	2.2	dppA	2.2	hybE	3.2	htpX	2.4	yebY	2.4	hcaR	4.3	yjiG	3.8
tdcC	2.6	yhiI	2.7	yjcH	2.3	manY	2.7	rnpB	2.2	ydiQ	2.2	yejB	3.2	hybE	2.5	yehR	2.4	hcaT	2.9	yjiH	3.3
cadA	2.6	hybE	2.8	ygeY	2.3	ebgA	2.7	rfbX	2.2	ssnA	2.2	ygfM	3.2	hypA	2.0	yehS	2.2	htpX	2.3	yjiL	2.8
hybD	2.6	ylbA	2.9	narP	2.3	map	2.7	ybfF	2.2	yeeL	2.2	ydaE	3.3	iadA	3.9	yehT	2.4	htrG	3.1	yjiM	4.0
gldA	2.6	hybC	2.9	glnH	2.3	proX	2.7	rbfA	2.1	yiaL	2.2	hcaR	3.3	intZ	2.7	yehX	2.3	hypA	2.6	yjjI	2.3
ynfE	2.6	yeiT	3.0	ybbA	2.4	yffO	2.7	ygjR	2.1	ybfP	2.2	mtr	3.4	iscA	2.2	yeiP	2.2	hypB	3.3	yjjK	2.8
ynfH	2.6	putA	3.0	glnQ	2.4	kdsB	2.7	gloA	2.1	ygfO	2.2	yqcE	3.4	iscS	2.4	yejB	2.3	iadA	2.8	ykgE	2.2
cadB	2.6	lsrB	3.1	rseA	2.4	folD	2.6	ravA	2.1	recE	2.2	ttdT	3.4	iscX	2.4	yejF	2.2	iscR	2.3	ykgF	2.1
pheA	2.6	fucO	3.2	ulaC	2.4	rpmE	2.6	rpoZ	2.1	hybA	2.2	fimZ	3.5	katG	2.3	yejO	3.7	katG	2.3	ykgG	3.5
yjiL	2.7	yeiA	3.2	fucU	2.4	gntX	2.6	yajQ	2.1	ybeQ	2.2	ydjO	3.5	kbaZ	2.7	yfaA	3.7	kdsB	4.1	ynbE	2.5
yjiE	2.8	lsrG	3.2	rsd	2.4	cysB	2.6	recR	2.1	sgbE	2.2	ygeY	3.5	kdsB	2.5	yfbN	2.3	leuW	2.3	yncJ	2.0
yhhJ	2.8	yjiM	3.3	xylG	2.4	hemE	2.6	manA	2.1	macA	2.2	ygjV	3.5	kefA	2.0	yfbO	2.1	lnt	2.6	yoeA	2.0
dmsC	2.9	alsA	3.3	yjcO	2.4	yrbC	2.6	recC	2.1	yraI	2.2	yejO	3.5	leuS	2.8	yfcM	2.2	lpp	2.3	ypdA	3.0
dcuB	2.9	yjiL	3.3	yahF	2.5	yfgM	2.6	ccmA	2.1	yfjU	2.2	ydeH	3.6	leuW	2.1	yfdE	2.6	lsrB	2.1	ypdB	2.2
hybE	2.9	yjiE	3.5	allD	2.5	nikR	2.6	cspA	2.1	prpE	2.2	yfdE	3.7	lpp	3.0	yfdG	2.0	lsrK	2.4	ypfJ	2.9
yhiI	3.0	xylF	3.6	yhjA	2.5	ytfB	2.6	mtn	2.1	hcaF	2.2	ydhC	3.7	lptA	2.1	yfdI	2.3	maeA	2.3	yphE	2.1

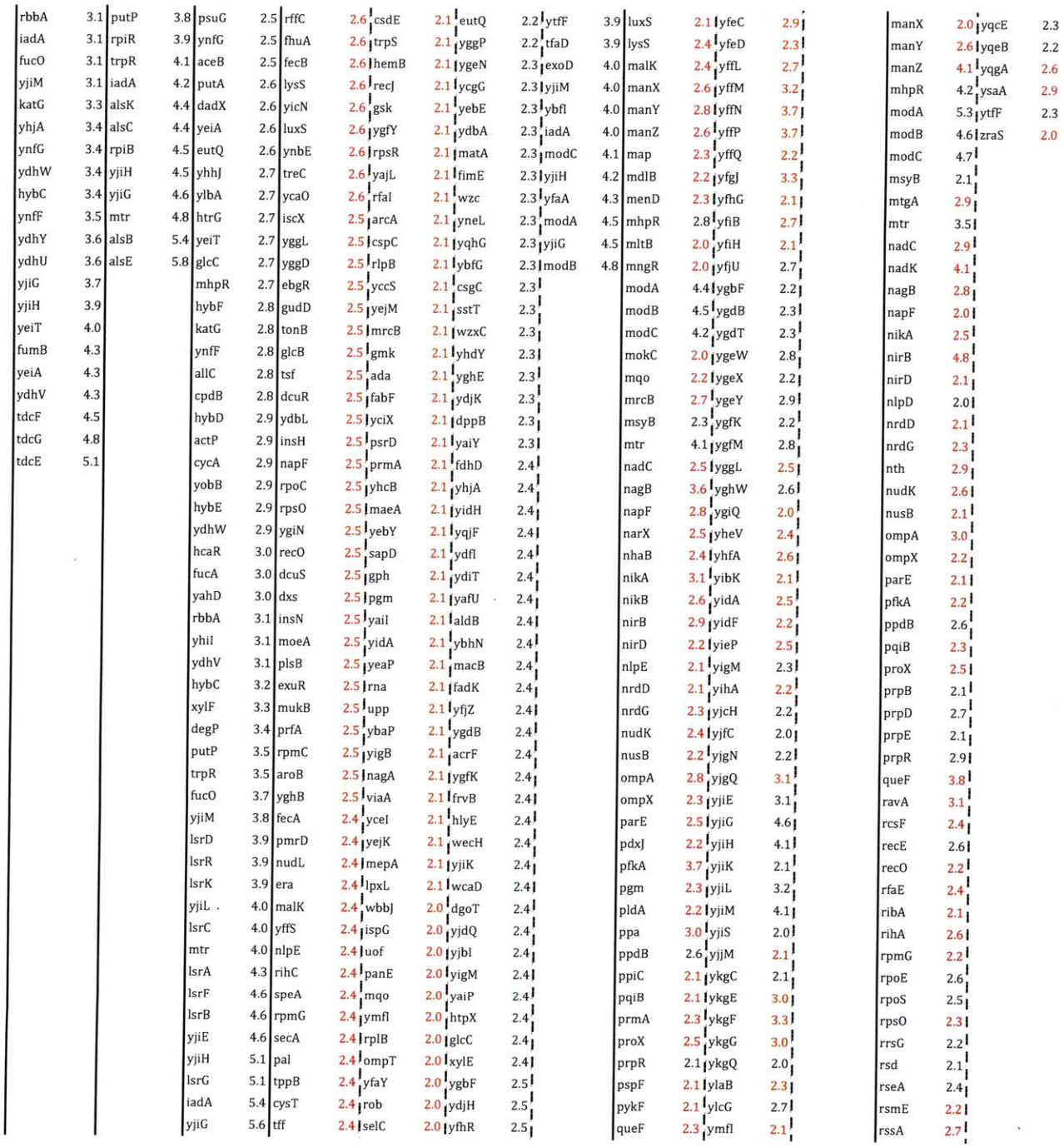
rbbA 3.1
iadA 3.1
fucO 3.1
yjiM 3.1
katG 3.3
yhjA 3.4
ynfG 3.4
ydhW 3.4
hybC 3.4
ynfF 3.5
ydhY 3.6
ydhU 3.6
yjiG 3.7
yjiH 3.9
yeiT 4.0
fumB 4.3
yeiA 4.3
ydhV 4.3
tdcF 4.5
tdcG 4.8
tdcE 5.1
putP 3.8
rpiR 3.9
trpR 4.1
iadA 4.2
alsK 4.4
alsC 4.4
rpiB 4.5
yjiH 4.5
yjiG 4.6
mtr 4.8
alsB 5.4
alsE 5.8
psuG 2.5
ynfG 2.5
aceB 2.5
putA 2.6
dadX 2.6
yeiA 2.6
eutQ 2.6
yhhJ 2.7
ylbA 2.7
htrG 2.7
yeiT 2.7
glcC 2.7
mhpR 2.7
hybF 2.8
katG 2.8
ynfF 2.8
allC 2.8
cpdB 2.8
hybD 2.9
actP 2.9
cycA 2.9
yobB 2.9
hybE 2.9
ydhW 2.9
hcaR 3.0
fucA 3.0
yahD 3.0
rbbA 3.1
yhiI 3.1
ydhV 3.1
hybC 3.2
xylF 3.3
degP 3.4
putP 3.5
trpR 3.5
fucO 3.7
yjiM 3.8
lsrD 3.9
lsrR 3.9
lsrK 3.9
yjiL 4.0
lsrC 4.0
mtr 4.0
lsrA 4.3
lsrF 4.6
lsrB 4.6
yjiE 4.6
yjiH 5.1
lsrG 5.1
iadA 5.4
yjiG 5.6
rffC 2.6
fhuA 2.6
fecB 2.6
lysS 2.6
yicN 2.6
luxS 2.6
ynbE 2.6
treC 2.6
ycaO 2.6
iscX 2.5
yggL 2.5
yggD 2.5
ebgR 2.5
gudD 2.5
tonB 2.5
glcB 2.5
tsf 2.5
dcuR 2.5
ydbL 2.5
insH 2.5
napF 2.5
rpoC 2.5
rpsO 2.5
ygiN 2.5
recO 2.5
dcuS 2.5
dxs 2.5
insN 2.5
moeA 2.5
plsB 2.5
exuR 2.5
mukB 2.5
prfA 2.5
rpmC 2.5
aroB 2.5
yghB 2.5
fecA 2.4
pmrD 2.4
nudL 2.4
era 2.4
malK 2.4
yffS 2.4
nlpE 2.4
rihC 2.4
speA 2.4
rpmG 2.4
secA 2.4
pal 2.4
tppB 2.4
cysT 2.4
tff 2.4
csdE 2.1
trpS 2.1
hemB 2.1
recJ 2.1
gsk 2.1
ygfY 2.1
rpsR 2.1
yajL 2.1
rfaI 2.1
arcA 2.1
cspC 2.1
rlpB 2.1
yccS 2.1
yejM 2.1
mrcB 2.1
gmk 2.1
ada 2.1
fabF 2.1
yciX 2.1
psrD 2.1
prmA 2.1
yhcB 2.1
maeA 2.1
yebY 2.1
sapD 2.1
gph 2.1
pgm 2.1
yaiI 2.1
yidA 2.1
yeaP 2.1
rna 2.1
upp 2.1
ybaP 2.1
yigB 2.1
nagA 2.1
viaA 2.1
yceI 2.1
yejK 2.1
mepA 2.1
lpxL 2.1
wbbJ 2.0
ispG 2.0
uof 2.0
panE 2.0
mqo 2.0
ymfI 2.0
rplB 2.0
ompT 2.0
yfaY 2.0
rob 2.0
selC 2.0
eutQ 2.2
yggP 2.2
ygeN 2.3
ycgG 2.3
yebE 2.3
ydbA 2.3
matA 2.3
fimE 2.3
wzc 2.3
yneL 2.3
yqhG 2.3
ybfG 2.3
csgC 2.3
sstT 2.3
wzxC 2.3
yhdY 2.3
yghE 2.3
ydjK 2.3
dppB 2.3
yaiY 2.3
fdhD 2.4
yhjA 2.4
yidH 2.4
yqjF 2.4
ydfI 2.4
ydiT 2.4
yafU 2.4
aldB 2.4
ybhN 2.4
macB 2.4
fadK 2.4
yfjZ 2.4
ygdB 2.4
acrF 2.4
ygfK 2.4
frvB 2.4
hlyE 2.4
wecH 2.4
yjiK 2.4
wcaD 2.4
dgoT 2.4
ydjQ 2.4
yjbI 2.4
yigM 2.4
yaiP 2.4
htpX 2.4
glcC 2.4
xylE 2.4
ygbF 2.5
ydjH 2.5
yfhR 2.5
ytfF 2.2
tfaD 2.2
exoD 2.3
yjiM 2.3
ybfI 2.3
iadA 2.3
modC 2.3
yjiH 2.3
yfaA 2.3
modA 2.3
yjiG 2.3
modB 2.3
luxS 3.9
lysS 3.9
malK 4.0
manX 4.0
manY 4.0
manZ 4.0
map 4.1
mdlB 4.2
menD 4.3
mhpR 4.5
mltB 4.5
mngR 4.8
modA 4.4
modB 4.5
modC 4.2
mokC 2.0
mqo 2.2
mrcB 2.7
msyB 2.3
mtr 4.1
nadC 2.5
nagB 3.6
napF 2.8
narX 2.5
nhaB 2.4
nikA 3.1
nikB 2.6
nirB 2.9
nirD 2.2
nlpE 2.1
nrdD 2.1
nrdG 2.3
nudK 2.4
nusB 2.2
ompA 2.8
ompX 2.3
parE 2.5
pdxJ 2.2
pfkA 3.7
pgm 2.3
pldA 2.2
ppa 3.0
ppdB 2.6
ppiC 2.1
pqiB 2.1
prmA 2.3
proX 2.5
prpR 2.1
pspF 2.1
pykF 2.1
queF 2.3
yfeC 2.9
yfeD 2.3
yffL 2.7
yffM 3.2
yffN 3.7
yffP 3.7
yffQ 2.2
yfgJ 3.3
yfhG 2.1
yfiB 2.7
yfiH 2.1
yfjU 2.7
ygbF 2.2
ygdB 2.3
ygdT 2.3
ygeW 2.8
ygeX 2.2
ygeY 2.9
ygfK 2.2
ygfM 2.8
yggL 2.5
yghW 2.6
ygiQ 2.0
yheV 2.4
yhfA 2.6
yibK 2.1
yidA 2.5
yidF 2.2
yieP 2.5
yigM 2.3
yihA 2.2
yjcH 2.2
yjfC 2.0
yjgN 2.2
yjgQ 3.1
yjiE 3.1
yjiG 4.6
yjiH 4.1
yjiK 2.1
yjiL 3.2
yjiM 4.1
yjiS 2.0
yjjM 2.1
ykgC 2.1
ykgE 3.0
ykgF 3.3
ykgG 3.0
ykgQ 2.0
ylaB 2.3
ylcG 2.7
ymfI 2.1
manX 2.0
manY 2.6
manZ 4.1
mhpR 4.2
modA 5.3
modB 4.6
modC 4.7
msyB 2.1
mtgA 2.9
mtr 3.5
nadC 2.9
nadK 4.1
nagB 2.8
napF 2.0
nikA 2.5
nirB 4.8
nirD 2.1
nlpD 2.0
nrdD 2.1
nrdG 2.3
nth 2.9
nudK 2.6
nusB 2.1
ompA 3.0
ompX 2.2
parE 2.1
pfkA 2.2
ppdB 2.6
pqiB 2.3
proX 2.5
prpB 2.1
prpD 2.7
prpE 2.1
prpR 2.9
queF 3.8
ravA 3.1
rcsF 2.4
recE 2.6
recO 2.2
rfaE 2.4
ribA 2.1
rihA 2.6
rpmG 2.2
rpoE 2.6
rpoS 2.5
rpsO 2.3
rrsG 2.2
rsd 2.1
rseA 2.4
rsmE 2.2
rssA 2.7
yqcE 2.3
yqeB 2.2
yqgA 2.6
ysaA 2.9
ytfF 2.3
zraS 2.0

Table 6-3: Z-score change for natural PonG1

Natural PonG1 treatement

6h				7h		8h	
abrB	2.7	pfkA	2.1	amiC	2.3	asnA	2.7
amiC	2.6	pstC	2.1	cdaR	3.6	cdaR	2.6
apt	2.3	raiA	2.4	cobC	2.1	feoB	2.7
bcr	2.1	ravA	2.3	cspF	2.2	fhuB	2.1
cdaR	3.9	rbsA	2.1	cspH	2.8	fimF	2.0
cobC	2.4	rnd	2.0	fimF	2.1	garK	2.5
dcuC	2.0	rraA	2.4	fimI	2.4	gudD	2.1
deoR	2.1	sdaB	2.4	fliL	2.1	gudX	2.2
dgsA	2.0	tdcA	3.7	fliN	2.0	nirB	2.1
feoA	2.4	ttdR	2.9	fliO	2.0	tonB	2.1
feoB	2.6	uspC	2.2	folK	2.3	ybhG	2.3
fimC	2.2	yadB	2.5	fruK	2.0	yfgJ	2.0
fimI	2.6	yaeH	2.1	ftsP	2.0	ylaC	2.2
focA	2.3	yahN	2.4	garD	2.2	yoeA	3.7
folB	2.0	ybjS	2.6	garK	2.9		
folK	3.4	ycbJ	2.5	garP	2.8		
frdB	2.1	yceA	2.4	garR	2.2		
fucP	2.3	ydeN	2.6	glnB	2.0		
garD	3.8	ydjY	2.2	gudD	2.9		
garK	3.5	yecF	2.1	gudP	2.9		
garL	2.9	yehD	2.3	gudX	2.7		
garP	4.5	yfbS	3.0	hypA	2.3		
garR	3.3	yfcZ	2.3	nagB	2.3		
gidB	2.1	yfeC	2.7	nikA	2.0		
glcB	2.1	yfeD	2.4	rraA	2.1		
glcF	2.3	yfeH	2.0	ryeC	2.5		
glcG	2.2	yfiD	2.0	sgrS	2.2		
gudD	3.0	ygcO	2.3	tdcA	3.4		
gudP	3.6	ygdE	2.6	tsr	2.1		
gudX	3.2	yghB	2.1	xseA	2.6		
hcp	2.1	yghZ	2.4	ydeN	2.0		
hypA	2.7	ygjR	2.1	yfeC	2.7		
hypB	2.1	yhbT	2.0	yfeD	2.1		
lpxH	2.2	yhbU	2.3	yfeH	2.2		
lpxT	2.1	yjdK	2.3	yggI	2.1		
mdoC	2.1	yjfN	3.2	yjfN	3.2		
melR	2.2	yjfO	2.5	yjfO	2.6		
menA	2.3	yjjM	2.7	ylaC	2.9		
mgsA	2.0	ykgE	3.4	ymjA	2.2		
mtfA	2.3	ykgF	2.5	yoeA	2.8		
nagB	2.4	ykgG	2.4	yqgA	2.6		
napC	2.3	ylaC	2.7	ysaA	2.3		
napF	3.5	yliG	2.1	zraS	2.1		
narK	2.1	ymjA	2.2				
nikA	3.2	yoeA	3.4				
nikB	2.1	ypfM	2.2				
nikC	2.1	yqgA	3.5				
nikD	2.0	yraL	2.2				
nirB	3.1	ysaA	3.8				
nirC	2.1	ytfB	2.0				
nirD	2.5	zraS	2.8				
pepE	2.2						

A map of the Z-score gene expression levels after treatment with the rebounding amidated PonG1-NH_2 is provided in Figure 6-9. A total of 798 genes were significantly affected (up or down regulated) upon treatment of wild-type *E. coli* K12 EMG2 with 10x MIC PonG1-NH_2. These genes were clustered according to similar expression patterns using simple hierarchical routine of the open source Cluter 3.0 software and were visualized using Java Treeview.

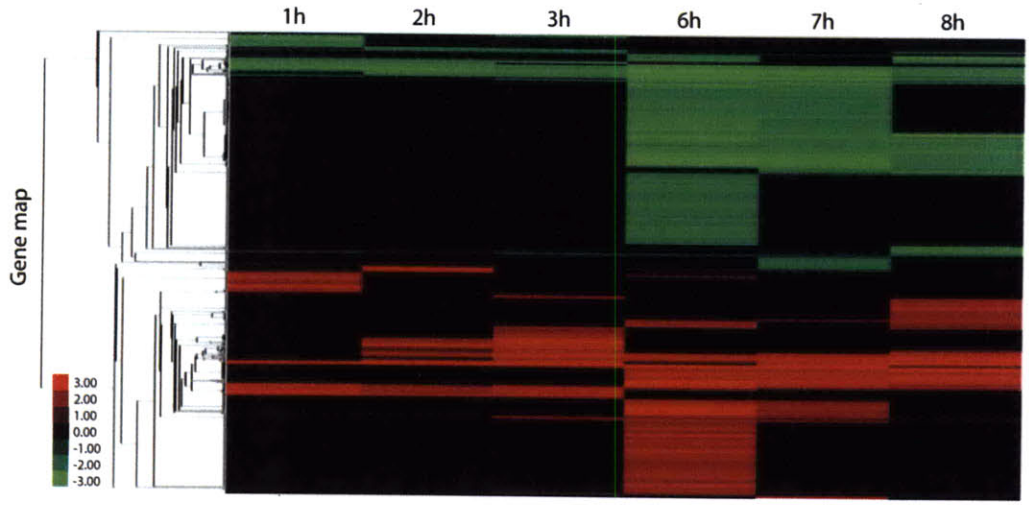

Figure 6-9: Gene expression levels rebounding amidated Ponericin G1-NH2

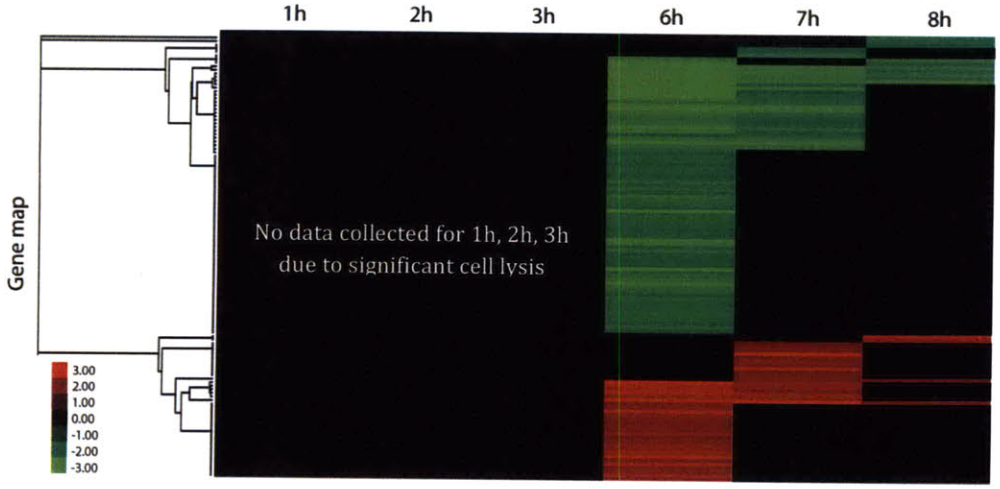

Figure 6-10: Gene expression map for cidal natural Ponericin G1.

A closer look a the gene expression levels along with the GO enrichments analysis detailed in section 6.7.4 show a strong and constant down regulation of the iron import genes upon treatment with Ponericin G1-NH2 (Table 6-4). We also performed a GO enrichment analysis on the gene expression data from treatment with Ponericin G1 alone but no clear pattern in pathway enrichment could be detected with strong statistical accuracy. This is primarily because differential expression analysis measures gene expression level, but does not differentiate primary targets from downstream secondary effects.

Table 6-4: Z-score change of iron import related gene upon treatment with PonG1-NH2.

Amidated PonG1-NH2 treatement												
1h		2h		3h		6h		7h		8h		
fecC	2.2	fecE	2.2	fecE	2.2	fecB	2.6	fecA	2.2	fecA	2.4	
fecB	2.1	fecB	2.1	fecA	2.0	fecA	2.4	fecB	2.3	fecB	2.8	
fecE	2.1	fecC	2.1	fecB	2.0					fecE	2.3	
fecD	2.1	fecA	2.1	fecC	2.0							

6.7.3. Mode-of-action by Network Identification (MNI) analysis

While the whole genome differential expression profile shows up-and-down regulated genes, it does not distinguish the initial genes targets or mediators of the AMP treatment from the many genes that respond secondarily to the initial effects. We therefore performed a Mode-of-action by Network Identification (MNI) analysis to distinguish the AMPs' actual pathway and gene targets from the indirect responders (*24*). The MNI approach performs well at identifying treatment mode-of-action because it makes use of information on the gene-regulatory network underlying the expression change (*25*), where as differential gene expression analysis uses no knowledge of regulatory influences.

The RMA normalized gene expression data of Table 6-2 and Table 6-3was loaded in the Matlab version of the MNI algorithm (http://gardnerlab.bu.edu) and analyzed using the default values of 1/3 for *Kfrac*, 3 for *NROUNDS*, 0.25 for *thP* and 100 for *TopN*. The raw output of the MNI algorithm identifies the top 100 highest ranked putative mediators and gene targets for PonG1-NH_2 and PonG1 at different time point and is shown in Table 6-5.

Table 6-5: MNI output showing the 100 highest ranked putative gene targets. The putative targets underlying the mode of action of PonG1-NH2 and PonG1 are shown for each time point. Pathway analysis was then performed on the MNI gene list using Gene Ontology enrichement and the gene associated with the identified pathways are shown in red (refer to Section 6.7.4 for details on GO enrichment analysis).

	Mode-of-action by Network Identification (MNI) analysis								
	Amidated PonG1-NH_2 treatement						Natural PonG1 treatement		
Rank	1h	2h	3h	6h	7h	8h	6h	7h	8h
1	aphA	potD	viiM	pepT	vdhC	bax	sdaB	vdhC	vsaA
2	cadA	cpdB	ansB	vffM	modA	viiM	birA	xseA	vtfI
3	fimG	mtr	putP	vdhC	mtr	vejO	apt	fruB	asnA
4	tdcE	putP	cpdB	vffP	xylF	modA	ispH	vlaC	vbiH
5	vdhV	fucR	vdhV	exoD	viiM	maeB	vlaC	lpxK	vbdD
6	vcbI	ansB	vhaL	vgeY	der	fadH	vehS	vlaB	vbiD
7	katG	viiM	iadA	rsxD	vdcH	iraP	rbsR	chiA	dctA
8	hybE	alsE	ftnB	vciD	fucO	mtr	vgdE	folK	vahN
9	vahN	katG	cstA	viiB	vtfI	vrbK	proX	rnd	maeB
10	pepE	iadA	katG	tfaD	vffP	vffN	fimI	vhiY	proX
11	ccmC	fimG	maeB	viiE	dctA	dctA	vlaB	rluB	tnaA
12	vdiY	alsA	viiE	iadA	vciD	vdcH	ppgG	ftsP	veeE
13	iadA	cstA	vdiY	vfaA	vlcG	xylF	folK	vedE	mppA
14	pck	vhaL	glnH	vgdT	uspF	vgdB	potD	apt	acnB
15	tdcG	glnH	iraP	vfbM	iadA	fadA	chaA	fadR	vdeN
16	ansB	alsK	yccA	kbaZ	vffL	htrG	gltP	fliF	vggG
17	cpdB	viiH	fucR	ansB	vff0	gabT	vgcF	ispH	vkgG
18	dcuB	xylF	lsrA	vffR	vafM	xylH	vfcL	vehS	veeD
19	vghZ	tppR	potD	modA	vffM	mhpR	glnS	rsxE	cpdB
20	vnfE	fimH	rihA	viiM	viiE	modB	tppB	vdiY	pabA
21	vhiA	acnB	vlbA	voaE	vejO	vtfI	hemN	vbiP	gsiC
22	hybO	htrG	gltK	rsmC	viiG	vciD	vfiH	cspF	tdcA
23	nrfF	hybC	vobB	vff0	vhbT	yccA	fimC	vehT	cstA
24	vdhU	gltK	uspF	vffN	fumA	fucA	gltX	potD	gcvP
25	nrfD	hybB	hybE	vff0	acnB	spy	accC	rsxC	gldA
26	vdiZ	mdh	lsrF	vrbK	vaiZ	fadI	maeA	vfcL	cysN
27	vdhY	iraP	fucA	vbfI	viiH	fucR	yccF	bcsC	aphA
28	viiI	alsB	dctA	der	vdaE	vbhO	rsxE	btuC	mglC
29	fumB	hcaR	viiH	vdeH	vffN	degP	cld	sdhB	narK
30	uxaC	fimA	mhpR	vtfF	dadX	veaC	cyoE	sdaB	vfeC
31	aspA	gcvP	vbdD	iscA	glnH	hcaR	lysS	vedF	vehD
32	uspF	maeB	tnaB	tff	modC	viiG	rnhA	rsxG	vehT
33	hypD	alsC	veiT	vgeX	exoD	iadA	vfbO	potA	yceH
34	hybF	fimI	vaiZ	intZ	vdbI	yceI	mrdB	yciT	rihC
35	dcuS	rpiB	dadX	vqeC	iraP	aldB	vecF	ycdY	cdaR
36	pspE	pssA	hybO	katG	acs	cstA	asnS	ymiA	melR
37	uxaB	veiA	degP	veiO	hcaR	cvaR	bglA	rrmA	tnaB
38	gldA	pspE	rbbA	vqcE	dppA	agp	era	rhtA	potD
39	viiM	mglB	ychN	ompW	tppR	emrA	yceA	phoO	vbhO
40	rbbA	vedE	vafM	exbB	fadB	veiB	argS	vgaM	napD
41	viiH	tnaB	gltL	veiB	fucR	glcC	truC	narK	gsiB
42	agp	dld	yicO	iscS	vgeW	pprR	hemB	glvS	symR
43	viiL	vbdD	xylF	vdaE	vqfA	ydcW	rdgC	nhaB	vebK
44	fucA	veiT	putA	iscU	maeB	katG	manZ	ubiG	rumA
45	caiF	fumA	acnB	ecnA	ompX	gabP	rnt	flgI	malE
46	nrfC	sthA	mdh	yihF	aldB	vdbI	rbsC	nth	veaT
47	tdcD	putA	htrG	lpp	msrB	astD	nuoL	thiI	nuoM
48	fimD	nuoL	aldA	aroB	modB	vqeB	lpxT	rihC	vdiA
49	fucO	lsrA	vqeB	chbG	yicH	vffL	menA	lpxT	vhbT
50	vqeC	vedF	vqeC	vgeW	htpX	astB	ychF	veaZ	vkgF
51	vdhX	dadX	ompW	maeB	vgeV	glnH	potA	vsaB	nuoL
52	nrfA	vbgE	lsrD	ssnA	vbhO	modC	veiK	yccF	vehU
53	vhhI	uspF	vdcH	vgfO	rveA	paaX	cmoB	proX	vbiK
54	vpfM	mglA	selD	amiA	actP	vqfA	nuoI	sucD	dld
55	tdcF	rihA	lsrC	rpmC	sucC	yifN	rbsA	fliM	cysI
56	vfcZ	yfiO	cvaR	guaD	degS	paaK	nuoI	prmC	vdiY
57	vdhW	glcB	agp	rpmG	vqeB	fadI	dxr	acnB	isrB
58	dtpB	msrB	sucC	vffL	fadH	lsrB	veaZ	rsxD	viiM
59	vnfG	gltL	slt	rfaE	vffR	vdeH	ptsG	cvoE	yifN
60	tdcA	veaC	fumA	leuW	mglB	feaR	panF	veeD	murO
61	vhbT	rpiR	vdiZ	hybE	dadA	vqeC	ycaO	yhcO	nagE

65	hvbA	yiiG	yicH	yqeB	yffS	fucO	nhaB	msbA	glcG
66	hvbG	ybgT	lsrG	yqfM	fucA	yaiZ	msbA	tppB	garD
67	hvpE	sdhD	msrB	rsmE	mtfA	sseA	yacG	fliO	mtfA
68	tnaB	fimC	ppyN	ydiL	yebE	fadD	yggN	ybiD	cysI
69	cyaR	fimD	psuG	agp	metK	astA	glyS	fliL	glcB
70	yqeB	glcG	hvbC	xdhA	sdhA	ydcV	rhtA	rnt	ebgC
71	dmsA	actP	dld	baeR	sseA	cycA	dsbG	asmA	ycbG
72	ychN	dctA	yiiG	psrD	mhpR	astC	potB	gatZ	yqeC
73	yiiG	sucC	lsrR	yiiH	emrA	hcaT	ubiG	yeeE	ycbI
74	yidK	sdhB	yecA	htpX	rfaE	htpX	gatZ	yedA	ykgE
75	yfbM	ylbA	sdhA	aldB	yffO	ompX	vaiG	gatY	elbB
76	frdB	lsrR	hybD	ybbD	agp	dppA	nuoH	yecF	mgsA
77	rihC	lsrF	sucD	lipB	yfiU	aldA	ansA	fliI	sucD
78	yfiD	yraP	lsrB	xylF	yihX	yicH	valS	gatA	mglA
79	exuT	yicH	ygeV	rpmF	hscB	acs	ampG	flgI	sseA
80	yeiA	rihC	gltA	yiiK	csdD	dadX	cmoA	potC	napF
81	ynfF	lsrB	rveA	yffS	suhB	acnB	gatA	ypiD	ucpA
82	dmsC	sucD	yedF	hscB	aldA	yebE	pncA	add	rihA
83	hvbC	fucO	lsrK	dnaX	fadI	ugpE	gsk	fliP	cysH
84	tdcC	fimF	lolE	modB	sucD	dadA	atpC	fliN	fumA
85	frdD	yiiL	sucA	mtr	katG	yiiH	lpxH	fabA	ychN
86	lysU	glgC	mtr	ygfK	ybdD	gltA	rbsK	fliG	aldA
87	frdC	mglC	fucO	yqeA	iscS	yffS	prmA	yebZ	nuoI
88	dcuC	mtfA	yiiL	glnB	cyaR	fadB	yciT	fliH	dcp
89	dmsB	cydB	ydcA	rplT	feaR	rveA	fadR	flhB	psdE
90	ompW	lolE	ghrA	mtr	intZ	ybdD	rrsG	yidI	yedF
91	yehD	slt	trpR	cstA	sdhB	fumA	pheP	deoR	fucO
92	yiiT	yaiZ	yeaC	trmI	ompW	mtfA	ydcP	hscC	pmrD
93	hybD	ppyN	mtfA	rlpB	yeaC	yihX	queC	potB	fucI
94	frdA	sdhA	gltI	ttdT	glcC	yhaL	ypiD	yibI	yafM
95	yeiT	lsrG	sdhB	focB	cstA	yfiU	yfiP	yibT	ygbZ
96	elbB	nuoM	yfgC	iscX	sdhD	ycfS	fdhE	flhA	rveC
97	tdcB	sucA	actP	hyuA	ppyE	astE	deoR	mppA	ybhG
98	fimF	sucB	sucB	modC	iscA	ymiA	yqeG	mgrB	agp
99	ydcH	aldA	hcaR	yiiG	ydiA	cspD	solA	lpxH	garP
100	dcuA	agp	hybB	rpmA	fadI	yqeF	mgrB	yehU	yaiZ

6.7.4. Pathway analysis using Gene Ontology (GO) enrichment

From the putative list of gene targets, the next step is to determine the pathways or classes that are significantly regulated. Pathway analysis involves looking for consistent but potentially small changes in gene expression by incorporating either pathway or functional annotations. It is therefore more subtle than the gene lists that result from univariate statistical analysis. (*26*).

Gene Ontology (GO) enrichment analysis identifies the cellular pathway affected by the treatment based on prior biological knowledge. It calculates, through a P-value, the probability that the pathway being correlated to the gene expression dataset is correctly identified due to an actual effect of the treatment as opposed to random occurrence. That is, lower the P-values indicate higher chances that the pathway is in fact a target of the treatment as opposed to being random. In other word, the GO analysis validates the plausibility that these pathways are affected by based on the MNI ranking order of the genes involved in the pathway of interest. These P-values describe the likelihood of obtaining the observed gene expression results. Therefore only the pathways, which are statistically likely to be affected, are

identified by the GO enrichment analysis. (*27*). The GO annotation classifies the pathways as influencing cellular component, molecular function and biological process (*28*) and annotated them to infer the actual networks and mechanisms by which the AMP treatment affects gene expression and cell function.

Therefore, the list of gene targets identified by MNI analysis is submitted to Gene Ontology enrichment analysis. The results and discussion of the enrichment analysis are presented in section 6.7.5 and section 6.7.6 as well as our hypothesis for the mode-of-action of the two AMPs, PonG1 and PonG1-NH2.

6.7.5. Amidated ponericin G1 affects iron transport and its recognition by the cell

Many of the 1h MNI targets of the static amidated AMP, PonG1-NH2, are involved in iron transport. Starting after 1h of treatment, there is a down regulation of proteins related to iron import such as fecA, fecB, fecC, fecD, and fecE. FecA is an outer membrane protein that is a transporter for Fe^{3+} citrate. When bound to Fe3+ citrate, FecA activates fecR, which is a protein in the cytoplasmic membrane that interacts with FecI, which is sigma factor of the sigma 70 type. FecI then goes and activates transcription of the fecA, fecB, fecC, fecD, fecE operon.

Given that fecABCDE are all down regulated and that the enzymes affected at 1h involve iron sulfur cores, it appears that the bacteriostatic amidated Ponericin G1-NH_2 affects iron transport or its recognition by the cell. However, since the transcription factor that regulates iron homeostasis, fur, doesn't seem to be involved, the cell are in fact "blinded" to not take up more iron, which in turn slows down metabolism and arrests cell growth. The main 2h targets of the amidated AMP seem to be in the TCA cycle - some of those proteins have iron sulfur clusters but others don't, so that could be a connection.

Table 6-6: Amidated PonG1-NH_2 Gene Ontology enrichment following MNI analysis

Function/process/component	Enrichment	Gene ontology
1 hour post treatment		

calcium ion binding	3.6E-08	GO:0005509
metal chelating activity	6.3E-08	GO:0046911
lead ion binding	1.4E-07	GO:0032791
heme binding	1.9E-07	GO:0020037
iron chaperone activity	1.9E-07	GO:0034986
metal ion binding	2.0E-07	GO:0046872
ferrous iron binding	2.0E-07	GO:0008198
ferric iron binding	2.0E-07	GO:0008199
iron ion binding	2.8E-07	GO:0005506
alkali metal ion binding	3.5E-07	GO:0031420
ion binding	4.5E-07	GO:0043167
2 iron, 2 sulfur cluster binding	4.7E-07	GO:0051537
3 iron, 4 sulfur cluster binding	4.7E-07	GO:0051538
4 iron, 4 sulfur cluster binding	4.7E-07	GO:0051539
iron-sulfur cluster binding	5.2E-07	GO:0051536
magnesium ion binding	5.5E-07	GO:0000287
metal cluster binding	7.3E-06	GO:0051540
nucleic acid binding	9.0E-06	GO:0003676
2 hours post treatment		
tricarboxylic acid cycle	6.3E-11	GO:0006099
reductive tricarboxylic acid cycle	6.3E-11	GO:0019643
acetyl-CoA catabolic process	3.0E-10	GO:0046356
3 hours post treatment		
tricarboxylic acid cycle	5.2E-10	GO:0006099
reductive tricarboxylic acid cycle	5.2E-10	GO:0019643
acetyl-CoA catabolic process	2.0E-09	GO:0046356
7 hours post treatment		
multicellular organismal lipid catabolic process	2.1E-08	GO:0044240
cellular lipid catabolic process	2.1E-08	GO:0044242
negative regulation of lipid catabolic process	2.1E-08	GO:0050995
tricarboxylic acid cycle	1.5E-07	GO:0006099
reductive tricarboxylic acid cycle	1.5E-07	GO:0019643
acetyl-CoA catabolic process	4.0E-07	GO:0046356
8 hours post treatment		
arginine catabolic process to glutamate	2.2E-07	GO:0019544
arginine catabolic process	2.8E-06	GO:0006527
glutamate metabolic process	2.8E-06	GO:0006536
multicellular organismal lipid catabolic process	3.0E-06	GO:0044240
cellular lipid catabolic process	3.0E-06	GO:0044242
negative regulation of lipid catabolic process	3.0E-06	GO:0050995
D-arginine metabolic process	4.5E-06	GO:0033055
very-long-chain fatty acid metabolic process	6.8E-06	GO:0000038
long-chain fatty acid metabolic process	6.8E-06	GO:0001676
icosanoid metabolic process	6.8E-06	GO:0006690
fatty acid catabolic process	6.8E-06	GO:0009062
wax metabolic process	6.8E-06	GO:0010166
suberin biosynthetic process	6.8E-06	GO:0010345
arachidonic acid metabolic process	6.8E-06	GO:0019369
fatty acid oxidation	6.8E-06	GO:0019395
oxylipin metabolic process	6.8E-06	GO:0031407
unsaturated fatty acid metabolic process	6.8E-06	GO:0033559
butanoic acid metabolic process	6.8E-06	GO:0043437
linoleic acid metabolic process	6.8E-06	GO:0043651
short-chain fatty acid metabolic process	6.8E-06	GO:0046459
lauric acid metabolic process	6.8E-06	GO:0048252
medium-chain fatty acid metabolic process	6.8E-06	GO:0051791
acyl-CoA metabolic process	1.0E-05	GO:0006637
negative regulation of fatty acid metabolic process	1.0E-05	GO:0045922

6.7.6. Natural Ponericin G1 targets tRNA synthetases

On the other hand, the natural version of the AMP is bactericidal and kills rapidly before the cells are able to develop resistance and regrow to their original count, typically within 6 hours. MNI analysis on the resistant cells at 6 hours does not pick out indentify iron-related genes as mediators of transcriptional changes but instead indicate a change that seems to point to tRNA synthetases. For this to occur, the AMP must be penetrating the cells and interfere directly with tRNA synthetases or affect the cell membrane in such a way as to lead to downstream transcriptional events.

Table 6-7: Natural PonG1 Gene Ontology enrichment following MNI analysis

Function/process/component	Enrichment	Gene ontology
6 hours post treatment		
arginyl-tRNA aminoacylation	1.68E-06	GO:0006420
glycyl-tRNA aminoacylation	2.40E-06	GO:0006426
alanine-tRNA ligase activity	8.27E-06	GO:0004813
arginine-tRNA ligase activity	8.27E-06	GO:0004814
aspartate-tRNA ligase activity	8.27E-06	GO:0004815
asparagine-tRNA ligase activity	8.27E-06	GO:0004816
cysteine-tRNA ligase activity	8.27E-06	GO:0004817
glutamate-tRNA ligase activity	8.27E-06	GO:0004818
glutamine-tRNA ligase activity	8.27E-06	GO:0004819
glycine-tRNA ligase activity	8.27E-06	GO:0004820
histidine-tRNA ligase activity	8.27E-06	GO:0004821
isoleucine-tRNA ligase activity	8.27E-06	GO:0004822
leucine-tRNA ligase activity	8.27E-06	GO:0004823
lysine-tRNA ligase activity	8.27E-06	GO:0004824
methionine-tRNA ligase activity	8.27E-06	GO:0004825
proline-tRNA ligase activity	8.27E-06	GO:0004827
serine-tRNA ligase activity	8.27E-06	GO:0004828
threonine-tRNA ligase activity	8.27E-06	GO:0004829
tryptophan-tRNA ligase activity	8.27E-06	GO:0004830
tyrosine-tRNA ligase activity	8.27E-06	GO:0004831
valine-tRNA ligase activity	8.27E-06	GO:0004832
tRNA aminoacylation for protein translation	8.27E-06	GO:0006418
ligase activity, forming aminoacyl-tRNA and related compounds	8.27E-06	GO:0016876
aminoacyl-tRNA synthetase auxiliary protein activity	8.27E-06	GO:0017100
pyrrolysyl-tRNA synthetase activity	8.27E-06	GO:0043767
phosphoserine-tRNA(Cys) ligase activity	8.27E-06	GO:0043816
aspartate-tRNA(Asn) ligase activity	8.27E-06	GO:0050560
glutamate-tRNA(Gln) ligase activity	8.27E-06	GO:0050561
lysine-tRNA(Pyl) ligase activity	8.27E-06	GO:0050562
aminoacyl-tRNA ligase activity	1.09E-05	GO:0004812
phenylalanine-tRNA ligase activity	1.09E-05	GO:0004826
asparaginyl-tRNA aminoacylation	1.98E-05	GO:0006421
aspartyl-tRNA aminoacylation	1.98E-05	GO:0006422
glutaminyl-tRNA aminoacylation	1.98E-05	GO:0006425
histidyl-tRNA aminoacylation	1.98E-05	GO:0006427
isoleucyl-tRNA aminoacylation	1.98E-05	GO:0006428
leucyl-tRNA aminoacylation	1.98E-05	GO:0006429
lysyl-tRNA aminoacylation	1.98E-05	GO:0006430
methionyl-tRNA aminoacylation	1.98E-05	GO:0006431
prolyl-tRNA aminoacylation	1.98E-05	GO:0006433
seryl-tRNA aminoacylation	1.98E-05	GO:0006434
threonyl-tRNA aminoacylation	1.98E-05	GO:0006435
tryptophanyl-tRNA aminoacylation	1.98E-05	GO:0006436
tyrosyl-tRNA aminoacylation	1.98E-05	GO:0006437
valyl-tRNA aminoacylation	1.98E-05	GO:0006438
tRNA aminoacylation	1.98E-05	GO:0043039
tRNA aminoacylation for mitochondrial protein translation	1.98E-05	GO:0070127
alanyl-tRNA aminoacylation	2.69E-05	GO:0006419
cysteinyl-tRNA aminoacylation	2.69E-05	GO:0006423
glutamyl-tRNA aminoacylation	2.69E-05	GO:0006424
phenylalanyl-tRNA aminoacylation	2.69E-05	GO:0006432
7 hours post treatment		
microtubule-based flagellum	4.89E-13	GO:0009434
flagellin-based flagellum	7.36E-13	GO:0009288
ciliary or flagellar motility	4.75E-10	GO:0001539
ciliary cell motility	4.75E-10	GO:0060285
flagellar cell motility	4.75E-10	GO:0060286
cell motility	7.53E-10	GO:0048870
flagellum	8.19E-08	GO:0019861
cell projection	9.49E-08	GO:0042995
microfilament motor activity	2.02E-07	GO:0000146
microtubule motor activity	2.02E-07	GO:0003777
flagellin-based flagellum part	1.25E-06	GO:0044461
flagellin-based flagellum basal body	3.41E-06	GO:0009425

6.8. Natural Ponericin G1 potentiates ribosomal antibiotics

Although almost identical in structure, PonG1 and PonG1-NH_2 act through very different mechanism-of-action with different targets. As a result the two peptides have different cidality profile.

Ponericin G1 has strong cidal activity and blocks tRNA synthetase in the ribosome. We hypothesize that PonG1 could be specifically potentiated with the addition ribosome targeting antibiotics, such as kanamycin from the aminoglycoside antibiotics. Kanamycin diffuses through porin channels and inhibits protein synthesis and increasing translation errors by interacting with three ribosomal proteins (*29*).

We determined the synergistic effect of the PonG1 and Kanamycin on antibiotic resistant *E. coli* population. A fresh culture of *E.coli* was first treated with 10x ofloxacin and the resistant population was allowed to regrow for 8 hours. These resistant cells were subjected to different treatment groups: ofloxacin-only, kanamycin-only, AmP-only treatments as controls and combination treatments of AmP+ofloxacin and AmP+kanamycin (Figure 6-11). The experiment was carried in triplicates and with both PonG1 and PonG1-NH2 as AmP. Treatment with ofloxacin, kanamycin, PonG1 and PonG1-NH2 alone were not effective at killing the culture of resistant cells; the cell count remained around 10^8CFU/ml even after 6 hours of treatment. On the other hand combination of the ribosome targeting PonG1 and the ribosomal antibiotic kanamycin lead to the highest cell killing with only 10^4 CFU/ml viable cells after 6 hours of treatment. Combination of kanamycin with PonG1-NH2 did not result in as large a decrease since the AmP and kanamycin do not act synergistically to target the ribosome. Combination of ofloxacin and PonG1-NH2 did not reduce the count of resistant cells, and combination with PonG1 lead to a reduction to $10^{5.5}$ CFU/ml after 6 hours which is about 30-fold less effective then the optimal combination of PonG1 and kanamycin.

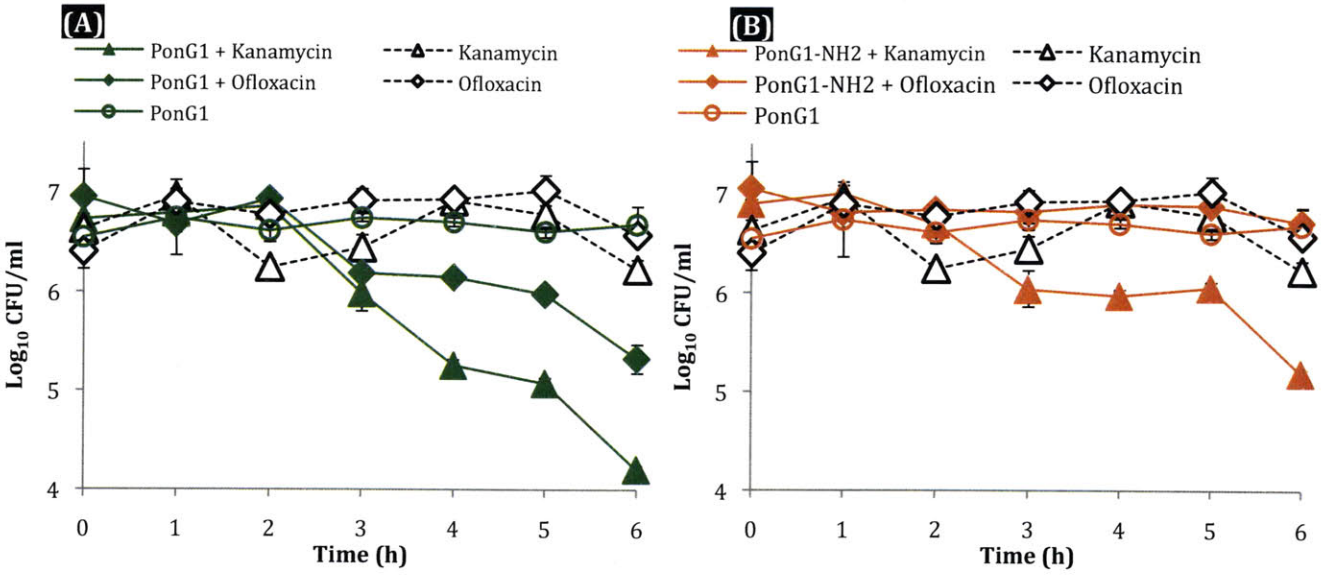

Figure 6-11: Synergistic effect for PonG1 and Kan. Ofloxacin resistant E.coli cells were treated with combination of ofloxacin or kanamycin with (A) PonG1 or (B) PonG1-NH2. PonG1 and kanamycin act synergistically by both targeting the ribosome and the combination treatment leads suppression of resistant culture by over 300-fold compare to single treatment with either kanamycin or PonG1 alone. Combination of PonG1 and ofloxacin or PonG1-NH2 and kanamycin also suppresses the bacterial culture although to a lesser extend.

6.9. Chapter conclusion

In summary, we measured the MIC and bactericidal of the ponericin family of AmPs. We discovered the MIC level and growth inhibition properties is not a good indicative of cidal activity the peptides. We re-classified the family of ponericins into ineffective AmPs, rebounding AmPs and bactericidal AmPs. We studied the cidal behaviors of AmPs using a high-speed AFM and and a microfluidic flow device. Both apparatus showed that the action of AmPs led to corrugation of the

bacterial cell membrane and that some cells are able to resist the action of the peptide more than others. We then focused our study on PonG1 to get a better understanding of its mechanism.

PonG1 demonstrated a rebounding behavior, that is a strong initial cidal effect followed by regrow of the baterial culture (Figure 2-2B). Images obtained using a microfluidic flow chamber shows a sub-population of the cell culture is affected by PonG1 and undergoes membrane disruption while other cells are able to resist the action of PonG1 and continue to divide and grow the chamber. Treatment with PonG1 leads to the misfolding of membrane proteins. The cells ability to sense and repair of these membrane defects through the CpxAR sensing system is key to developing resistance to PonG1 (Figure 6-6). Finally, PonG1 also causes DNA damage, which the cells overcome by activating SOS response (Figure 6-8). The cells ability to sense and activate the SOS response through the DpiAB system is beneficial but not essential for cell resistance (Figure 6-7) indicating that other sensing mechanism can lead to the activation of SOS response. Gene expression analysis shows that PonG1 affect tRNA synthetase occurring the cell's ribosome activity (Table 6-6). When combined with other ribosome targeting antimicrobials such as kanamycin, PonG1 is synergistically potentiated. The combination treatment is able to able to suppress cultures of antibiotic resistant *E.coli* that are not affect by either PonG1 or kanamycin treatment alone (Figure 6-11).

6.10. References

1. H. G. Boman, in *Jounral of Internal Medicine.* (2003), pp. 197-215.
2. M. Zasloff, in *Nature.* (2002), vol. 415, pp. 389-95.
3. R. E. W. Hancock, H.-G. Sahl, in *Nat Biotechnol.* (2006), vol. 24, pp. 1551-1557.
4. J. Orivel *et al.*, in *J Biol Chem.* (2001), vol. 276, pp. 17823-9.
5. A. Barry *et al.*, in *Clinical and Laboratory Standards Institute.* (1999), vol. 19, pp. M26-A.
6. L. F. Fehri *et al.*, in *Antimicrob Agents Chemother.* (2005), vol. 49, pp. 4154-65.
7. D. Andreu *et al.*, in *FEBS Lett.* (1992), vol. 296, pp. 190-4.
8. E. Y. Chekmenev, B. S. Vollmar, M. Cotten, in *BBA - Biomembranes.* (2010), vol. 1798, pp. 228-234.
9. G. E. Fantner, R. J. Barbero, D. S. Gray, A. M. Belcher, in *Nature Nanotechnology.* (2010).
10. M. Pietiäinen *et al.*, in *Microbiology (Reading, Engl).* (2005), vol. 151, pp. 1577-92.
11. MacRitchie, Buelow, Price, Raivio, in *Adv Exp Med Biol JO* -. (2008), vol. 631 IS -, pp. 80-110 DO -.
12. Yormiar. (2005), pp. 1-14.
13. Miller *et al.*, in *Science JO* -. (2004), vol. 305, pp. 1629-1631.
14. B. Michel, in *PLoS Biol.* (2005), vol. 3, pp. e255.
15. R. T. Cirz *et al.*, in *PLoS Biol.* (2005), vol. 3, pp. e176.
16. T. J. Wigle, S. F. Singleton, in *Bioorg Med Chem Lett.* (2007), vol. 17, pp. 3249-53.
17. A. M. Lee, C. T. Ross, B. B. Zeng, S. F. Singleton, **48**, 5408 (2005).
18. M. S. KÖRIS, in *Boston University PhD Thesis.* (2010).
19. J. J. Faith *et al.*, *PLoS Biol* **5**, e8 (Jan 1, 2007).
20. R. A. Irizarry *et al.*, *Nucleic Acids Res* **31**, e15 (Feb 15, 2003).
21. R. A. Irizarry *et al.*, *Biostatistics (Oxford, England)* **4**, 249 (Apr, 2003).
22. B. M. Bolstad, R. A. Irizarry, M. Astrand, T. P. Speed, *Bioinformatics* **19**, 185 (Jan 22, 2003).
23. P. Hegde *et al.*, *Biotechniques* **29**, 548 (2000).
24. D. di Bernardo *et al.*, in *Nat Biotechnol.* (2005), vol. 23, pp. 377-83.
25. H. Xing, T. S. Gardner, in *Nat Protoc.* (2006), vol. 1, pp. 2551-4.

26. R. K. Curtis, M. Oresic, A. Vidal-Puig, *Trends Biotechnol* **23**, 429 (2005).

27. S. Draghici, P. Khatri, R. P. Martins, G. C. Ostermeier, S. A. Krawetz, *Genomics* **81**, 98 (2003).

28. M. Ashburner *et al.*, **25**, 25 (2000).

29. H. Umezawa, *Adv Carbohydr Chem Biochem* **30**, 183 (1974).

Chapter 7. Therapeutic opportunities for engineered bacteriophages (PhDCEP Capstone)

Throughout this thesis, I have worked in close collaboration with Timothy Lu and Michael Koeris from the Collins' Lab at Boston University. The three of us engineered bacteriophages to express various foreign proteins and confer new functionalities to the bacteriophages in order to turn them into potential new human therapeutics. Timothy Lu first developed a T7 lytic bacteriophage capable of breaking down resistant biofilms by inducing the expression of the DspB enzyme[1]. He also developed an M13 lysogenic bacteriophage capable to suppressing the evolution of bacterial resistance by expressing a lexA3 protein repressor of the bacterial SOS pathway[2]. Finally, in Chapter 3, we report the creation of enhanced M13 and T7 bacteriophages, which prevent the evolution of bacterial resistance to phages and result in the long-term suppression of bacterial cultures. The three of us realized the need to bring these technologies outside of the labs and into the clinics to treat actual patients.

In this chapter, we establish a development plan for a start up company with the goal to develop and commercialized our engineered bacteriophages into new human therapeutics. We quantifie the market opportunity, establish a market entry point in the antibiotics space, analyse risks and provide different mitigation strategies associated with such this venture. We named this company Novophage Therapeutics, to emphasize the mission to develop new bacteriophage-based therapeutics.

---

[1] Lu and Collins. PNAS. 2007
[2] Lu and Collins. PNAS. 2009

Novophage

"Antibiotic resistance is a global threat that has the potential to

wipe out many of the major health benefits that have occurred over the last century"

Lindsay Baden, MD, Harvard Medical School, Infectious Disease Physician

"A product that decreases antibiotic-resistance rates and

improves patient outcomes would be very exciting and useful to clinicians and hospitals"

Joel Katz, MD, Brigham & Women's Hospital, Infectious Disease Specialist

"The ability to control hospital-based infections would

add tens of millions of dollars straight to a medical center's bottom line."

John Paul, recently retired CFO, University of Pittsburgh Medical Center

Table of Contents

7.1. Executive summary

7.1.1. The opportunity: infection and drug resistance to current therapies

In 2007, 1.7 million cases of hospital-acquired infections and 99,000 deaths occurred in the US alone. The total medical cost for these infections is $21.3 billion each year. These infections are becoming more difficult to treat because of the increasing prevalence of antibiotic-resistant bacteria such as methicillin-resistant *Staphylococcus aureus* (MRSA). In 2005, 94,000 hospital-acquired MRSA cases were reported (31.8 per 100,000), of which 18,650 were fatal. Existing antibiotics ($8 billion US in 2007) are unable to effectively treat these superbugs and a significant clinical need still exists.

Novophage has developed a differentiated biological therapy to increase the efficacy of antibiotic treatments, to significantly slow the onset of antibiotic resistance, and to effectively treat biofilms. We achieve these advances through the co-treatment of infections with our genetically enhanced bacteriophages and existing antibiotics. Bacteriophages are viruses ubiquitous to the natural environment that selectively target and destroy bacteria and bacteria only. Our genetically engineered bacteriophages are superior to natural bacteriophages because we have identified active proteins, enzymes, and other antimicrobial agents that we selectively co-express in our bacteriophages.

Novophage provides win-win solutions for all parties involved with healthcare. From a public health perspective, our technology provides unprecedented means for slowing the spread of antibiotic resistance, a dramatically worsening problem in modern medicine. For clinicians, patients, hospitals, and insurance companies, our technology significantly enhances the effectiveness of antimicrobial treatments, reduces hospital stays and costs, and improves overall outcomes. For pharmaceutical companies, our technology enables the extension of effective clinical lifetimes for existing and new antibiotics through reformulation with our bacteriophage.

7.1.2. The first product: therapeutic for hospital-acquired MRSA infections

Novophage will develop a therapy administered topically or intravenously for the treatment of hospital-acquired surgical site infections. This therapy will combine our genetically enhanced bacteriophage and an antibiotic to treat surgical site infections by MRSA.

Our engineered bacteriophages are modifications of natural bacteriophages; those natural bacteriophages have separately already been approved for use in human food products by the FDA in 2006. Currently, Exponential Biotherapies successfully completed a Phase I US-based clinical trial involving the use of natural bacteriophage in humans and Intralytix's bacteriophage is in pre-clinical testing. In 2007, Biocontrol successfully completed a Phase II clinical trial in the UK for ear infections and reported positive results.

We have demonstrated a 30,000-fold increase in the bactericidal activity of antibiotics when combined with our engineered bacteriophage. Furthermore, unlike current standard-of-care antibiotics, we have shown that our product can reduce the evolution of antibiotic resistance by at least 600-fold. In an industry-standard mouse infection model with *Escherichia coli*, our product increased the survival of infected mice from 20% to 80% when used in conjunction with traditional antibiotic therapy. This study has been published in the *Proceedings of the National Academy of Sciences* March 3rd, 2009.

Novophage's core inventions for composition and methods are protected by a series of four patent applications and one provisional patent held by MIT and BU. We have obtained a verbal agreement to pursue an exclusive licensing agreement. We have several options to mitigate commercialization risk and generate early revenue.

We have identified several suitable partners because our technology can extend the patent lifetimes and effective clinical lifetimes of antibiotics. The products of six big pharmaceutical companies account for $4 billion in sales of patent-protected antibiotics. Loss of patent protection is a significant

threat that pharmaceutical companies in the antimicrobial industry are facing. Several blockbuster antibiotics are facing loss of patent protection in 2009 (Avelox – $580 million sales in 2007) and 2010 (Levaquin – $1.4 billion sales in 2007).

In addition, Novophage can generate early revenue by out-licensing technology. The technology has immediate applicability for the use in the food safety and agribiotech industries.

7.1.3. Next steps

We have working prototypes of our engineered bacteriophages that have been validated in *in vitro* and *in vivo* experiments, which we are currently optimizing. We will translate this proof-of-concept work and develop a clinical prototype for our lead indication: surgical site infections by *S. aureus*. We seek $500,000 to build our team, to continue with the product development program, to complete in-licensing of the technology, and to secure additional financing for further product development and testing.

7.2. Market opportunity

The CDC estimates that patients acquire nearly 2 million bacterial infections each year in US hospitals, resulting in direct health care costs of $28-34 billion (2007 USD)[3]. Over $8 billion was spent in the US on antibiotic therapy in 2002[4]. Bacterial infections are becoming increasingly difficult to treat for two reasons: 1) the increasing prevalence of antibiotic-resistant bacteria such as methicillin (oxacillin)-resistant Staphylococcus aureus (MRSA); and 2) many years of under-investment in new therapeutic strategies.

In the mid-1980s, 1-5% of *S. aureus* isolates were methicillin-resistant, and today 60% to 70% of *S. aureus* strains found in hospitals are multidrug-resistant MRSA[5]. In 2005 over 94,000 cases of invasive MRSA infections alone occurred in the US with nearly 19,000 deaths[6].

Since the early 1980's only two new classes of antibiotics have been approved by the FDA[7], and in fact, many pharmaceutical companies abandoned or dramatically slowed discovery in the infectious diseases in the late 1980's and early 1990's[8]. Reflecting this decrease in investment, the global antibiotic market actually shrank from 2004 to 2006 due to a shift of sales from brand products to generic products following recent patent expirations (down 1.8% in 2006 to $22.6 billion from $23.4 billion in 2004)[9].

In short, "With increasing levels of antibiotic resistance, an insecure pipeline, and a dwindling number of companies investing in anti-infective agents, we have reached an unsettling impasse in

---

[3] CDC Report by R. Douglas Scott II. March 2009. The Direct Medical Costs of Healthcare-Associated Infections in U.S. Hospitals and the Benefits of Prevention.
[4] Kalorama Information. April 2003 Market Report: World Market for Anti-Infectives. US represents only 35% of the global prescription antibiotic market.
[5] Science. 2008; 321: 356-361. From Henry Chambers, infectious disease specialist at the University of California, San Francisco.
[6] JAMA. 2007; 298 (15): 1763-1771.
[7] Oxazolidinones (linezolid) & cyclic lipopeptides (daptomycin)
[8] N Engl J Med. 2004; 351(6): 523-526.
[9] Kalorama Information. April 2007 Market Report: Anti Infectives, Vol II: Antibacterials.

medicine," according to Dr. Richard P. Wenzel, former President of the International Society for Infectious Disease and Chairman of the Department of Internal Medicine at Virginia Commonwealth University[10].

Novophage Therapeutics will introduce a new biological therapy that slows the onset of antibiotic resistance and increases the efficacy of current antibiotics based on knowledge and engineering from MIT, Boston University, and Harvard Medical School. Novophage Therapeutics will penetrate the antibiotic market by offering efficacious treatments for highly antibiotic-resistant bacterial infections. Infectious disease doctors can therefore better manage the fight against multidrug-resistant strains through co-administration of our engineered bacteriophages with current clinical standards-of-care.

Novophage will enter the market by focusing on MRSA complicated skin and skin structure infections (cSSSI) acquired in hospital settings such as abscesses, infected ulcers, infected wounds, and surgical site infections. Complicated SSSI accounts for almost 10% of all hospital admissions for infections in the US[11]. Additionally, out of 94,000 invasive MRSA cases in the US reported in 2005, approximately 40,200 cases were cSSSI[12]. While Novophage Therapeutics is currently focused on the US market (US is 35% of the global prescription antibiotics market), *S. aureus* is also the main pathogen for SSSI in Latin American and Europe where MRSA resistance rates are 29% and 23%, respectively[13].

The entry strategy into the antibiotic market via cSSSI is similar to strategies used by the recently approved antibiotic drugs: 1) daptomycin known as Cubicin by Cubist Pharmaceuticals; and 2) tigecycline known as Tygacil developed by Wyeth. Daptomycin was the first lipopeptide antibiotic and received its first approval for cSSSI in 2003. Two years post-approval, off-label use included vancomycin-resistant enterococci (VRE), bacteremia, and endocarditis[14]. The 2008 net product sales of

---

[10] N Engl J Med. 2004; 351(6): 523-526.
[11] Centers for Disease Control. MMWR 2001; 50: 381-384.
[12] MRSA infections acquired in the community are approximately 15% of all MRSA infections with SSSI representing 75% of these infections. MRSA infections acquired related to health care delivery are approximately 85% of all MRSA infections with SSSI representing 37% of these infections. JAMA. 2003;290(22):2976-2984.
[13] Diagnostic Microbiology and Infectious Disease. 2007;57:7-13. Incidence determined from data reported from 1998-2004.
[14] Drug Therapy Topics 2005; 34 (6): 29-31.

Daptomycin/Cubicin were $414 million. Tigecyclin was also a first in class antibiotic for glycocyclines with its first approval for cSSSI, as well as complicated intra-abdominal infections (cIAI). Off-label use of tigecycline was reported for ventilator associated pneumonia[15] and septic patients[16]. Q4 sales for Tygacil in 2008 were $60 million.

The cSSSI market is an appealing therapeutic entry point because the unmet need with MRSA is significant; the situation for identifying patients is controlled; and the patient population is significant. Furthermore, FDA approval for cSSSI will enable off-label use and future regulatory approval in other clinical indications as is commonplace for antibiotics. Therefore, the market potential for Novophage Therapeutics is much larger than just MRSA infections or cSSSI since the therapeutic approach is applicable to many different areas of infectious diseases as indicated in Table 2-1.

Table 7-1: Market size for antibiotic segmented by therapeutic indication.

Therapeutic Indication	Global Market[17] (Millions USD 2006)	US Market[18] (Millions USD 2006)	US Market *MRSA*[19] (Millions USD 2006)
Skin and Skin Structure Infections (SSSI)	$2878	$1213	$220
Respiratory & ear Infections	$10,411	$4635	$155 (pneumonia only)
Urinary Tract Infections	$1226	$565	$32
Bloodstream Infections	Undetermined	Undetermined	$134

The significant costs associated with hospital-acquired infections, combined with the rise in antibiotic resistance and the dearth of novel options, create a unique opportunity for Novophage to enter

---

[15] Pharmacotherapy 2007;27(7):980–987).
[16] Journal of Antimicrobial Chemotherapy 2008 61(3):729-733.
[17] Kalorama Information. April 2007 Market Report: Anti Infectives, Vol II: Antibacterials. Some markets may be larger as market report had significant categories identified as "Other."
[18] Kalorama Information. April 2007 Market Report: Anti Infectives, Vol II: Antibacterials. Revenue for antibiotic class for a given therapeutic areas was weighted by US share of market for that antibiotic class.
[19] Prevention and Control of Healthcare-Associated Infections In Massachusetts. JSI Research and Training Institute, Inc. in Collaboration with the Massachusetts Department of Public Health. January 31, 2008.

the market at price parity with the current proprietary treatment options. Treatment cost (wholesale) based on 2006 Red Book for Cubicin is $0.365/mg or approximately $720 per treatment course[20].

7.3. Novophage's solution

7.3.1. The problem

As mentioned, antibiotic-resistant bacterial infections are a quickly rising and worldwide problem. Significant under-investment in new ways to combat bacterial infections has resulted in a depleted therapeutic pipeline, limiting the number of options infectious disease doctors have to defeat infections. Patients with severe infections at best have longer stays in the hospital and at worst lose limbs or die.

7.3.2. The solution

Novophage Therapeutics offers a differentiated antibiotic adjuvant therapy with three unique characteristics:

- It significantly slows the onset of antibiotic resistance by disrupting the mechanisms bacteria use to evolve resistance;
- It increases the killing efficacy of antibiotics against bacteria in biofilms by producing enzymes to degrade biofilms; and
- It potentiates killing of bacteria directly by producing additional antimicrobial agents

Novophage's novel approach uses genetically-enhanced bacteriophages. Bacteriophages are viruses ubiquitous in the natural environment that selectively infect and destroy bacteria only. Novophage's scientific founders harnessed new knowledge and tools in molecular and genetic biology to selectively insert and modify genes in the bacteriophage genome to enhance the natural killing functions

[20] http://www.cubicin.com/cost-data/ at 4 mg/kg/day dose and 70 kg person for 7 days.

of bacteriophages such as self-replication and the ability to burst through bacterial cell walls. When the enhanced bacteriophages are used in combination with corresponding classes of antibiotics, the combination therapy is more effective at bacterial killing and slows the onset of antibiotic resistance relative to antibiotic therapy alone.

The figure below illustrates the action of antibiotics alongside the three different features of the engineered bacteriophage and how the bacteriophage uses the infected bacteria's own cellular machinery to produce agents that prevent resistance, that breakdown biofilms, and that directly enhance killing of bacteria.

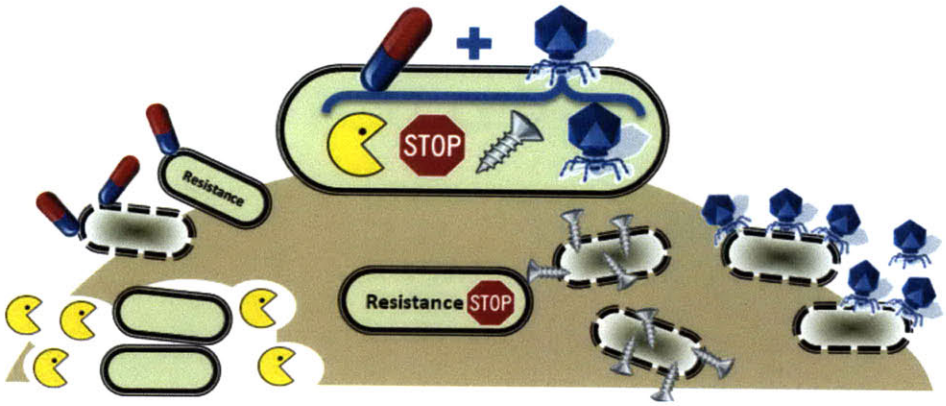

Figure 7-1: Mechanism of action of enhanced bacteriophages and antibiotics. The bacteriophages (blue) in combination with antibiotics (red and blue capsule) attack the bacterial cell. The bacteriophages infect the cell and force production of four entities: 1) more bacteriophages; 2) repressors of bacterial DNA damage repair mechanisms (stop sign); 3) biofilm-degrading enzymes (pac-man); and 4) broad-spectrum antimicrobial peptides (screw). The repressors slow the evolution of resistance in bacterial cells, enabling antibiotics to work longer. The biofilm-degrading enzymes and the antimicrobial peptides are released upon bacterial cell lysing (destruction) by the natural action of the bacteriophages. The enzymes and antimicrobial peptides work extracellularly, degrading the biofilm to expose more bacterial cells in the biofilm to antibiotics and puncturing the membranes of other bacterial cells, respectively.

To enter the market, Novophage Therapeutics will develop a product for MRSA cSSSI. The product will be a two-part combination of an enhanced bacteriophage and a current standard of care antibiotic. Clinical outcomes are expected to be higher cure rates than the antibiotic alone based on suppression of antibiotic resistance and increased bacterial killing.

7.3.3. Scientific evidence

Three different, useful modifications of natural bacteriophages have been demonstrated *in vitro,* and one of the three modifications has been tested *in vivo*. These proof-of-concept experiments used engineered bacteriophages targeting *E. coli* to suppress the evolution of bacterial resistance to antibiotics, to increase its activity on biofilms, and to widen the activity spectrum against a broader array of pathogens.

The first modification involves inserting a gene encoding a repressor of a bacteria's repair mechanism - the SOS response - into the bacteriophage[21]. When this enhanced bacteriophage infects harmful bacteria in the body, the harmful bacteria produce the repressor. The repressor then prevents the bacteria from repairing the damage inflicted by an antibiotic (e.g., a quinolone) that has simultaneously been administered with the enhanced-bacteriophage. The repressor gene encoded, *lexA3*, disables the SOS response that is induced upon bacterial DNA damage caused by antibiotics such as the quinolones, aminoglycosides, and penicillins, among others.

Data published in the *Proceedings of the National Academy of Sciences* by one of the scientific co-founders illustrates that enhanced bacteriophage combined with ofloxacin[22] yields a >30,000-fold improvement in the bacterial killing activity compared to ofloxacin alone in *E. coli*. The combination of enhanced bacteriophage plus gentamicin yields a 10,000-fold improvement and enhanced bacteriophage

---

[21] Lu and Collins. PNAS. 2009; Electronic publication March 2009.

[22] Quinolone class of antibiotic.

plus ampicillin yields a 100,000-fold improvement. Furthermore, the combination therapy reduces the evolution of antibiotic resistance by more than 600-fold relative to ofloxacin alone.

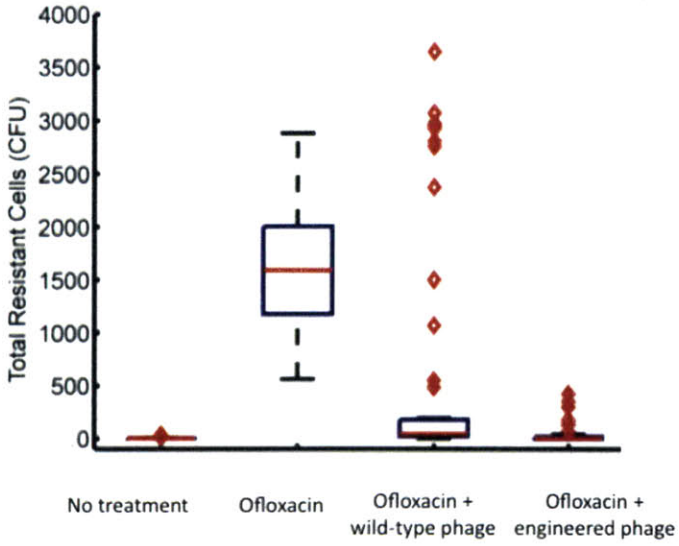

Figure 7-2: Novophage enhanced bacteriophage prevents emergence of antibiotic resistant bacteria. Lane 1 represents the control of no treatment; lane 2 is ofloxacin treatment where the median number of mutants is 1600; lane 3 is natural bacteriophage treatment plus ofloxacin; and lane 4 is lexA3-enhanced bacteriophage plus ofloxacin treatment. The number of resistant cells increases with antibiotic treatment, but in the presence of the enhanced bacteriophage, the number of resistant cells remains low.

The most powerful demonstration of this proposed mechanism as a viable therapeutic strategy is in the results of a mouse *E. coli* bacteremia model. Ten mice per treatment group were infected intraperitoneally with pathogenic *E. coli* and after 1 hour were administered one of four treatments: 1) no antibiotic, 2) ofloxacin antibiotic only, 3) natural T7 bacteriophages, 4) combination of enhanced bacteriophage and ofloxacin antibiotic.

After 5 days of studies, only 10% of the mice that were not administered antibiotics survived, while 20% of the mice treated with the standard of care ofloxacin antibiotic survived. Mice treated with

natural bacteriophage had a survival rate of 30%. However, 80% of the mice treated with our Novophage combination of genetically engineered bacteriophages and antibiotics survived the infection, thus showing a 4-fold improvement in survival over the current standard of care antibiotic treatment. No additional safety or toxicity issues were observed in the mice relative to enhanced bacteriophage administration.

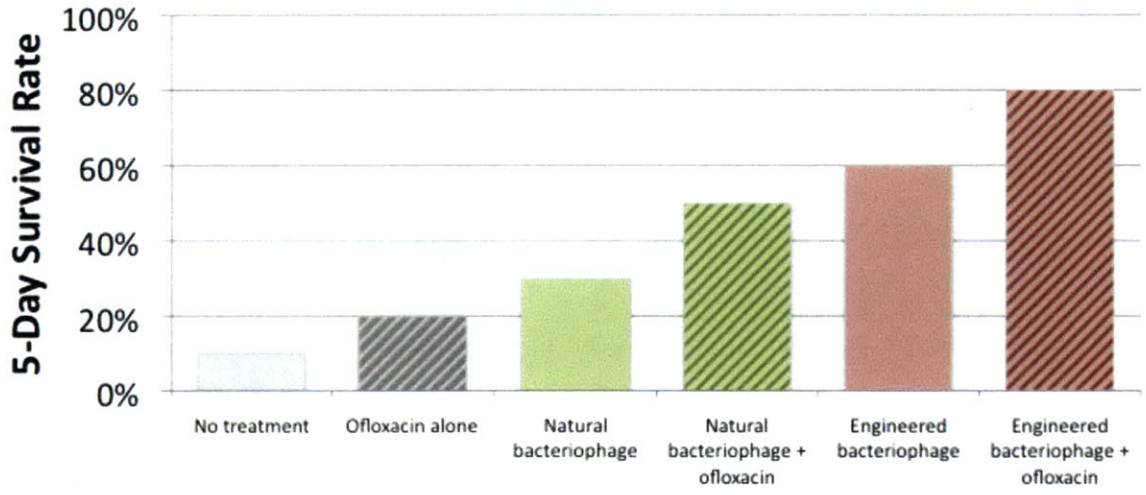

Figure 7-3: Novophage enhanced bacteriophage in combination with antibiotic increases survival of mice in a bacteremia model. Five day survival of mice in an intraperitoneal E. coli infection model. 10 mice per cohort were injected with E. coli and, after the onset of bacteremia, dosed with placebo, ofloxacin, natural bacteriophage, or a combination of natural bacteriophage and antibiotics or our combination therapy of enhanced bacteriophage and ofloxacin.

A second modification to the bacteriophage is the addition of genes encoding biofilm-degrading enzymes[23]. As before, upon infection of harmful bacteria by enhanced bacteriophage, the bacteria produce biofilm-degrading enzymes. The enzymes then begin to disrupt the polysaccharides that provide structural integrity for the biofilm, degrading the biofilm matrix and permitting antibiotic access to the bacteria living in the biofilm. Data published in the *Proceedings of the National Academy of Sciences* by one

[23] Lu and Collins. PNAS. 2007;104 (27): 11197–11202.

of the scientific co-founders shows bacteriophage designed to produce the biofilm-degrading enzyme Dispersin B in infected bacteria led to a >10,000x destruction of the biofilm as measured by viable cell counts.

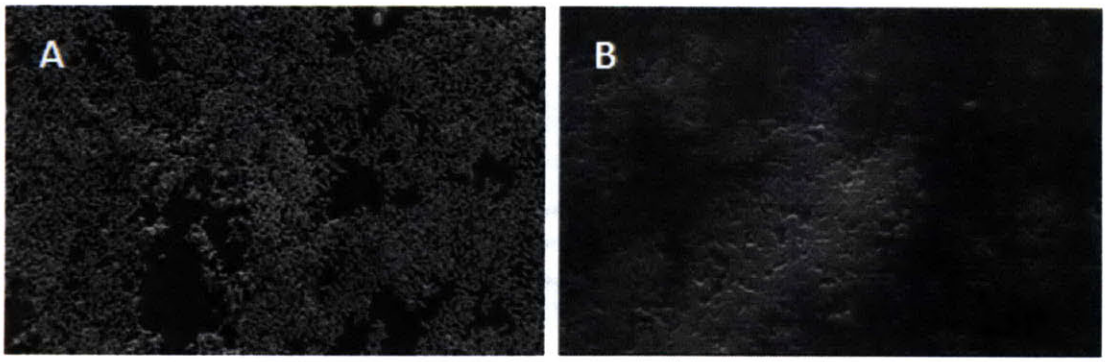

Figure 7-4: Enhanced bacteriophage treatment of biofilm reduces the number of live bacteria on and within the biofilm. A. Untreated biofilm of E. coli where only the top layers of cells are visible; the lower layers of cells are shielded. B. Biofilm treated with DispersinB –enhanced bacteriophage. No clear and defined E. coli cells are visible and very few viable cells were recovered; the residue is cellular debris.

Third, a gene encoding antimicrobial proteins has been inserted into the engineered bacteriophage to confer broad-spectrum bactericidal activity. These antimicrobial agents are short peptides of 15 – 25 amino acids in length that penetrate the membrane of bacteria thereby lysing them as well as attacking intracellular targets to decrease viability[24]. Preliminary, unpublished data demonstrates the efficacy of further enhancing bacteriophage to express these peptides in combination with the previously described engineered features.

Finally, based on the mechanism of action and initial *in vitro* results with *S. aureus* growth, this approach may work as broad-spectrum therapy, that is, for both gram positive and gram-negative bacterial infections.

---

[24] Brogden Nat. Rev. Microbio. (2005), Vol. 3 (3) pp. 238-50

7.3.4. Treatment & efficacy for MRSA cSSSI today

Treatments today that are approved for MRSA cSSSI include vancomycin, linezolid, daptomycin, and tigecycline. Vancomycin is the gold standard for MRSA cSSSI, a generic drug delivered intravenously (IV). However, vancomycin is highly toxic and poorly metabolized, leading to difficulties for the physician who must deal with administration. Cubist Pharmaceuticals' Daptomycin (Cubicin) has been shown to be equivalent to vancomycin in a once-per-day IV delivery. Pfizer's Linezolid (Zyvox) has been shown to be more effective than vancomycin even in an oral formulation in large Phase 3 trials. Whereas Wyeth's Tigecycline (Tygacil) is a broad-spectrum (gram positive and gram negative) antibiotic that can also be used for vancomycin resistance enterococci (VRE) and is less toxic than vancomycin. It is delivered IV and has been shown to be equivalent to vancomycin. Ofloxacin is a fluoroquinolone that belongs to an older class of drugs that has seen resurgence in use, particularly with community-acquired MRSA infections. While many of the above treatments are effective many patients with tolerable toxic side effects, Novophage's solution of combining antibiotic and enhanced bacteriophages promises to be more efficacious for similar side effects or less toxic by lowering the necessary dose of a toxic antibiotic. The rationale for this novel therapeutic approach is to combine the broad-spectrum activity of antibiotics with specific bacteriophages to address the high incidence of antibiotic-resistance in these infections, particularly for *S. aureus* and the resistant sub-strain MRSA.

7.4. Competition

There are three main competitors in the antibiotic adjuvant space with programs in the clinical stage: MPEX Pharmaceuticals, Biocontrol Limited and Exponential Biotherapies.

- MPEX Pharmaceuticals is a San Diego-based company in the antibiotic adjuvant space currently pursuing drug efflux pump inhibitors in gram negative bacteria. While this approach potentiates antibiotics against resistant bacteria including *Pseudomonas aeruginosa*, its efficacy is limited because it does not directly address the primary mode of resistance especially in gram positive

infections in which efflux pumps are less of a concern. These compounds are in the early stages and have not entered human clinical trials.

- Biocontrol Limited is a UK-based company developing natural bacteriophage cocktails as human therapies targeting infections of the outer ear caused by *Pseudomonas aeruginosa*. Successful Phase I safety trials and more recently Phase II efficacy trials were completed for topical application of the bacteriophage cocktail with patients in London. Biocontrol Limited plans on addressing other indications as well including cystic fibrosis and infections of burn wounds. Independently, a bacteriophage cocktail to treat burn wound infections by *Pseudomonas* and *Staphylococcus* is currently being evaluated in Belgium.
- Exponential Biotherapy is a Virginia-based company developing a natural bacteriophage cocktail therapy to treat vancomycin-resistant Enterococci (VRE) infections in the urinary tract. These infections are resistant to virtually all known antibiotics, yet Exponential Biotherapies obtained 100% healing rate in rodents after intravenous injection of the bacteriophage cocktail. After completing Phase I trials in 30 healthy humans to prove the non-toxicity of bacteriophages, they received FDA approval to proceed with Phase II trials.

While natural bacteriophage products such as those being pursued by Biocontrol and Exponential Biotherapy show potential as antimicrobial therapies and food antimicrobial products, the engineering approach Novophage has taken offers clear advantages over natural bacteriophages.

Our key advantages include:

- **Combating Resistance:** Bacteria are apt to develop resistance to natural bacteriophage treatment. Our engineered bacteriophages are able to overcome that limitation.
- **Biofilm Destruction:** Unlike natural bacteriophages that do not target biofilms, Novophage engineered the co-expression of biofilm busting enzymes to break down the extracellular "slime"

matrix that protects harmful bacterial biofilms which colonize implantable devices and catheters. These same biofilms also form on food products and are particularly difficult to treat.

- **Novelty:** Natural bacteriophage companies patent the method by which natural bacteriophages are isolated, methods which can easily be circumvented by one skilled in the art. Novophage Therapeutics protects not only methodologies for developing our products but also the composition of our engineered bacteriophages through patent filings.

Since 2006, natural bacteriophages have entered the commercial space as antimicrobials in the food safety and agricultural industry through commercialization by three active companies. EBI Food Safety is a Dutch company offering an FDA approved bacteriophage food antimicrobial product to treat meat, poultry, vegetable and dairy products against *Listeria.* The company established an industrial-scale bacteriophage production facility in the Netherlands from which its products are distributed to major food companies in the EU and the US.

Intralytix and OmniLytics are two US companies offering FDA approved natural bacteriophages cocktails targeting *Listeria* and *E. coli.* Both companies are now developing natural bacteriophage cocktails as human therapeutics targeting wounds caused by multidrug-resistant *S. aureus,* but are still in pre-clinical stages.

7.5. Intellectual property

Novophage's core inventions for sequence modifications to bacteriophages, methods of creating modified bacteriophages, and related methods of treatment are protected by five patent applications jointly held by the Massachusetts Institute of Technology and Boston University. The five applications are either submitted as a provisional application (1), in the PCT stage (2), or national (2)

Unlike patents granted on natural bacteriophages, which can only cover the method of isolation and not the organism, Novophage's core intellectual property covers the method of expression of biofilms

busting enzymes, resistance suppressors, and additional broad-spectrum antimicrobial agents from bacteriophages in general, i.e. not limited to any specific bacteriophage species. Furthermore we are covering the specific composition of the classes of these agents and the specific genetic sequences that we have engineered into the bacteriophages.

Novophage has a verbal agreement with both Technology Development Offices at both institutions that exclusive license is available to the company and negotiations are ongoing; a pro forma term sheet has been circulated. A Freedom-to-Operate analysis has been carried out and appears to be clear at this point. The team is continuing to advance technology development, to file patent applications on new discoveries, and to refine intellectual property strategies to protect likely business opportunities with the help of team mentors.

7.6. Risks and mitigation

A primary means to address the risks outlined below is for the team to recruit relevant and experienced people to the company as consultants, advisors, and employees. The team is actively seeking and meeting with mentors, some of whom the team hopes to engage with in closer relationships over time and as the needs of the company become more apparent.

7.6.1. Lead therapeutic development

We propose to mitigate the risks associated with the development of our novel combination antimicrobial therapy through the following sets of experiments that will validate the viability of our approach, culminating in a pre-clinical assay of the technology in the relevant animal models. First, we are transferring our work from *E. coli* bacteriophage into *S. aureus* bacteriophage K. This includes the transfer of our modular engineered inserts into bacteriophage K and screening the initial recombinants for activity on *in vitro S. aureus* cultures.

7.6.2. Screening of LexA3/AmP/DspB combinations

We will construct and screen a combinatorial library of our modules[25] to find the most effective combination of the LexA3 SOS repressor, the Dispersin B and the six different AmPs[26] we want to combine. Our primary outcome will be bactericidal activity on a planktonic *S. aureus* culture, followed by the same in a biofilm assay. After these early tests, we will test the lead phages against heterogeneous biofilms to simulate the more clinically relevant scenario of a mixed-species biofilms. This work involves molecular biology and should be completed in 4 - 8 weeks.

7.6.3. Animal models of surgical site infections

We will approach our first indication - MRSA complicated skin and skin structure (cSSSIs) - using a validated animal model. We will treat the infection and the primary endpoint will be survival as compared to best-in-class treatment, linezolid.

7.6.4. Expansion of product line to MDR *Pseudomonas aeruginosa*

At the same time as we are developing the *S. aureus* bacteriophage, we will develop a bacteriophage to target multidrug-resistant (MDR) *Pseudomonas aeruginosa* in order to utilize our enhanced biofilm-degrading ability against cystic fibrosis (CF) infections. The effort needed in the early stages of the development of this therapeutic dovetails with the development of our lead candidate therapeutic, i.e. the *S. aureus* bacteriophage. The advantage of targeting *P. aeruginosa*, and specifically CF, is the highly motivated patient population and several high-profile players in the area such as the CF Foundation, which is keen on testing novel approaches for the treatment of CF. Our delivery and proposed combination with existing antibiotics makes that therapeutic an ideal candidate for co-administration in clinical trials.

---

[25] The module contains all three main components plus other components necessary for expression.
[26] Based on our initial *in vitro* screens against *E. coli* and *S. aureus* we selected the six most active AmPs.

7.6.5. Safety profile

We will thoroughly test the safety of our engineered bacteriophages, specifically looking for issues related to pyrogenicity27, cytotoxicity28 and immunogenicity29. Based on clinical trial evidence to date using natural bacteriophages, no toxicities have been reported in Phase I human toxicity studies. For example, Exponential Biotherapies successfully completed a Phase I US-based clinical trial involving the use of natural bacteriophages in humans. Furthermore, in 2007, Biocontrol successfully completed a Phase II clinical trial in the UK for ear infections and reported positive results.

Additional preclinical testing will include further understanding of the bacteriophage clearance mechanism and timing as assessed through absorption, distribution, metabolism, and excretion studies. Evaluation of the likelihood of removal of benign bacteria in the body and possible related adverse events will also be tested. In addition, the therapeutic window will be evaluated in preclinical studies by determining minimum inhibition concentrations and maximum tolerated doses relative to adverse effects.

7.6.6. Manufacturing

Quality control endpoints in the manufacturing process will include testing of the pH, sterility, pyrogenicity, and cytotoxicity of pre-production batches of enhanced bacteriophage. Initially all batches will be tested for viral morphology by transmission electron microscopy (TEM) as well as sequenced to guarantee homogeneity.

---

[27] For endotoxin testing, the Limulus Amoebocyte Lysate (LAL) assay is the first line regulatory test but the phages may interfere with this test. A second test is the rabbit pyrogenicity test used when there is interference with the endotoxin test. Merabishvili et al, PLoS ONE (2009), Vol. 4 (3) pp. e4944.

[28] Cytotoxicity will be assessed in a cell survival assay using a human primary keratinocyte tissue culture assay. Based on literature and clinical trials, we do not expect to see any negative effect on survival rates following bacteriophage treatment.

[29] Immunogenic response will be assessed by the serum-response of guinea pigs. Hartman et al., Inf. Imm. (1991), Vol. 59 (11) pp. 4075-83. Repeat dosing with high doses of bacteriophage will be assessed through measuring the level of antibody reponse. In addition, adverse immunogenic reactions to proteins purposely released by the phage such as Dispersin B will be determined. Based on our experience and current literature. We do not anticipate adverse immunological reactions in vertebrates. Ramasubbu et al., JMB (2005), Vol. 349, pp. 475-486. Purified Dispersin B to treat diabetic foot ulcers is in preclinical development by Kane Biotech (summer of 2009).

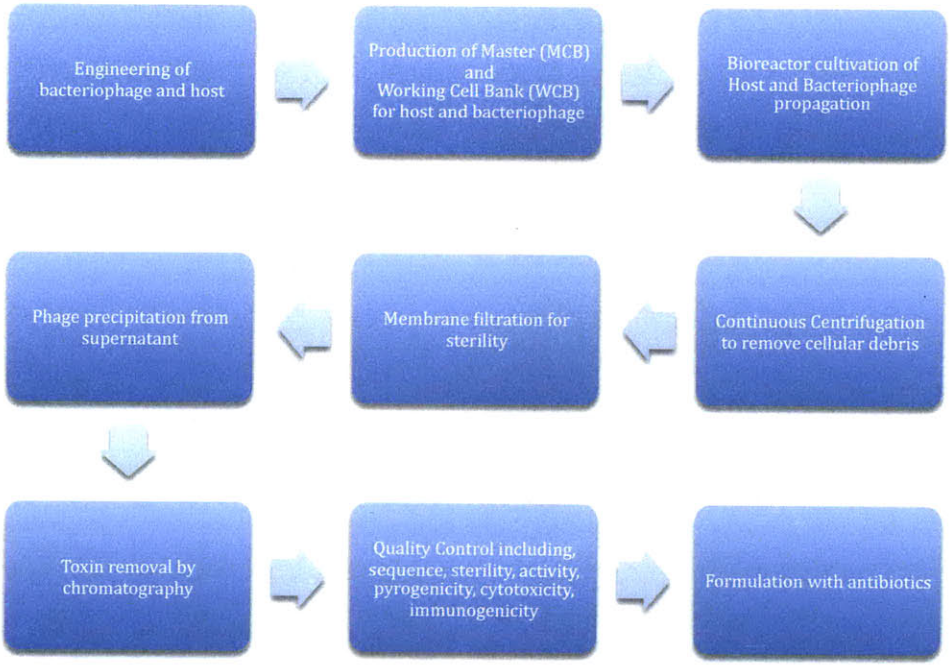

Figure 7-5: Manufacturing batch process for bacteriophages.

Figure 7-5 illustrates our current understanding of the manufacturing and purification steps necessary to produce therapeutic quality bacteriophage preparations. This understanding was developed with the kind help of Steve Sofen, VP at Genzyme. The critical step of the process are the removal of cellular debris and toxins to prevent adverse immune response in patients. The technology required for these steps is well established and understood.

7.6.7. Toxin-removal from bacteriophage batches

A major hurdle for bacteriophage therapy to overcome is assuring that final product batches are free of contamination that would lead to adverse reactions in the patient. These contaminations are mainly bacterial endotoxins for gram-negative bacteria and superantigens for gram-positive bacteria[30] that are necessarily present in the manufacturing process through the use of bacteria in the process. We plan to test several ways of cost-effectively removing toxins from batches using both commercially

[30] Endotoxins are a class of cellular debris composed of fragments of the bacterial cell wall that elicit a strong immune reaction in humans. Superantigens are a class of proteins in gram-positive bacteria

available kits as well as custom purification systems. The main principles of purification are successive steps of ultra-filtration[31] followed by adsorption of the remaining toxins to a column of high affinity binding partner. The primary drivers of cost in this purification scheme are the membranes and resins for ion exchange chromatography.

Another concern in manufacturing enhanced bacteriophages is genetic drift, i.e. changes in the genome of the bacteriophage leading to challenges in the ability to manufacture reproducible batches. We plan to minimize this risk by using bacteriophages that do not integrate into the bacterial genome, called non-temperate phages. This non-integration reduces the transfer of bacterial genetic material between successive rounds of viral replication and cuts down the transfer of pathogenicity islands[32]. Additionally, we will screen our bacteriophage genome for regions sensitive to mutation and modify these regions as necessary. If necessary, a further step to lock the bacteriophage genome is to replace the native viral DNA polymerases, with high-fidelity polymerases that reduce the mutation rate by more than 2 orders of magnitude.

7.6.8. Regulatory

Facing mounting pressure from the public and healthcare sectors due to the rapid spread of drug-resistant bacteria and the lack of new antibiotics, the FDA has become more accepting of alternative therapies, including the use of bacteriophages. We do not minimize the challenges of the FDA approval process but believe it is a manageable risk, based on recent go-aheads by the FDA for both Phase I and Phase II trials for cocktails of natural bacteriophages. The team plans to engage the FDA in the early stages of preclinical testing to understand if the experiments and data to be generated fit FDA expectation and guidelines. In terms of clinical trials, we expect shorter and well-defined trials, because endpoints for antibiotics are well established and the treatment course is shorter relative to other diseases such as cancer.

---

[31] Ultra-filtration through polysulfone membranes with a pore size of <30nm.
[32] Chen and Novick, Science (2009), Vol. 323 (5910), pp. 139-41

Furthermore, we have talked with two FDA regulatory experts. We understand that natural bacteriophages applied as food antimicrobials and as human therapeutics are establishing precedents in the FDA regulatory path. Both FDA experts expressed that engineered bacteriophages appear a manageable regulatory issue. One expert strongly indicated that our approach would not fall under the jurisdiction of the Recombinant Advisory Committee. The second regulatory expert indicated that engineered bacteriophages could be even more appealing than natural bacteriophages because of the control over the genome, specifically the ability to make them non-replicative and non-mutating.

7.6.9. Adoption by infectious disease physicians

We plan to closely cooperate with infectious disease physicians and clinical laboratory leaders to understand their concerns regarding our therapeutic approach as we are developing our lead therapeutic. To this end we will convene a panel of the key opinion leaders in the field and local specialists. Going forward we will closely collaborate with Brigham and Women's Hospital clinical leaders to design clinical trials.

7.7. Business development opportunities

The antibiotic products of six large pharmaceutical companies account for $10 billion in global sales. Loss of patent protection is a significant threat faced by these companies. Pfizer's Zithromax patents expired in 2005, and several more blockbuster antibiotics are facing patent expiration including Avelox ($580 million 2007 sales; expiration 2009) and Levaquin ($1.4 billion 2007 sales; expiration 2010). Novophage's product can effectively extend the patent lifetimes of antibiotics. Through partnership agreements, Novophage can leverage its novel products to gain access to distribution and manufacturing expertise.

Currently Novophage is in preliminary discussions with a large Boston-based biotechnology firm as well as a large pharmaceutical company about possible synergies and partnerships; these discussions are focusing on co-development agreements.

In the food safety sector, Novophage has an opportunity to generate an early revenue stream by licensing our technology to established players that already utilize natural bacteriophages in their business. The US food antimicrobials market is valued at $200 million and is growing at 4% annually. Four million foodborne pathogen cases each year are directly due to bacterial contamination during the industrial preparation process. These contaminations create an enormous social and economic strain on society, estimated at upwards of $35 billion annually in medical costs and lost productivity. The food industry itself is losing more than $400 million annually due to recalls, overhauls and stock market value reductions. Novophage provides familiar, yet more efficacious biological solutions for foodborne infections by using engineered bacteriophages to treat pathogenic bacteria in food products. Potential partners may include EBI Food Safety, OmniLytics and Intralytix.

7.8. Milestones and financials

7.8.1. Company information

Novophage Therapeutics was incorporated as a Delaware-based C corporation in March 2009. The goal for the next 12 months is to demonstrate in a MRSA cSSSI animal model that a *S. aureus*-targeted enhanced bacteriophage improves survival above the current standard of care with minimal safety and toxicity issues. Additionally, the company will identify the best antibiotic-enhanced bacteriophage combination for the first product to treat MRSA cSSSI. Finally, the team will determine the COGS associated with manufacturing the product. The company expects these activities to require less than $500,000.

The goal for 12-24 months is to more fully characterize the first product opportunity from *in vitro* and *in vivo* drug metabolism/pharmacokinetics and pathology/toxicology viewpoints. In addition, the company will conduct a pre- investigational new drug (IND) meeting with FDA to review the data to be generated and submitted for approval to enter phase I clinical trials. Further disease animal studies are expected to prepare for an IND filing with FDA. The team expects these activities to require approximately $6,500,000. Beyond this time frame, the company expects to complete the *in vivo* studies referenced above and to then enter GLP/GMP studies in preparation of an IND filing to enter phase 1 human trials. The team expects to begin ramping up preclinical work on a second product development program. These activities will require approximately $14,000,000.

Phase III trials are expected to run about $26,000 per patient with 1,000 patients per year, based on Cubist Pharmaceutical's Phase III study of Cubicin, for a total of $26M each in years 6 and 7[33]. Antibiotics clinical trials are typically less costly than other clinical trials, which range between $50M and $300M[34].

7.8.2. Company financials

See below for a detailed look into the projected financials.

---

[33]Phase 3 Data on CUBICIN Published in Journal Clinical Infectious Diseases: CUBICIN Efficacy Comparable to Standards of Care Against MSSA and MRSA. http://www.thefreelibrary.com/Phase+3+Data+on+CUBICIN+Published+in+Journal+Clinical+Infectious...-a0118242356

[34]Journal Health Economics 22 (2003):151-185. DiMasi and Grabowski.

Cash Flow Projections

	2009	2010	2011	2012	2013	2014	2015	2016	201
	Year 0	Year 1	Year 2	Year 3	Year 4	Year 5	Year 6	Year 7	Year
Beginning Cash	$70,000.00	$30,000.00	$3,641,500.00	$226,000.00	$9,112,472.80	($90,385.12)	$23,412,975.65	$13,046,361.85	($48,378,9
Cash from Operations	($540,000.00)	($2,888,500.00)	($3,415,500.00)	($5,113,527.20)	($9,202,857.91)	($11,496,639.24)	($60,366,613.79)	($61,425,305.49)	$4,539,3
Cash from Investing	$500,000.00	$6,500,000.00	$0.00	$14,000,000.00	$0.00	$35,000,000.00	$50,000,000.00	$0.00	
Capital Expense	$0.00	$0.00	$0.00	$0.00	$0.00	$0.00	$0.00	$0.00	
Change in Cash	($40,000.00)	$3,611,500.00	($3,415,500.00)	$8,886,472.80	($9,202,857.91)	$23,503,360.76	($10,366,613.79)	($61,425,305.49)	$4,539,3
Ending Balance	$30,000.00	$3,641,500.00	$226,000.00	$9,112,472.80	($90,385.12)	$23,412,975.65	$13,046,361.85	($48,378,943.64)	($43,839,5

Investment rounds	Amount
Grants	$500,000.00
Series A	$6,500,000.00
Series B	$14,000,000.00
Series C	$35,000,000.00
Series D	$50,000,000.00

OFFSET	Grants	Series A	Series B	Series C	Series D

Profit & Loss

		2009 Year 0	2010 Year 1	2011 Year 2	2012 Year 3	2013 Year 4	2014 Year 5	2015 Year 6	2016 Year 7	2017 Year 8	2018 Year 9	2019 Year 10
Sales												
	S. aureus phage	$0.00	$0.00	$0.00	$0.00	$0.00	$0.00	$0.00	$0.00	$31,337,150.00	$188,022,900.00	$501,394,400.00
	Out-licensing	$0.00	$50,000.00	$100,000.00	$290,495.10	$421,149.08	$832,190.59	$1,275,441.57	$1,752,821.13	$2,266,350.35	$2,818,157.39	$3,410,482.83
	Total Sales	$0.00	$50,000.00	$100,000.00	$290,495.10	$421,149.08	$832,190.59	$1,275,441.57	$1,752,821.13	$33,603,500.35	$190,841,057.39	$504,804,882.83
COGS	55%	$0.00	$27,500.00	$55,000.00	$159,772.31	$231,631.99	$457,704.82	$701,492.86	$964,051.62	$18,481,925.19	$104,962,581.56	$277,642,685.56
Gross Margin	45%											
Net Revenue		$0.00	$22,500.00	$45,000.00	$130,722.80	$189,517.09	$374,485.76	$573,948.71	$788,769.51	$15,121,575.16	$85,878,475.82	$227,162,197.27
Expenses												
	R & D											
	Salaries & Benefits	$240,000.00	$550,000.00	$670,000.00	$730,000.00	$930,000.00	$930,000.00	$930,000.00	$930,000.00	$930,000.00	$930,000.00	$930,000.00
	Equipment	$50,000.00	$875,000.00	$787,500.00	$1,661,250.00	$2,643,125.00	$4,374,375.00	$28,992,687.50	$29,701,225.00	$3,926,347.50	$14,243,914.88	$14,118,914.88
	Consumables	$125,000.00	$350,000.00	$525,000.00	$787,500.00	$1,181,250.00	$1,653,750.00	$2,149,875.00	$2,579,850.00	$2,837,835.00	$2,979,726.75	$2,979,726.75
	Animal Studies	$75,000.00	$400,000.00	$75,000.00	$200,000.00	$75,000.00	$200,000.00	$75,000.00	$200,000.00	$75,000.00	$200,000.00	$75,000.00
	Clinical Trials	$0.00	$0.00	$0.00	$392,500.00	$965,000.00	$1,930,000.00	$26,000,000.00	$26,000,000.00	$0.00	$10,000,000.00	$10,000,000.00
	Total	$490,000.00	$2,175,000.00	$2,057,500.00	$3,771,250.00	$5,794,375.00	$9,088,125.00	$58,147,562.50	$59,411,075.00	$7,769,182.50	$28,353,641.63	$28,103,641.63
	Manufacturing											
	Salaries & Benefits	$0.00	$80,000.00	$180,000.00	$175,000.00	$250,000.00	$250,000.00	$250,000.00	$250,000.00	$250,000.00	$250,000.00	$250,000.00
	Equipment	$40,000.00	$100,000.00	$500,000.00	$125,000.00	$125,000.00	$125,000.00	$250,000.00	$250,000.00	$1,000,000.00	$750,000.00	$750,000.00
	Consumables	$5,000.00	$25,000.00	$100,000.00	$500,000.00	$500,000.00	$500,000.00	$5,000,000.00	$5,000,000.00	$10,000,000.00	$10,000,000.00	$10,000,000.00
	Total	$45,000.00	$205,000.00	$780,000.00	$800,000.00	$875,000.00	$875,000.00	$5,500,000.00	$5,500,000.00	$11,250,000.00	$11,000,000.00	$11,000,000.00
	Regulatory											
	Salaries & Benefits	$0.00	$125,000.00	$125,000.00	$190,000.00	$315,000.00	$315,000.00	$315,000.00	$315,000.00	$315,000.00	$315,000.00	$315,000.00
	Misc/Other	$0.00	$0.00	$0.00	$0.00	$0.00	$0.00	$0.00	$0.00	$0.00	$0.00	$0.00
	Total	$0.00	$125,000.00	$125,000.00	$190,000.00	$315,000.00	$315,000.00	$315,000.00	$315,000.00	$315,000.00	$315,000.00	$315,000.00
	Marketing											
	Salaries & Benefits	$0.00	$0.00	$220,000.00	$220,000.00	$220,000.00	$315,000.00	$315,000.00	$315,000.00	$315,000.00	$315,000.00	$315,000.00
	PR/Literature	$0.00	$0.00	$10,000.00	$15,000.00	$20,000.00	$30,000.00	$40,000.00	$50,000.00	$60,000.00	$70,000.00	$80,000.00
	Trade Shows	$0.00	$1,000.00	$10,000.00	$10,000.00	$10,000.00	$10,000.00	$10,000.00	$10,000.00	$10,000.00	$10,000.00	$10,000.00
	Misc/Other											
	Total	$0.00	$1,000.00	$240,000.00	$245,000.00	$250,000.00	$355,000.00	$365,000.00	$375,000.00	$385,000.00	$395,000.00	$405,000.00
	Sales											
	Salaries & Benefits	$0.00	$0.00	$325,000.00	$325,000.00	$325,000.00	$445,000.00	$445,000.00	$445,000.00	$445,000.00	$445,000.00	$445,000.00
	Travel	$0.00	$0.00	$3,000.00	$3,000.00	$3,000.00	$3,000.00	$3,000.00	$3,000.00	$3,000.00	$3,000.00	$3,000.00
	Misc/Other											
	Total	$0.00	$0.00	$328,000.00	$328,000.00	$328,000.00	$448,000.00	$448,000.00	$448,000.00	$448,000.00	$448,000.00	$448,000.00
	G&A											
	Salaries & Benefits	$0.00	$470,000.00	$570,000.00	$570,000.00	$570,000.00	$570,000.00	$570,000.00	$570,000.00	$570,000.00	$570,000.00	$570,000.00
	Rent	$0.00	$60,000.00	$60,000.00	$60,000.00	$1,000,000.00	$1,000,000.00	$1,000,000.00	$1,000,000.00	$1,000,000.00	$1,000,000.00	$1,000,000.00
	Telecom/Postage	$0.00	$10,000.00	$10,000.00	$10,000.00	$75,000.00	$25,000.00	$25,000.00	$25,000.00	$25,000.00	$25,000.00	$25,000.00
	Legal	$50,000.00	$10,000.00	$10,000.00	$10,000.00	$1,000,000.00	$10,000.00	$10,000.00	$10,000.00	$10,000.00	$10,000.00	$10,000.00
	Rent	$0.00	$60,000.00	$60,000.00	$60,000.00	$60,000.00	$60,000.00	$60,000.00	$60,000.00	$60,000.00	$60,000.00	$60,000.00
	Total	$50,000.00	$610,000.00	$710,000.00	$710,000.00	$2,705,000.00	$1,665,000.00	$1,665,000.00	$1,665,000.00	$1,665,000.00	$1,665,000.00	$1,665,000.00
	Operating Expenses	$540,000.00	$2,911,000.00	$3,460,500.00	$5,244,250.00	$9,392,375.00	$11,871,125.00	$60,940,562.50	$62,214,075.00	$10,582,182.50	$31,176,641.63	$30,936,641.63
Operating Profit		($540,000.00)	($2,888,500.00)	($3,415,500.00)	($5,113,527.20)	($9,202,857.91)	($11,496,639.24)	($60,366,613.79)	($61,425,305.49)	$4,539,392.66	$54,701,834.20	$196,225,555.65

Research & Development Budget

		Year 0	Year 1	Year 2	Year 3	Year 4	Year 5	Year 6	Year 7	Year 8	Year 9	Year 10
Lab Material				150.00%	150.00%	150.00%	140.00%	130.00%	120.00%	110.00%	105.00%	100.00%
	Equipment	$50,000.00	$125,000.00	$187,500.00	$281,250.00	$421,875.00	$590,625.00	$767,812.50	$921,375.00	$1,013,512.50	$1,064,188.13	$1,064,188.13
	Consumables	$125,000.00	$350,000.00	$525,000.00	$787,500.00	$1,181,250.00	$1,653,750.00	$2,149,875.00	$2,579,850.00	$2,837,835.00	$2,979,726.75	$2,979,726.75
		$0.00	$0.00	$0.00	$0.00	$0.00	$0.00	$0.00	$0.00	$0.00	$0.00	$0.00
		$0.00	$0.00	$0.00	$0.00	$0.00	$0.00	$0.00	$0.00	$0.00	$0.00	$0.00
	Total	$175,000.00	$475,000.00	$712,500.00	$1,068,750.00	$1,603,125.00	$2,244,375.00	$2,917,687.50	$3,501,225.00	$3,851,347.50	$4,043,914.88	$4,043,914.88
Animal Studies												
	Rodents	$75,000.00	$150,000.00	$75,000.00	$75,000.00	$75,000.00	$75,000.00	$75,000.00	$75,000.00	$75,000.00	$75,000.00	$75,000.00
	Canines	$0.00	$250,000.00	$0.00	$125,000.00	$0.00	$125,000.00	$0.00	$125,000.00	$0.00	$125,000.00	$0.00
	Total	$75,000.00	$400,000.00	$75,000.00	$200,000.00	$75,000.00	$200,000.00	$75,000.00	$200,000.00	$75,000.00	$200,000.00	$75,000.00
Clinical Trials					Phase I	Phase IIa	PhaseIIb	Phase III	PhaseIII	Approval	Phase IV	Phase IV
	Patient #	0	0	0	25	50	100	1,000	1,000	0	10,000	10,000
	Cost / Patient	$0.00	$0.00	$0.00	$15,700.00	$19,300.00	$19,300.00	$26,000.00	$26,000.00		$1,000.00	$1,000.00
	Total	$0.00	$0.00	$0.00	$392,500.00	$965,000.00	$1,930,000.00	$26,000,000.00	$26,000,000.00	$0.00	$10,000,000.00	$10,000,000.00
Grand Total		$250,000.00	$875,000.00	$787,500.00	$1,661,250.00	$2,643,125.00	$4,374,375.00	$28,992,687.50	$29,701,225.00	$3,926,347.50	$14,243,914.88	$14,118,914.88

Production cost

Manufacturing		Laboratory 1	Scale-Up 2	Pilot-Set-Up 0.02	Clinical Trials 3	Clinical Trials 4	Clinical Trials 5	Clinical Trials 6	Clinical Trials 7	Approval 8	Market 9	Market 10
	Capital Equipment	$40,000.00	$100,000.00	$500,000.00	$125,000.00	$125,000.00	$125,000.00	$250,000.00	$250,000.00	$1,000,000.00	$750,000.00	$750,000.00
	Consumables	$5,000.00	$25,000.00	$100,000.00	$500,000.00	$500,000.00	$500,000.00	$5,000,000.00	$5,000,000.00	$10,000,000.00	$10,000,000.00	$10,000,000.00
	Total	$45,000.00	$125,000.00	$600,000.00	$625,000.00	$625,000.00	$625,000.00	$5,250,000.00	$5,250,000.00	$11,000,000.00	$10,750,000.00	$10,750,000.00

taffing Plan

	0	1	2	3	4	5	6	7	8	9	10	Annual Salary	Year 0	Year 1	Year 2	Year 3	Year 4	Year 5	Year 6	Year 7	Year 8	Year 9	Year 10
D																							
CTO	0	1	1	1	1	1	1	1	1	1	1	$150,000.00	$0.00	$150,000.00	$150,000.00	$150,000.00	$150,000.00	$150,000.00	$150,000.00	$150,000.00	$150,000.00	$150,000.00	$150,000.00
Scientists	0	2	2	2	4	4	4	4	4	4	4	$100,000.00	$0.00	$200,000.00	$200,000.00	$200,000.00	$400,000.00	$400,000.00	$400,000.00	$400,000.00	$400,000.00	$400,000.00	$400,000.00
Technicians	0	2	4	5	5	5	5	5	5	5	5	$60,000.00	$0.00	$120,000.00	$240,000.00	$300,000.00	$300,000.00	$300,000.00	$300,000.00	$300,000.00	$300,000.00	$300,000.00	$300,000.00
Consultant	3	1	1	1	1	1	1	1	1	1	1	$80,000.00	$240,000.00	$80,000.00	$80,000.00	$80,000.00	$80,000.00	$80,000.00	$80,000.00	$80,000.00	$80,000.00	$80,000.00	$80,000.00
Total	3	6	8	9	11	11	11	11	11	11	11	$390,000.00	$240,000.00	$550,000.00	$670,000.00	$730,000.00	$930,000.00	$930,000.00	$930,000.00	$930,000.00	$930,000.00	$930,000.00	$930,000.00
nufacturing																							
CMO	0	0	1	1	1	1	1	1	1	1	1	$100,000.00	$0.00	$0.00	$100,000.00	$100,000.00	$100,000.00	$100,000.00	$100,000.00	$100,000.00	$100,000.00	$100,000.00	$100,000.00
Engineers	0	0	0	1	2	2	2	2	2	2	2	$75,000.00	$0.00	$0.00	$0.00	$75,000.00	$150,000.00	$150,000.00	$150,000.00	$150,000.00	$150,000.00	$150,000.00	$150,000.00
Consultant	0	1	1	0	0	0	0	0	0	0	0	$80,000.00	$0.00	$80,000.00	$80,000.00	$0.00	$0.00	$0.00	$0.00	$0.00	$0.00	$0.00	$0.00
Total	0	1	2	2	3	3	3	3	3	3	3	$255,000.00	$0.00	$80,000.00	$180,000.00	$175,000.00	$250,000.00	$250,000.00	$250,000.00	$250,000.00	$250,000.00	$250,000.00	$250,000.00
ulatory																							
Regulatory Affairs	0	1	1	1	2	2	2	2	2	2	2	$125,000.00	$0.00	$125,000.00	$125,000.00	$125,000.00	$250,000.00	$250,000.00	$250,000.00	$250,000.00	$250,000.00	$250,000.00	$250,000.00
Consultant	0	0	0	1	1	1	1	1	1	1	1	$65,000.00	$0.00	$0.00	$0.00	$65,000.00	$65,000.00	$65,000.00	$65,000.00	$65,000.00	$65,000.00	$65,000.00	$65,000.00
Total	0	1	1	2	3	3	3	3	3	3	3	$190,000.00	$0.00	$125,000.00	$125,000.00	$190,000.00	$315,000.00	$315,000.00	$315,000.00	$315,000.00	$315,000.00	$315,000.00	$315,000.00
rketing																							
VP Marketing	0	0	1	1	1	1	1	1	1	1	1	$125,000.00	$0.00	$0.00	$125,000.00	$125,000.00	$125,000.00	$125,000.00	$125,000.00	$125,000.00	$125,000.00	$125,000.00	$125,000.00
Product Manager	0	0	1	1	1	2	2	2	2	2	2	$95,000.00	$0.00	$0.00	$95,000.00	$95,000.00	$95,000.00	$190,000.00	$190,000.00	$190,000.00	$190,000.00	$190,000.00	$190,000.00
Other	0	0	0	0	0	0	0	0	0	0	0	$80,000.00	$0.00	$0.00	$0.00	$0.00	$0.00	$0.00	$0.00	$0.00	$0.00	$0.00	$0.00
Total	0	0	2	2	2	3	3	3	3	3	3	$300,000.00	$0.00	$0.00	$220,000.00	$220,000.00	$220,000.00	$315,000.00	$315,000.00	$315,000.00	$315,000.00	$315,000.00	$315,000.00
les																							
VP Sales	0	0	1	1	1	1	1	1	1	1	1	$175,000.00	$0.00	$0.00	$175,000.00	$175,000.00	$175,000.00	$175,000.00	$175,000.00	$175,000.00	$175,000.00	$175,000.00	$175,000.00
Regional Sales	0	0	1	1	1	1	1	1	1	1	1	$70,000.00	$0.00	$0.00	$70,000.00	$70,000.00	$70,000.00	$70,000.00	$70,000.00	$70,000.00	$70,000.00	$70,000.00	$70,000.00
Support	0	0	2	2	2	5	5	5	5	5	5	$40,000.00	$0.00	$0.00	$80,000.00	$80,000.00	$80,000.00	$200,000.00	$200,000.00	$200,000.00	$200,000.00	$200,000.00	$200,000.00
Consultant	0	0	0	0	0	0	0	0	0	0	0	$80,000.00	$0.00	$0.00	$0.00	$0.00	$0.00	$0.00	$0.00	$0.00	$0.00	$0.00	$0.00
Total	0	0	4	4	4	7	7	7	7	7	7	$365,000.00	$0.00	$0.00	$325,000.00	$325,000.00	$325,000.00	$445,000.00	$445,000.00	$445,000.00	$445,000.00	$445,000.00	$445,000.00
neral & Admin.																							
CEO	0	1	1	1	1	1	1	1	1	1	1	$200,000.00	$0.00	$200,000.00	$200,000.00	$200,000.00	$200,000.00	$200,000.00	$200,000.00	$200,000.00	$200,000.00	$200,000.00	$200,000.00
VP Finance	0	1	1	1	1	1	1	1	1	1	1	$150,000.00	$0.00	$150,000.00	$150,000.00	$150,000.00	$150,000.00	$150,000.00	$150,000.00	$150,000.00	$150,000.00	$150,000.00	$150,000.00
VP Business Dev	0	1	1	1	1	1	1	1	1	1	1	$120,000.00	$0.00	$120,000.00	$120,000.00	$120,000.00	$120,000.00	$120,000.00	$120,000.00	$120,000.00	$120,000.00	$120,000.00	$120,000.00
Accounting	0	0	1	1	1	1	1	1	1	1	1	$50,000.00	$0.00	$0.00	$50,000.00	$50,000.00	$50,000.00	$50,000.00	$50,000.00	$50,000.00	$50,000.00	$50,000.00	$50,000.00
Admin. Staff	0	0	1	1	1	1	1	1	1	1	1	$50,000.00	$0.00	$0.00	$50,000.00	$50,000.00	$50,000.00	$50,000.00	$50,000.00	$50,000.00	$50,000.00	$50,000.00	$50,000.00
Total	0	3	5	5	5	5	5	5	5	5	5	$570,000.00	0	470000	570000	570000	570000	570000	570000	570000	570000	570000	570000
and Total	3	10	20	22	25	29	29	29	29	29	29	$1,815,000.00	$240,000.00	$1,225,000.00	$2,090,000.00	$2,210,000.00	$2,610,000.00	$2,825,000.00	$2,825,000.00	$2,825,000.00	$2,825,000.00	$2,825,000.00	$2,825,000.00

Chapter 8. Thesis conclusion

The rise in antibiotic resistant infections poses a great threat to human health and resulted in increased morbidity and mortality in patients. The work in this thesis described new strategies focusing on the family of antimicrobial peptides to counter these resistant infections.

We first determined the antimicrobial activity of a panel of over 500 natural and designed AmPs by measuring the peptide's minimum inhibitory concentration against four pathogens – *E. coli*, *P. aeruginosa*, *S. epidermidis* and *S. aureus*. This represented the largest ever-compiled database of AmP activity. The activity database is of tremendous value to the scientific community as it allows, for the first time, direct comparison of AmP activity based on a single standardized protocol. In addition, we supplemented the database with hemolytic toxicity measurements for selected AmPs that demonstrated strong antimicrobial activity. As a result, researchers now have the knowledge necessary to select and work with AmPs that are non-toxic and most active against specific bacterial target.

While natural AmPs typically have a broad activity spectrum against different pathogens, they are not optimized for a specific antimicrobial function or bacterial target. We developed a design algorithm that utilizes conserved motif found in the amino acid sequences of natural AmPs in order to produce new peptides with antimicrobial activity. We used the database of AmP activity to rank the motifs' putative antimicrobial strength and designed new peptides using active motifs. Finally, we incorporated design criteria to mimic natural AmP and guide the choice of amino acid in order to derive new peptide sequences. The incorporation of activity information and the design criteria increased the success rate in designing active peptides from 45% to 73% and increased the antimicrobial

strength of the designs. In the current algorithm, motif were ranked was solely based on their MIC value for *E. coli*. We envision that future would involve ranking motifs based on multiple criteria such as minimizing toxicity, maximizing resistance to protease degradation, or maximizing bacterial specificity. Finally, new design criteria could be applied to also favor sequence to achieved specific and desired functions for the peptides.

After gaining the ability to design new and active peptides sequence, we then focused our attention onto understanding the AmP mechanism and developing new AmP potentiation strategies. Our study of the family of Ponercin AmPs showed that MIC is an incomplete determinant for antimicrobial activity and that cidal behavior must also be accounted for. Using AFM and microfluidic flow device, we correlated the cidal activity of Ponericin G1 with corrugation of the cell membrane. We then determined that the membrane stress sensing and repair of misfolded membrane proteins via the CpxAR system allows bacteria to resist the action of Ponericin G1 as well as DNA repair via induction of the cell's SOS response by RecA. We finally determined that Ponericin G1 also target tRNA synthetase in the ribosome and that Ponericin G1 can be synergistically potentiated by 300-fold by combining it with kanamycin, an antibiotic also targeting the ribosome to treat antibiotic resistant *E. coli* infections. We also identified that the amidated version of Ponericing G1 disrupts the iron import mechanism and future work will verify this hypothesis by supplementing iron chelators in the media to observe additional synergistic potentiation effect.

After having developed new strategies to potentiate AmPs as therapeutics, we developed new means to deliver AmPs or genes encoding AmPs directly at the site of infection. Since a large portion of infections originate at the surface of implantable devices, we developed films coatings that incorporate AmPs in order to prevent the initial

attachment of bacteria and ensure the sterility of these surfaces. We demonstrated that the kinetics of AmP release could be adjusted via the number of layers, the co-released of agents or the nature of the film polymers. We also showed that the released AmPs still actively prevented bacterial growth and remained non-toxic towards mammalian cells. Future work would include the incorporation of such antimicrobial surface in an infection animal model to demonstrate the feasibility of this approach *in vivo*.

After delivery AmPs, we developed new methods to deliver of genes inducing the toxic expression of AmPs and other lytic agents directly into bacteria using reengineered bacteriophages. Expression of these lytic agents from lysogenic bacteriophages resulted in bactericidal activity, and demonstrated, for the first time, a long-term cidal effect for over 20 hours. We then enhanced the efficacy of this antimicrobial approach by expressing the same agents in lytic bacteriophage, which resulted in complete suppression of the bacterial culture and prevented bacterial regrowth and resistance to bacteriophages. Future extension of this technology would seek to treat bacterial co-cultures to broaden the activity spectrum of the bacteriophage.

Finally, we identified a market opportunity for an antimicrobial company commercializing such genetically engineered bacteriophages and developed a clear market entry and expansion strategies. The idea won at seven major business plan competition throughout the US. A company was then incorporated to pursue the opportunity and bring the technology developed in this thesis to patients. Future work will begin with the pre-clinical trials of the technology in animal model. In conclusion, this thesis establishes new advances in the delivery, the design and the potentiation of therapies to treat antibiotic resistant infections.

– Change is the end result of all true learning –

Leo Buscaglia